2. Convective-Stratiform Separation Algorithm (CSSA) Development and Evaluation

This section summarizes the work performed in FY 2003 to improve the prototype Convective-Stratiform Separation Algorithm (CSSA) and to evaluate the performance of the prototype Range-dependent bias Correction Algorithm (RCA) as supported by CSSA.

2.1 Introduction

In FY02, CSSA was developed further and evaluated qualitatively for a variety cases from 12 different WSR-88D sites. While visual examination of the results indicated generally good performance in separating convective cores from stratiform areas, a truer test of CSSA lies in the performance of the RCA as supported by CSSA under the 'stratify-and-adjust' paradigm (Seo et al. 2002). Here, we present the case studies carried out to evaluate the performance of CSSA-RCA.

CSSA as described in Seo et al. (2002) relies on three attributes; the maximum reflectivity in the vertical (r_x), the vertically-averaged local spatial correlation of reflectivity (ρ_r), and the local spatial correlation of the top-height of apparent convective core (ρ_h). In Seo et al. (2002), it was also recognized that vertically-integrated liquid water (VIL) is a skillful attribute for convective-stratiform separation. Because VIL is an existing WSR-88D product, it is tempting to consider the VIL only-based CSSA as a significantly less expensive alternative to the 'full-blown' CSSA based on multiple attributes. To assess viability of such a VIL only-based separation approach, here we compare the VIL only-based CSSA (referred to herein as the VIL-only CSSA) with the full-blown CSSA based on the four attributes; r_x, ρ_r, ρ_h and VIL (referred to herein as the full CSSA).

2.2 Description of the full CSSA

Seo et al. (2002) provides a description of the CSSA based on r_x, ρ_r and ρ_h. Though the mathematical description of the algorithm with VIL added is completely analogous to that without it (Seo et al. 2002), in the following we describe the 4-attribute version of CSSA in some detail for completeness and future reference.

Given at each azran bin the four attributes, r_x, ρ_r, ρ_h and VIL, the algorithm estimates the conditional probability that the bin belongs to the convective or stratiform area of precipitation. In the indicator approach adopted for CSSA (see Seo et al. 2002 for rationale), the conditioning variables are not the absolute magnitude of the attributes themselves, but only their binary encoding based on whether the attributes are greater or less than some preset thresholds. The objective is to estimate the conditional probability, Prob[Bin $\in$ stratiform | $r_x < r_{xci}$, $\rho_r \geq \rho_{rcj}$, $\rho_h \geq \rho_{hck}$, VIL < VIL_l; $i=1,...,n_1$, $j=1,...,n_2$, $k=1,...,n_3$, $l=1,...,n_4$], where Prob[ ] denotes the probability of occurrence of the event bracketed, and n_1, n_2, n_3 and n_4 denote the number of thresholds used for r_x, ρ_r, ρ_h and VIL, respectively. The above conditional probability is then approximated by the following conditional expectation involving indicator variables (i.e., the binary encoding of the attributes via thresholding):

$$\text{Prob}[\text{ Bin} \in \text{stratiform} \mid r_x < r_{xci},\ \rho_r \geq \rho_{rcj},\ \rho_h \geq \rho_{hck},\ VIL \prec VIL_l\ ;\ i=1,...,n_1,\ j=1,...,n_2,\ k=1,...,n_3,\ l=1,...,n_4]$$

$$\approx E[I_s \mid I_{rxi} = i_{rxi},\ I_{\rho rj} = i_{\rho rj},\ I_{\rho hk} = i_{\rho hk},\ I_{VILl}=i_{VILl};\ i=1,...,n_1,\ j=1,...,n_2,\ k=1,...,n_3,\ l=1,...,n_4] \qquad (1)$$

Throughout this section, random variables are denoted by upper case letters and the experimental outcome of them are denoted by the corresponding lowercase letters. In Eq.(1), r_{xci}, ρ_{rcj}, ρ_{hck} and VIL_{cl} are the i-th, j-th, k-th and l-th thresholds for r_x, ρ_r, ρ_h and VIL, respectively, and the indicator variables, I_s, I_{rxi}, $I_{\rho rj}$, $I_{\rho hk}$ and VIL_k are defined as:

$$i_s = \begin{cases} 0 & \text{if the bin is in the convective core} \\ 1 & \text{otherwise} \end{cases} \qquad (2)$$

$$i_{rxi} = \begin{cases} 1 & \text{if } r_{xi} < r_{xci} \\ 0 & \text{otherwise} \end{cases} \qquad (3)$$

$$i_{\rho rj} = \begin{cases} 0 & \text{if } \rho_{rj} < \rho_{rcj} \\ 1 & \text{if otherwise} \end{cases} \qquad (4)$$

$$i_{\rho hk} = \begin{cases} 0 & \text{if } \rho_{hk} < \rho_{hck} \\ 1 & \text{otherwise} \end{cases} \qquad (5)$$

$$VIL_l = \begin{cases} 1 & \text{if } VIL_l < VIL_{cl} \\ 0 & \text{otherwise} \end{cases} \qquad (6)$$

The conditional expectation of I_s in Eq.(1) is estimated via the following linear estimator:

$$E[I_s \mid I_{rxi} = i_{rxi},\ I_{\rho rj} = i_{\rho rj},\ I_{\rho hk} = i_{\rho hk},\ I_l=i_{vill}\ ;\ i=1,...,n_1,\ j=1,...,n_2,\ k=1,...,n_3,\ l=1,...,n_4]$$

$$= \sum_{i=1}^{n_i} \lambda_{rxi}\, i_{rxi} + \sum_{j=1}^{n_j} \lambda_{\rho rj}\, i_{\rho rj} + \sum_{k=1}^{n_k} \lambda_{\rho hk}\, i_{\rho hk} + \sum_{l=1}^{n_l} \lambda_{VILl}\, i_{VILl} \qquad (7)$$

where λ_{rxi}, $\lambda_{\rho rj}$, $\lambda_{\rho hk}$ and λ_{VILl} denote the weights associated with the indicator variables, i_{rxi}, $i_{\rho rj}$, $i_{\rho hk}$ and i_{VILl}, respectively. The weights are obtained by solving the following indicator version of ordinary kriging (see, e.g., Deutsch and Journel 1991, Seo 1996):

Minimize;

$$J = E[(I_s - I_s^*)^2 \mid I_{rx} = i_{rxi}, I_{\rho r} = i_{\rho rj}, I_{\rho h} = i_{\rho hk}, I_l = i_{vill};\ i=1,...,n_1,\ j=1,...,n_2,\ k=1,...,n_3,\ l=1,...,n_4] \quad (8)$$

subject to;

$$\sum_{i=1}^{n_1} \lambda_{rxi} + \sum_{j=1}^{n_2} \lambda_{\rho rj} + \sum_{k=1}^{n_3} \lambda_{\rho hk} + \sum_{l=1}^{n_4} \lambda_{VILl} = 1 \quad (9)$$

where I_s^* in Eq.(8) is given by Eq.(7). The above constrained minimization is identical to ordinary kriging for which the weights are obtained by solving the following linear system:

$$\begin{bmatrix} \mathbf{Cov(I_{rx},I_{rx})} & \mathbf{Cov(I_{rx},I_{\rho r})} & \mathbf{Cov(I_{rx},I_{\rho h})} & \mathbf{Cov(I_{rx},I_{VIL})} & \mathbf{U_1^T} \\ \mathbf{Cov(I_{\rho r},I_{rx})} & \mathbf{Cov(I_{\rho r},I_{\rho r})} & \mathbf{Cov(I_{\rho r},I_{\rho h})} & \mathbf{Cov(I_{\rho r},I_{VIL})} & \mathbf{U_2^T} \\ \mathbf{Cov(I_{\rho h},I_{rx})} & \mathbf{Cov(I_{\rho h},I_{\rho r})} & \mathbf{Cov(I_{\rho h},I_{\rho h})} & \mathbf{Cov(I_{\rho h},I_{VIL})} & \mathbf{U_3^T} \\ \mathbf{Cov(I_{VIL},I_{rx})} & \mathbf{Cov(I_{VIL},I_{\rho r})} & \mathbf{Cov(I_{\rho h},I_{\rho h})} & \mathbf{Cov(I_{VIL},I_{VIL})} & \mathbf{U_4^T} \\ \mathbf{U_1} & \mathbf{U_2} & \mathbf{U_3} & \mathbf{U_4} & \mathbf{0} \end{bmatrix}$$

$$\bullet \begin{bmatrix} \boldsymbol{\lambda_{rx}} \\ \boldsymbol{\lambda_{\rho r}} \\ \boldsymbol{\lambda_{\rho h}} \\ \boldsymbol{\lambda_{VIL}} \\ \mu \end{bmatrix} = \begin{bmatrix} \mathbf{Cov(I_s,I_{rx})} \\ \mathbf{Cov(I_s,I_{\rho r})} \\ \mathbf{Cov(I_s,I_{\rho h})} \\ \mathbf{Cov(I_s,I_{VIL})} \\ \mathbf{1} \end{bmatrix} \quad (10)$$

In the above, μ is the Lagrange multiplier, $\mathbf{U_1}$, e.g., is the $(1xn_1)$ unit vector; $\mathbf{U_1} = (1,1,..,1)$, $\mathbf{Cov(I_s,I_{rx})}$, e.g., is the (n_1x1) indicator covariance vector; $\mathbf{Cov(I_s,I_{rx})} = [Cov(I_s,I_{rx1}),...,Cov(I_s,I_{rxn1})]^T$, and $\mathbf{Cov(I_{rx},I_{\rho r})}$, e.g., the (n_1xn_2) indicator covariance matrix;

$$\mathbf{Cov(I_{rx},I_{\rho r})} = \begin{bmatrix} Cov(I_{rx1},I_{\rho r1}) & ... & Cov(I_{rx1},I_{\rho rn2}) \\ Cov(I_{rx2},I_{\rho r1}) & ... & Cov(I_{rx2},I_{\rho rn2}) \\ & ... & \\ & ... & \\ Cov(I_{rxn1},I_{\rho r1}) & ... & Cov(I_{rxn1},I_{\rho rn2}) \end{bmatrix} \quad (11)$$

As noted in Seo et al. (2002), the rationale behind the indicator approach is that it approximates multi-variate probability with a set of bivariate probabilities. To illustrate how indicator covariance may describe bivariate probability, we rewrite $Cov(I_s,I_{VIL1})$ in $\mathbf{Cov(I_s,I_{VIL})}$ as:

$$Cov(I_s,I_{VIL1})$$

$$= E[I_s\, I_{VIL1}] - E[I_s]\, E[I_{VIL1}] \quad (12a)$$

$$= \text{Prob[Bin} \in \text{stratiform,}\ _{\text{VIL}} < _{\text{VILc1}} \text{] - Prob[Bin} \in \text{stratiform] Prob[}\ _{\text{VIL}} < _{\text{VILc1}} \text{]} \quad (12b)$$

$$= \{ \text{Prob[Bin} \in \text{stratiform} \mid _{\text{VIL}} < _{\text{VILc1}} \text{] - Prob[Bin} \in \text{stratiform]} \} \text{ Prob[}\ _{\text{VIL}} < _{\text{VILc1}} \text{]} \quad (12c)$$

Note that, if VIL is indeed a skillful attribute for discriminating convective cores from stratiform areas (or vice versa), the conditional probability, Prob[Bin $\in$ stratiform | $_{\text{VIL}} < _{\text{VILc1}}$], should be greater than the unconditional probability, Prob[Bin $\in$ stratiform], thus resulting in a positive indicator covariance. If only one attribute is considered (e.g., VIL only in the VIL only-based CSSA), it can be easily shown that the above formulation is reduced to simple thresholding; i.e., the azran bin is in the convective core if VIL $\geq$ VIL_c, and in the stratiform region if VIL $<$ VIL_c.

2.3 Estimation of Indicator Statistics

CSSA as described above requires specification of the indicator statistics in Eq.(10). Ideally, the statistics should be estimated from a large sample in a site- and seasonality-specific manner. Because estimation of the indicator statistics in the right-hand side of Eq.(10) requires ground-truthing (i.e. having to identify where the 'true' convective cores are: see Eq.(2)), large-sample estimation of indicator statistics may not be considered operationally viable. As such, the approach taken in Seo et al. (2002) and as here is to estimate the indicator statistics from a small but 'informative' sample. Such a sample should contain, in the least, a precipitation event with widespread, well-developed and clearly distinguishable areas of convective and stratiform precipitation. As in Seo et al. (2002), we use the southern plains squall line at KINX (Tulsa, OK) (see Table 1) for this. The particular data set used to estimate the statistics are the volume scans 240, 245, 255 and 265 of KINX_N04206: see Seo et al. 2002 for reflectivity maps).

The choice for the above particular set of volume scans is based on extensive sensitivity analysis involving the following steps: 1) select a set of volume scans, 2) estimate the indicator statistics, 2) run CSSA-RCA for the KINX case, 3) examine the results, 4) repeat Steps 2 and 3 with a different set of thresholds, and 5) repeat Steps 1 through 4 with different set of volume scans. In ground-truthing convective and stratiform areas, it was assumed that all azran bins with VIL < 6 kg/m^2 in the trailing stratiform region of the precipitation field are 'truly' stratiform (even though the rest of the bins in the trailing stratiform region, i.e., those with VIL > 6 kg/m^2, are, naturally, also 'truly' stratiform). The reason for this apparent self-contradiction is that the extremely intense brightband enhancement seen in KINX_N04206 (exceeding r_x of 50 (dBZ) and VIL of 10 (kg/m^2) in some areas) is rather rare (in the southern plains or elsewhere) and hence is not very representative. (Increasing the VIL threshold in ground-truthing, so that all trailing stratiform region is identified as 'true' stratiform, does not help the situation because it tends to deteriorate the overall performance of CSSA.) Throughout this work, the number of thresholds chosen for the attributes is 3 for all; i_{rxc1} = 38 (dBZ), i_{rxc2} = 40 (dBZ), i_{rxc3} = 42 (dBZ), $i_{\rho r1}$ = 0.97, $i_{\rho r2}$ = 0.98, $i_{\rho r3}$ = 0.99, $i_{\rho h1}$ = 0.9, $i_{\rho h2}$ = 0.99, and $i_{\rho h3}$ = 0.999, i_{VIL1}=5.5 (kg m^{-2}), i_{VIL2}=6.0 (kg m^{-2}), i_{VIL3}=6.5 (kg m^{-2}).

2.4 Evaluation and Results

To evaluate the performance of CSSA-RCA, the following experiment was performed: 1) perform convective-stratiform separation using the full CSSA, 2) estimate/update the mean vertical profile of reflectivity (VPR) using the volume scan reflectivity data only from the area identified as stratiform, 3) apply the mean VPR-derived adjustment factors to the reflectivity data in the stratiform area only, convert reflectivity in all areas to rainfall, and accumulate rainfall in all areas, 4) repeat Steps 1 through 3 for all volume scans over the period of interest, 5) repeat the above steps using the VIL-only CSSA, and 6) repeat all of the above steps for the seven cases listed below (a subset of the twelve used in Seo et al. 2002). Note that, from the list of twelve, we deliberately excluded the pure stratiform cases for which both the VIL-only and the full CSSA perform very well (Seo et al. 2002) and hence of little interest from the CSSA-RCA evaluation point of view.

Because of other (i.e. than VPR effects) significant sources of error in radar rainfall estimation that are not accounted for in this work, quantitative evaluation of CSSA-RCA using rain gauge data is rather difficult and is left as a future endeavor. Here, we focus on evaluating the performance of CSSA-RCA in all phases of the algorithm based on careful visual examination of both the intermediate results and the final rainfall maps, as described below in some detail. Except as shown for the KINX development data figures, each case is described by the same set of figures.

The 'VIL' field (see, e.g., Fig.1) is simply the field of vertically-integrated liquid water (in kg/m^2) as mapped onto the base elevation angle. The Z-M conversion relationship used is the WSR-88D default, $M=3.44x10^{-6}Z^{4/7}$ where Z is the reflectivity factor in $mm^6\ m^{-3}$ and M is the liquid water content in $kg\ m^{-3}$

The 'VIL-only CSSA' field (see, e.g., Fig. 2) is the binary rendition of the VIL field based on the threshold of 6 kg/m^2: the red and cyan represent the areas identified as convective and stratiform, respectively.

The first 'full CSSA' field (see, e.g., Fig. 3) represents the field of conditional probability, as estimated by the 4-attribute CSSA (see above), that the particular azran bin is in the convective area. The larger/smaller the probability is, the more/less likely that the bin is in the convective area. Because the level of skill that each attribute contributes to the separation depends, to a varying degree, on the slant range and the density of the Volume Coverage Pattern (VCP) (an aspect not accounted for in the current algorithm), and because the correlation attributes, ρ_r and ρ_h, are susceptible to data quality (Seo et al. 2002), it is not to be expected that the spatial pattern of conditional probability is reasonable everywhere. Our primary interest is rather in the discriminatory skill that the conditional probability may possess in separating the convective and stratiform areas.

The second 'full CSSA' field (see, e.g., Fig. 4) is the same as the first, except that a threshold probability of 0.80 is used to separate the convective (in magenta) and stratiform (in cyan) areas. The threshold probability is tied to the particular data set used in the estimation of the indicator statistics and hence is a constant (i.e. as long as the same statistics are used). The choice of 0.80 is based on the sensitivity analysis described above. This yes/no field is referred to as the "categorical" CSSA.

The 6-panel xy-plots for 'VIL-only CSSA' (see, e.g., Fig. 5) shows; **(top-left)** the reflectivity factor ($mm^6\ m^{-3}$)-vs-height (km) display of the individual data points from the area identified as stratiform in the current volume scan by the VIL-only CSSA, **(top-center)** the estimated true (in solid line) and apparent (in dotted line) mean VPRs in the stratiform area, **(top-right)** the estimated error standard deviation associated with the estimated true mean VPR in the stratiform area, **(bottom-left)** the adjustment factor derived from the estimated true mean VPR in the stratiform area as a function of slant range in the first elevation angle, **(bottom-center)** the same as bottom-left but in the second elevation angle, and **(bottom-right)** the same as bottom-left but in the third elevation angle.

The 6-panel xy-plots for 'full CSSA' (see, e.g., Fig. 6) is the same as that for VIL-only CSSA, except that the full CSSA is used to identify the stratiform area.

The 'w/o RCA' field (see, e.g., Fig.7) represents the rainfall map (see Table 1 for the accumulation duration) as estimated without CSSA or RCA. It is generated not by the WSR-88D Precipitation Processing Subsystem (PPS, Fulton et al. 1998) but by applying the convective Z-R relationship to the Level II reflectivity data and accumulating in time. There were no quality control steps except for the hail cap of 56 dBZ.

The 'w/RCA, full CSSA' field (see, e.g., Fig. 8) represents the rainfall map for the same duration as estimated by the full CSSA-RCA: i.e., for each volume scan, run the full CSSA and identify the stratiform area, estimate/update the mean VPR from the stratiform area only, apply the mean VPR-derived adjustment factors to the stratiform area only, and accumulate rainfall in all areas. Note that, because no adjustments are made to the areas identified as convective, the 'w/RCA, full CSSA' field should be identical to the 'w/o RCA' field in those areas that are identified as convective throughout the accumulation duration.

The 'w/RCA, VIL-only CSSA' field (see, e.g., Fig.9) is generated in the same way as the 'w/RCA, full CSSA' field except that VIL-only CSSA is used in place of the full CSSA.

The 'Subtracted by RCA, full CSSA' field (see, e.g., Fig.10) represents the rainfall amounts subtracted by RCA based on the full CSSA. Typically, the area of subtraction corresponds to the area of brightband enhancement (i.e. where the base elevation angle intercepts the melting layer in the stratiform region).

The 'added by RCA, full CSSA' field (see, e.g., Fig.11) represents the rainfall amounts added by RCA based on the full CSSA. Typically, the area of addition is at the farthest ranges where the base elevation angle samples the ice particles above the freezing level.

The 'Subtracted by RCA, VIL-only CSSA' field (see, e.g., Fig.12) is the same as the 'Subtracted by RCA, full CSSA' field except that the VIL-only CSSA is used in place of the full CSSA.

The 'Added by RCA, VIL-only CSSA' field (see, e.g., Fig.13) is the same as the 'Added by RCA, full CSSA' field except that the VIL-only CSSA is used in place of the full CSSA.

Table 1. List of cases.

Identifier	Site	Tape #	Date	Storm Type	Used For
KDDC[1]	Dodge City, KS	N01158	7/14/93	organized-convective	validation
KEVX[2]	Eglin AFB, FL	N09652	10/4/95	hurricane (Opal)	validation
KFDR[3]	Frederick, OK	N01114	5/9/93	squall line	validation
KHGX[4]	Houston, TX	N02961	10/17/94	organized-convective	validation
KINX[5]	Tulsa, OK	N04206	5/8/95	squall line	calibration
KMLB[6]	Melbourne, FL	A20054	3/25/92	chaotic-convective	validation
KOKX[7]	New York, NY	N23993	10/19/96	stratiform	validation

[1] Volume Scans 240 through 292
[2] Volume Scans 81 through 216
[3] Volume Scans 41 through 96
[4] Volume Scans 11 through 100
[5] Volume Scans 236 through 312
[6] Volume Scans 60 through 119
[7] Volume Scans 21 through 85

2.4.1 KDDC (Dodge City, KS)

Figs. 2 and 4 show that the area identified as convective by the full CSSA is larger than that by the VIL-only CSSA. The top-left panels in Figs. 5 and 6 indicate that the VIL-only CSSA significantly under-delineates convective areas (probably from misidentifying the convective areas as stratiform in the fringes of high-VIL cores). The full CSSA too under-delineates convective areas but to a significantly lesser extent. The top-center panels in Figs. 5 and 6 show that the mean VPR based on the full CSSA exhibits the familiar stratiform profile, whereas that based on the VIL-only CSSA is significantly biased near the surface due to the under-delineation of convective areas. The bottom panels in Figs. 5 and 6 show that the adjustment factors derived from the two profiles are very much different, due in large part to the biased near-surface profile from the VIL-only CSSA. Figs. 7 through 13 suggest that the VIL-only CSSA tends to under-correct overestimation of rainfall due to brightband enhancement and over-correct far-range underestimation of rainfall due to sampling of ice particles. That the VIL-only CSSA under-delineates convective areas may also be seen in Fig.12 in which 'streaky' areas of subtraction may be observed (an impossible signature for brightband enhancement).

2.4.2 KEVX (Eglin AFB, FL)

This is a pure tropical rainfall case (Hurricane Opal), and hence convective-stratiform separation does not apply. In practice, the adjustment factors will have to be estimated from the entire radar umbrella without CSSA. Nevertheless, we apply CSSA-RCA here as a way of assessing robustness of the procedure. The unadjusted rainfall map (see Fig. 21) suggests far-range underestimation of rainfall (note the suddenly diminishing rainfall pattern near the farthest ranges in individual rainbands). In this case, RCA based on the full CSSA (see Fig. 22) results in deterioration of far-range underestimation, whereas RCA based on the VIL-only CSSA (see Fig. 23) improves rainfall estimation. The reason for the improvement is that the VIL-only CSSA significantly under-delineates convective areas (see Fig.15) and, as such, the mean VPR based on the VIL-only CSSA (see Fig.18) is not very different from the mean VPR over the entire radar umbrella (see Fig.20). Accordingly, the adjusted rainfall map based on the VIL-only CSSA (see Fig.23) is close to that without CSSA (see Fig.24). This case suggests that, in cases of pure tropical rainfall, CSSA should be bypassed and mean VPR should be estimated from the entire radar umbrella.

2.4.3 KFDR (Frederick, OK)

Figs. 31 and 32 indicate that the VIL-only CSSA under-delineates convective areas. The difference between the VIL-only and the full CSSA results, however, is not significant and the two resulting adjusted rainfall maps (see Figs. 34 and 35) are rather similar. As in KDDC, the 'streaks' in the areas of subtracted rainfall based on the VIL-only CSSA point to under-delineation of convective areas by the VIL-only CSSA.

2.4.4 KHGX (Houston, TX)

This case also indicates under-delineation of convective areas by the VIL-only CSSA. It introduces significant biases in mean VPR below approximately 3.5 km (see Fig. 44), and produces adjustment factors that are very much different from those based on the full CSSA (see Fig. 45). Figs. 46 through 52 indicate that such biases have rather large impact on rainfall accumulations: note in Fig. 48 the gross overestimation of rainfall based on the VIL-only CSSA. This case illustrates the rather stringent accuracy requirement for CSSA to realize consistently positive impact of CSSA-RCA on radar rainfall estimation.

2.4.5 KINX (Tulsa, OK)

This is the squall line case used to estimate the indicator statistics (Volume Scan 265, on which Figs. 53 through 58 are based, is one of the four volume scans used in the estimation of indicator statistics). As such, this case represents calibration rather than validation. Figs. 57 and 58 indicate that the VIL-only CSSA slightly underestimates the convective areas, resulting in comparably biased mean VPRs both below and above the freezing level. The impact of this bias on rainfall accumulation is that, compared to the full CSSA, the VIL-only CSSA under-corrects brightband enhancement and over-corrects far-range underestimation of precipitation (see Figs. 75 through 81). Figs. 59 through 74 capture the passage of the trailing stratiform region, and illustrate some of the difficulties associated with convective-stratiform separation. Note that, even in stratiform precipitation, VIL can easily exceed 6 kg/m^2 over a large area. Increasing the VIL threshold to improve identification of stratiform areas, however, necessarily deteriorates identification of convective areas. The full CSSA, owing to its multi-attribute nature, is less susceptible to large VIL in the stratiform region, but suffers from misidentification of stratiform areas at close ranges. This tendency to misidentify stratiform as convective at close ranges is due to the range-dependency of the attributes: at close ranges, the sampling volume associated with reflectivity measurements is significantly smaller, resulting in biased estimates of the attributes. It is expected that the range dependency may be reduced by explicitly accounting for the differences in the sampling volume.

2.4.6 KMLB (Melbourne, FL)

This is a pure convective case, and hence convective-stratiform separation does not apply. As in KEVX, however, we ran CSSA-RCA to assess the robustness of the procedure. Figs. 82 through 85 show that the full CSSA correctly identifies (as convective) most of the areas of significant rainfall whereas the VIL-only CSSA significantly under-delineates convective areas. Figs. 86 and 87 show that the under-delineation results in the adjustment factors from the VIL-only CSSA being significantly larger than those from the full CSSA even in mid-ranges. The rainfall maps (Figs. 88 through 94) based on both adjustments are not unrealistic. It is not clear, however, whether either adjustment offers an improvement over the other, or over the unadjusted.

2.4.7 KOKX (Brookhaven, NY)

This is largely a stratiform case with embedded lines of moderate convection. Figs. 99 indicates that the VIL-only CSSA under-delineates the convective areas, resulting in a modest bias in the mean VPR near the surface and larger adjustment factors at far ranges (see Figs. 100 and 101). The reflectivity-vs-height scatter-plots (the top-left panels in Figs. 100 and 101) show that the full CSSA is more successful, though not completely, in screening out convective areas. The adjusted rainfall maps based on the VIL-only and the full CSSA are rather similar, with the VIL-only probably mis-subtracting some rainfall from the lines of convection that are misidentified as stratiform (see Fig. 106). It is worth noting in Figs. 101 through 103 that the difference between the unadjusted and the adjusted rainfall maps is rather striking and serves to illustrate the importance of CSSA-RCA in radar rainfall estimation.

2.5 Summary, Conclusions and Recommendations

The Convective-Stratiform Separation Algorithm (CSSA, Seo et al. 2002) has been extended to include vertically-integrated liquid water (VIL) as an additional predictor attribute. The resulting 4-attribute CSSA is evaluated in multiple case studies by feeding the separation results to the Range-dependent bias Correction Algorithm (RCA, Seo et al. 2000). Because VIL is an existing WSR-88D product, VIL-only based stratiform-convective separation, if found viable, may be a significantly less expensive alternative to the full CSSA. To assess performance of the VIL-only CSSA, the two are inter-compared in the multiple case studies.

The major conclusions and recommendations drawn from this work are as follows:

Performance of the Range-dependent bias Correction Algorithm (RCA) is sensitive to that of the Convective-Stratiform Separation Algorithm (CSSA). For RCA to operate as an all-season and all-storm type application, reliable high-level performance of CSSA is essential.

Performance of the 'full' CSSA, which uses four different attributes as predictors, is generally satisfactory whereas that of the 'VIL-only' CSSA, which uses VIL as the sole predictor, is not. As such, implementation of the VIL-only CSSA as an interim alternative is not recommended.

Range dependency of the predictor attributes is found to be one of the factors adversely affecting the performance of CSSA. Improvements are recommended to reduce such range dependency and to employ efficient computational schemes for evaluation of local-statistical attributes.

Though the performance of CSSA is generally satisfactorily for a wide range of storms, it is less robust for certain types of storms, including purely tropical and purely convective. Further case studies, both historical and real-time, are recommended to further mature the algorithm and the operations concept and to develop specific operational guidance.

REFERENCES

Deutsch, C. V., and Journel, A. G., 1992: *GSLIB Geostatistical software library and users' guide*. Oxford University Press.

Fulton, R. A., J. P. Breidenbach, D-J. Seo, D. A. Miller, and T. O'Bannon, The WSR-88D rainfall algorithm. *Wea. Forecasting*, **13**, 377-395, 1998.

Fulton, R., D. Miller, J. Breidenbach and D.-J. Seo, 2001: Final Report Interagency MOU among the NEXRAD Program, The WSR-88D Radar Operations Center, and The NWS Office of Hydrologic Development. Hydrology Laboratory, Office of Hydrologic Development, National Weather Service, Silver Spring, MD.

Seo, D.-J., 1996: Nonlinear estimation of spatial distribution of rainfall - An indicator cokriging approach. *Stoch. Hydrol. Hydraul.*, **10**, 127-150.

_____, J. P. Breidenbach, R. A .Fulton, D. A. Miller, and T. O'Bannon, 2000: Real-time adjustment of range-dependent biases in WSR-88D rainfall data due to nonuniform vertical profile of reflectivity, *J. Hydrometeorol.***, 1(3)**, 222-240.

_____, F. Ding and R. Fulton, 2002: Final Report Interagency MOU among the NEXRAD Program, The WSR-88D Radar Operations Center, and The NWS Office of Hydrologic Development. Hydrology Laboratory, Office of Hydrologic Development, National Weather Service, Silver Spring, MD.

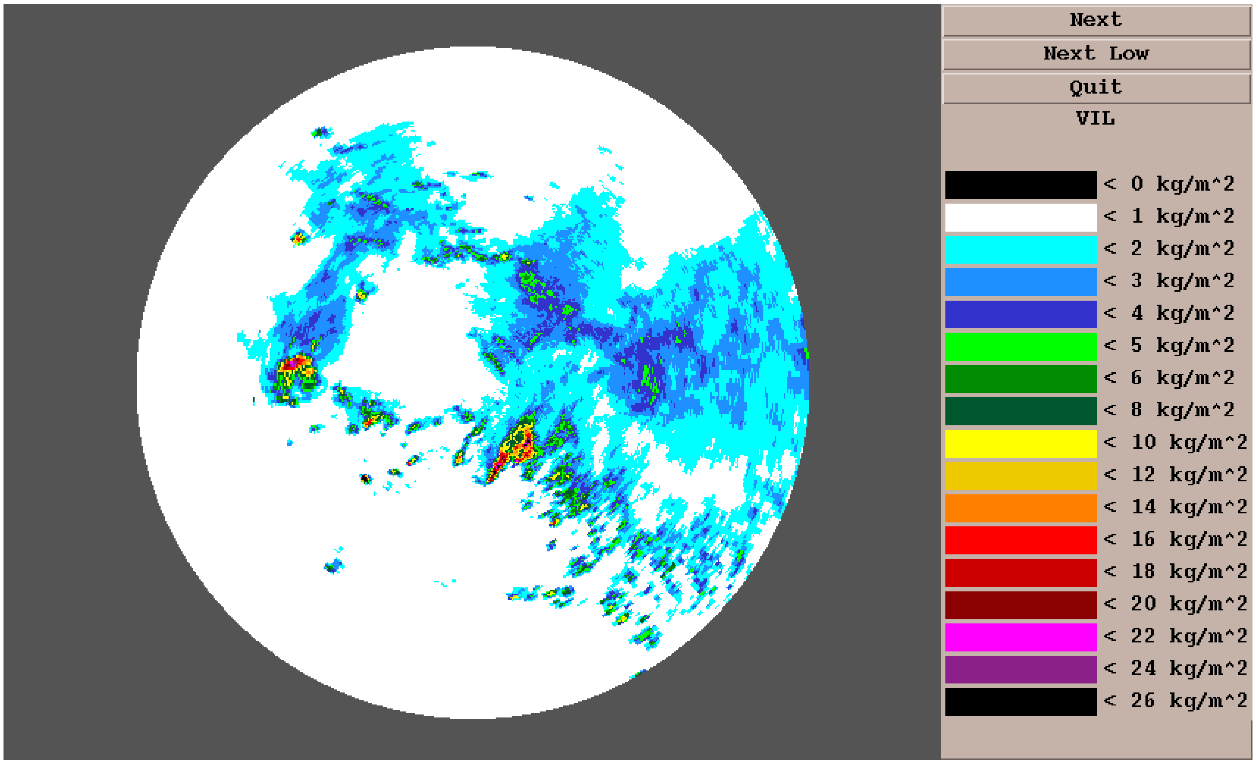

Figure 1. Vertically-integrated liquid (VIL) within KDDC umbrella, 14 July 1993.

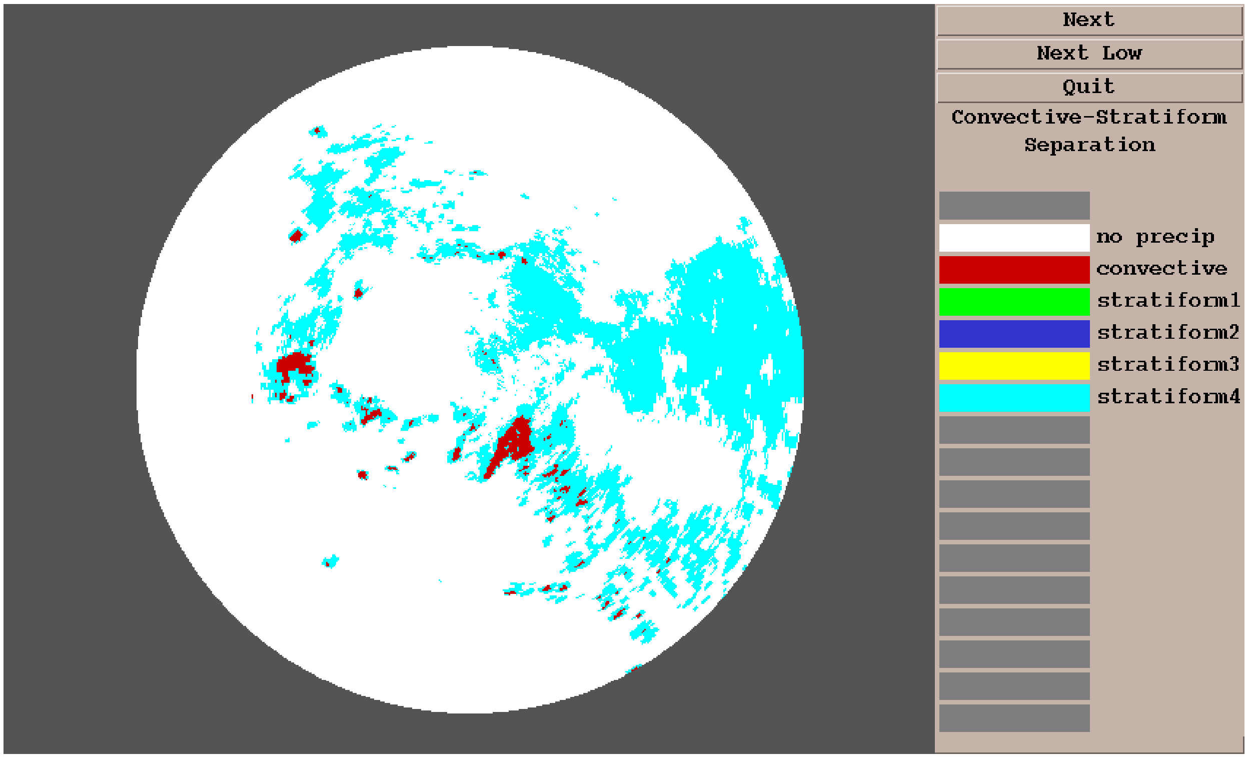

Figure 2. Convective-stratiform separation (CSSA) algorithm output based only on VIL, KDDC umbrella, corresponding to image in Fig. 1.

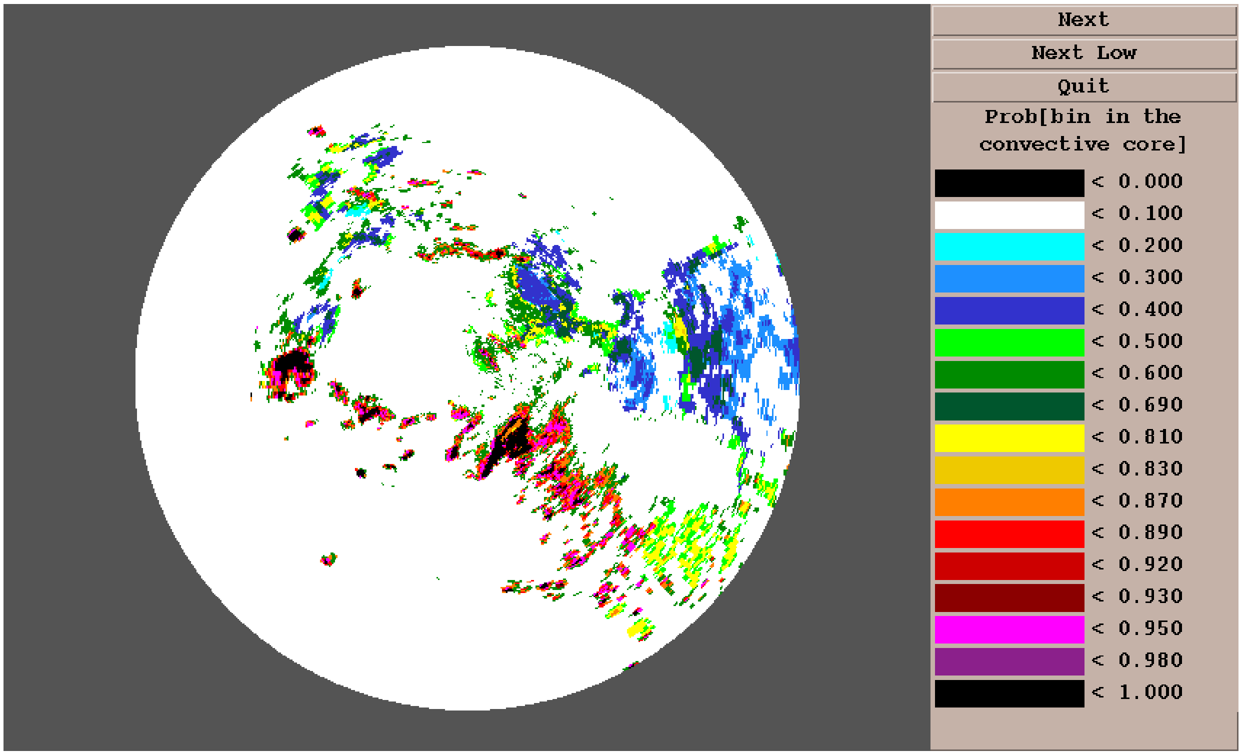

Figure 3. As in Fig. 2, except full-predictor CSSA output corresponding to field in Fig. 1.

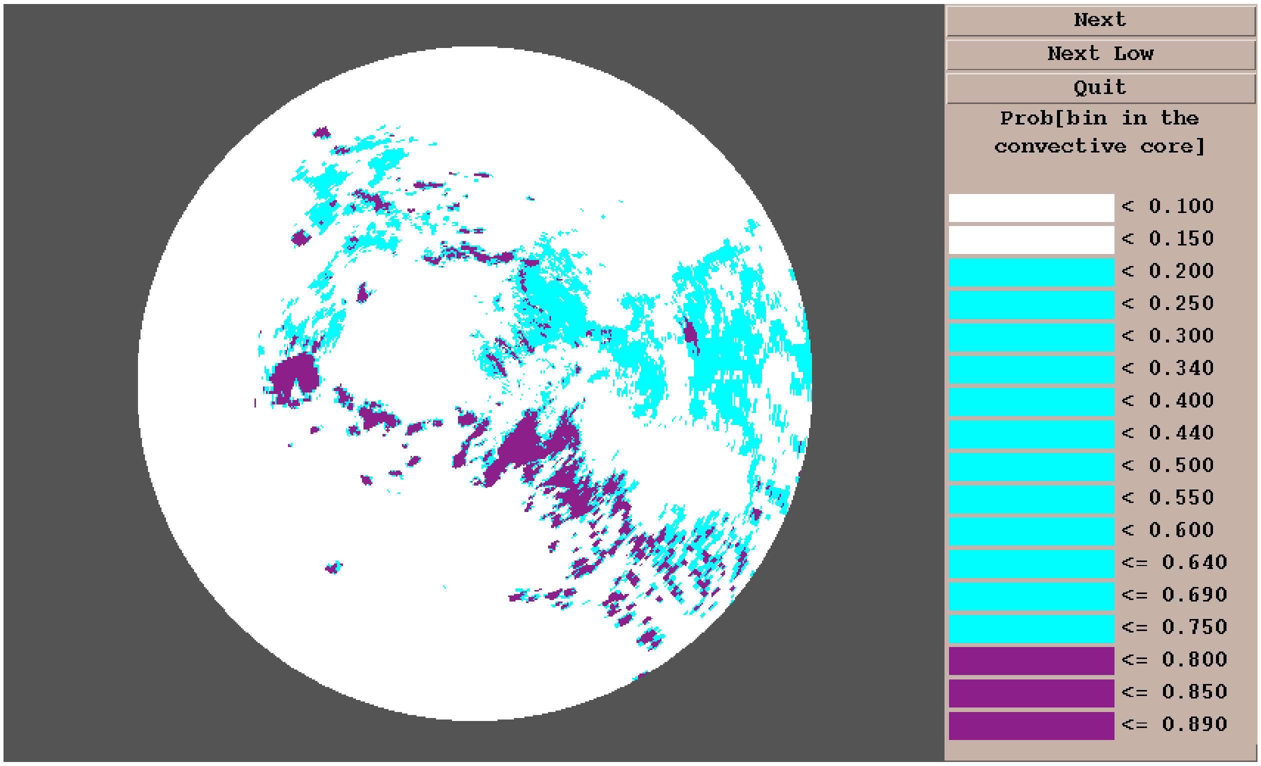

Figure 4. Categorical CSSA corresponding to continuous values shown in Fig. 3.

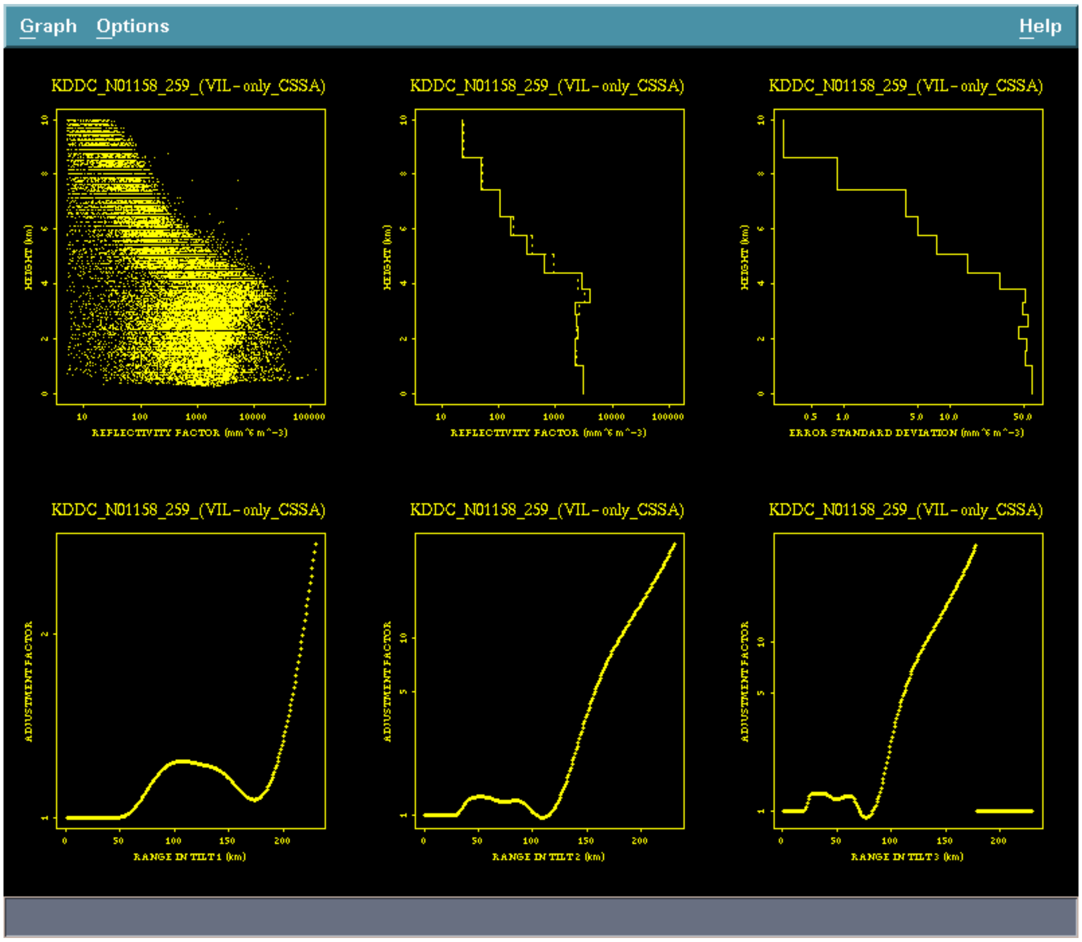

Figure 5. Vertical profile of reflectivity (VPR) and adjustment-factor curves based on VIL-only CSSA, for KDDC.

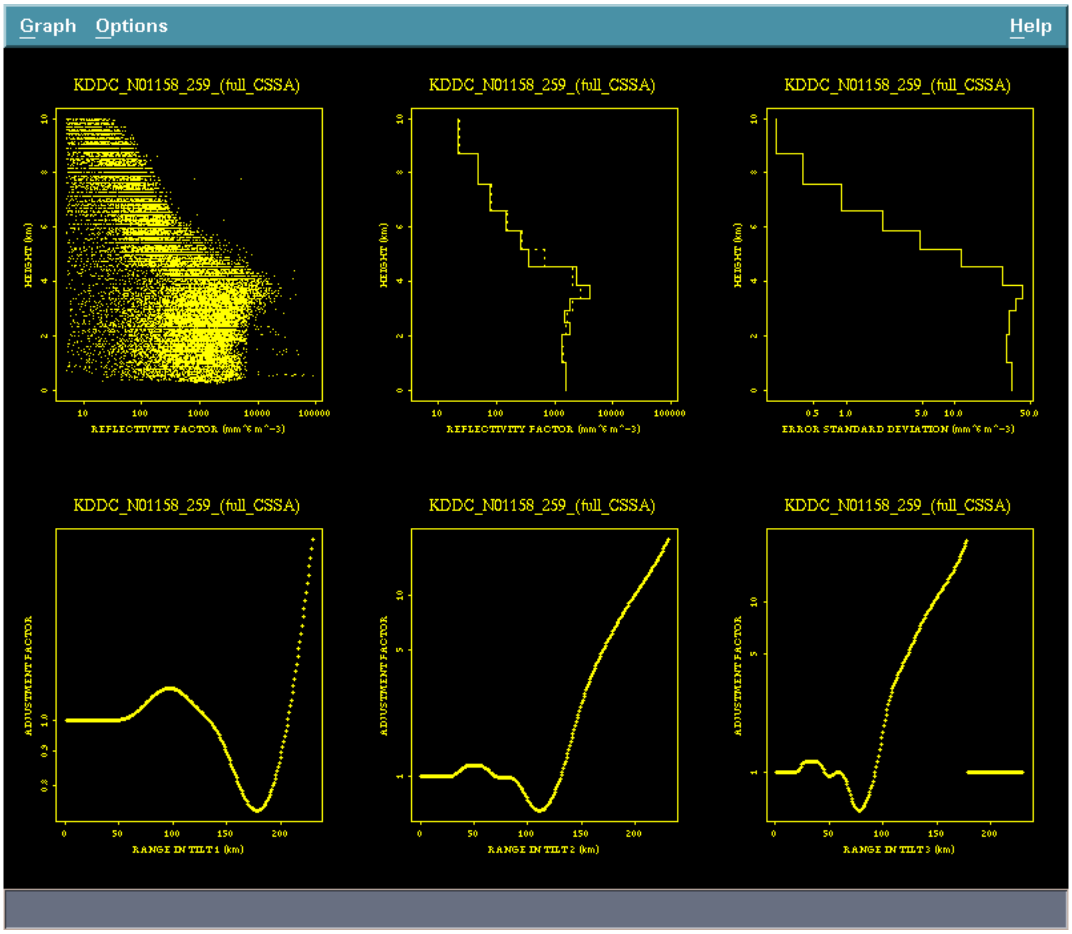

Figure 6. Vertical profile of reflectivity (VPR) and adjustment-factor curves based on full-predictor CSSA, for KDDC

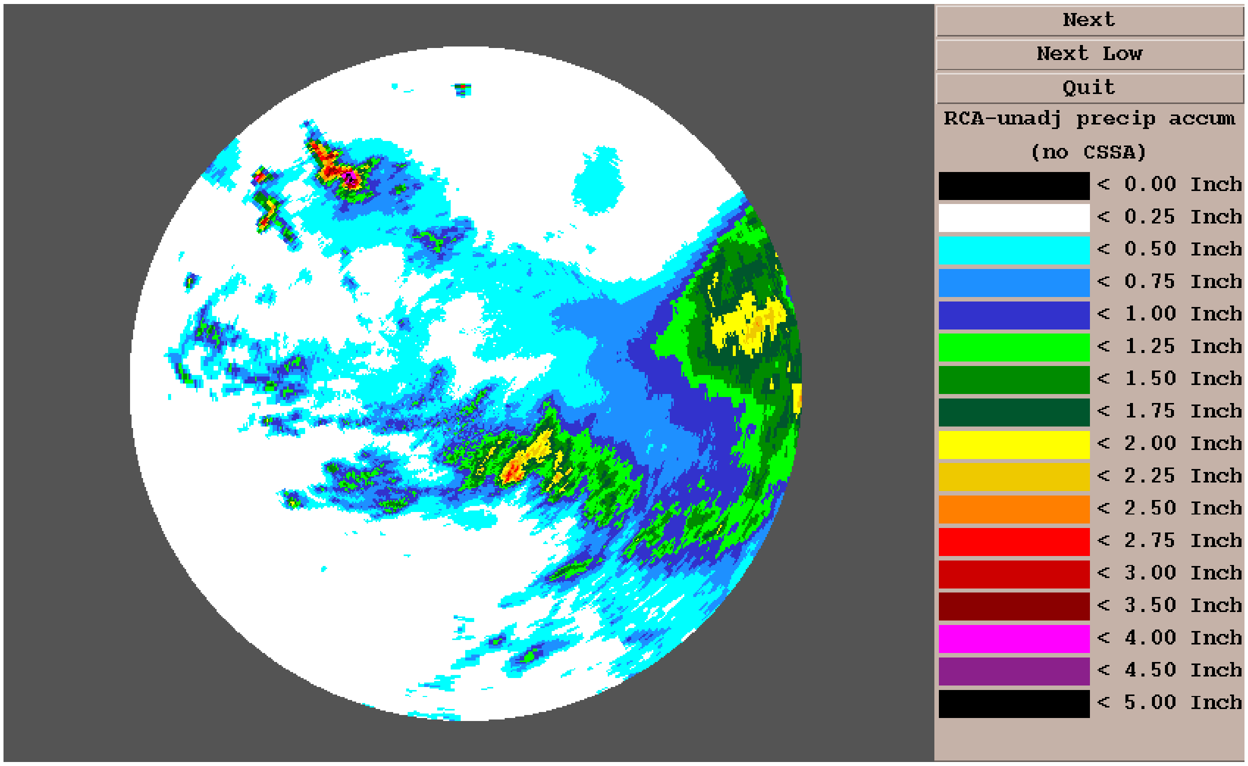

Figure 7. Rainfall estimates for KDDC umbrella over ~5 h, 14 July 1993, without range correction.

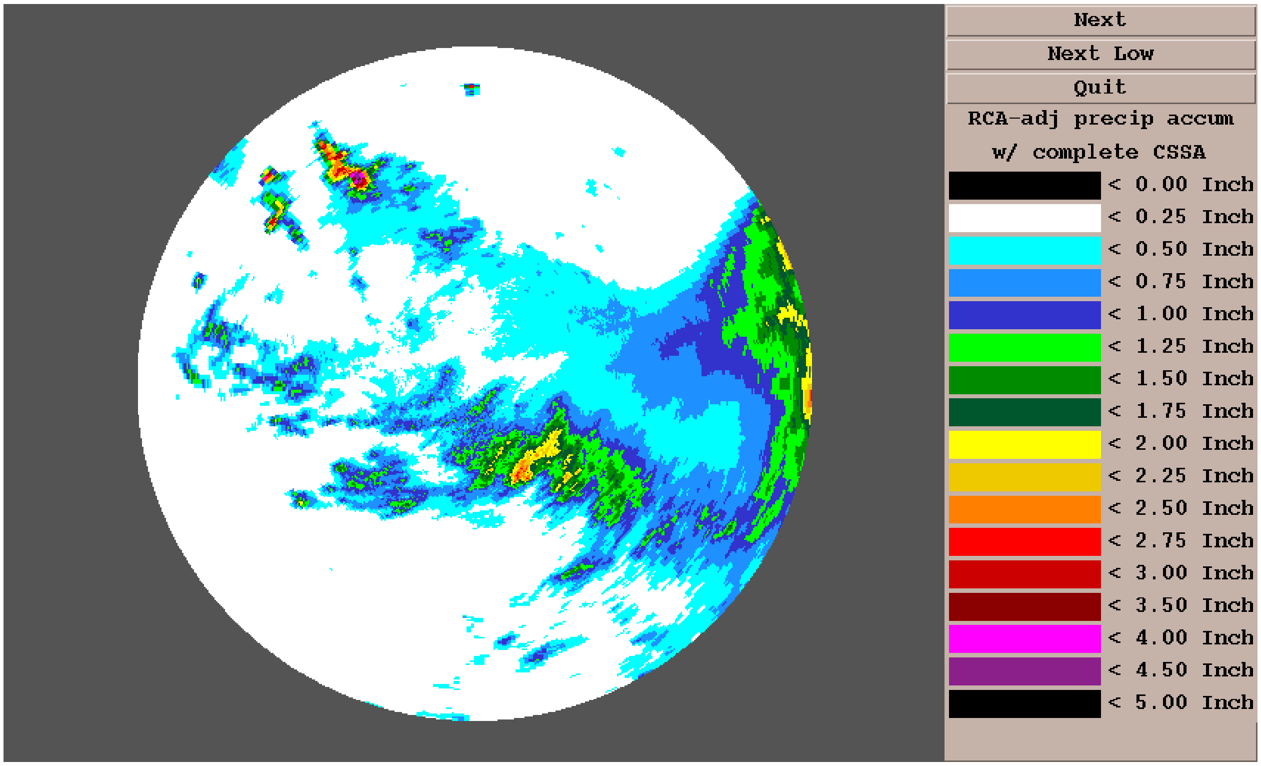

Figure 8. As in Fig. 7, except rainfall with with range correction algorithm, full CSSA applied.

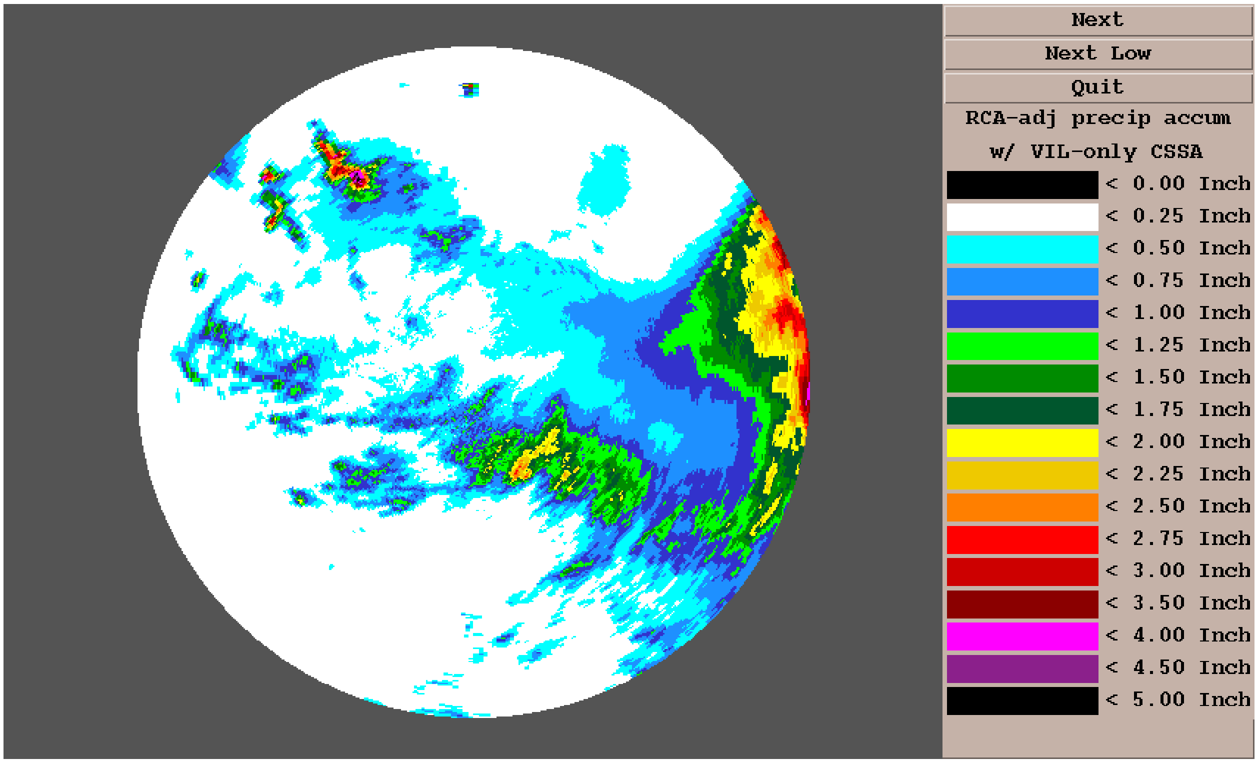

Figure 9. As in Fig. 7, except with range correction with VIL-only CSSA applied.

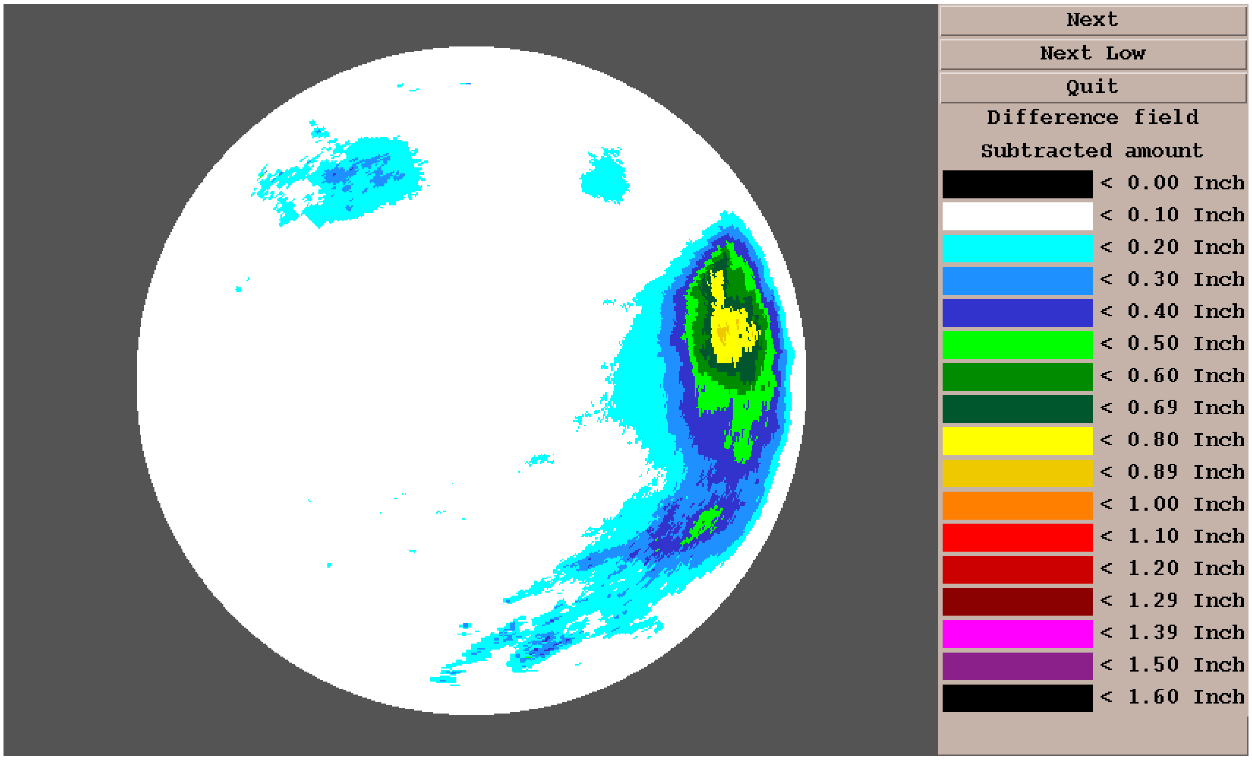

Figure 10. Position and amount of rainfall apparently subtracted by RCA/full CSSA, corresponding to Figs. 7 and 8.

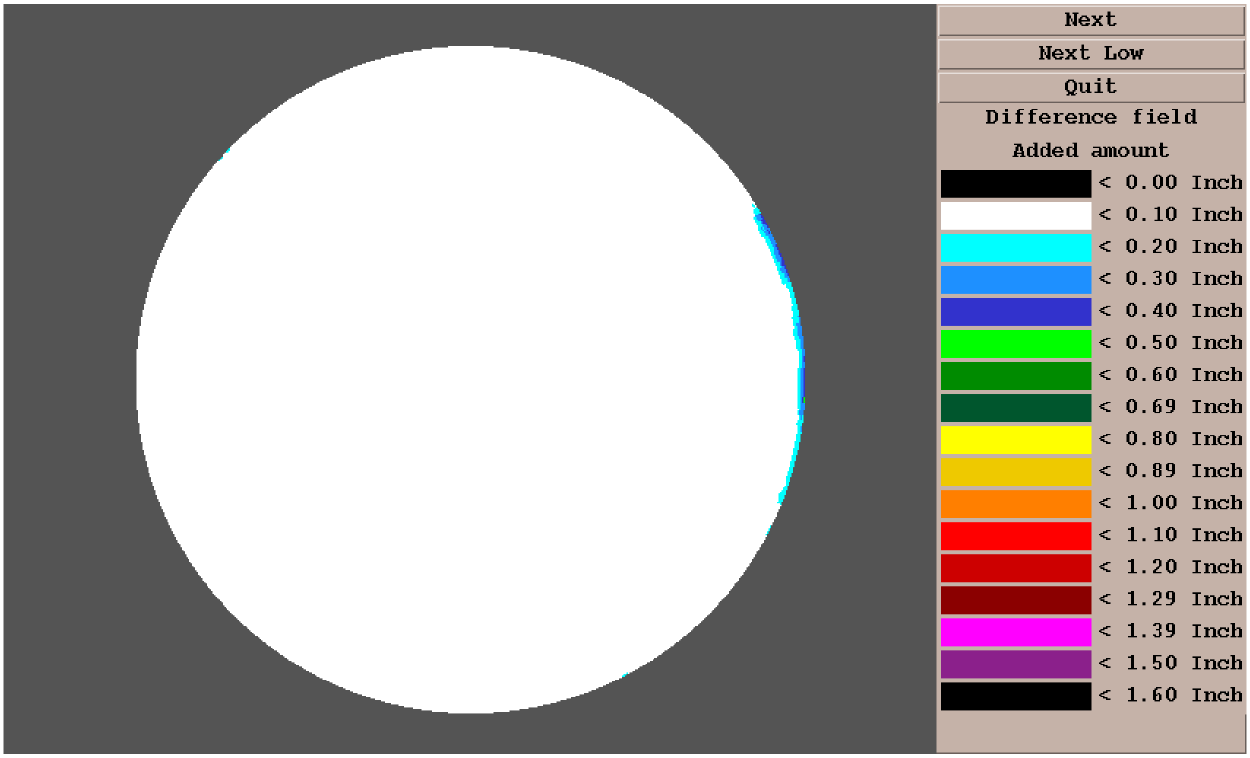

Figure 11. Position and amount of rainfall apparently added by RCA/full CSSA, corresponding to Figs. 7 and 8. Addition took place near 230-km limit, eastern quadrant.

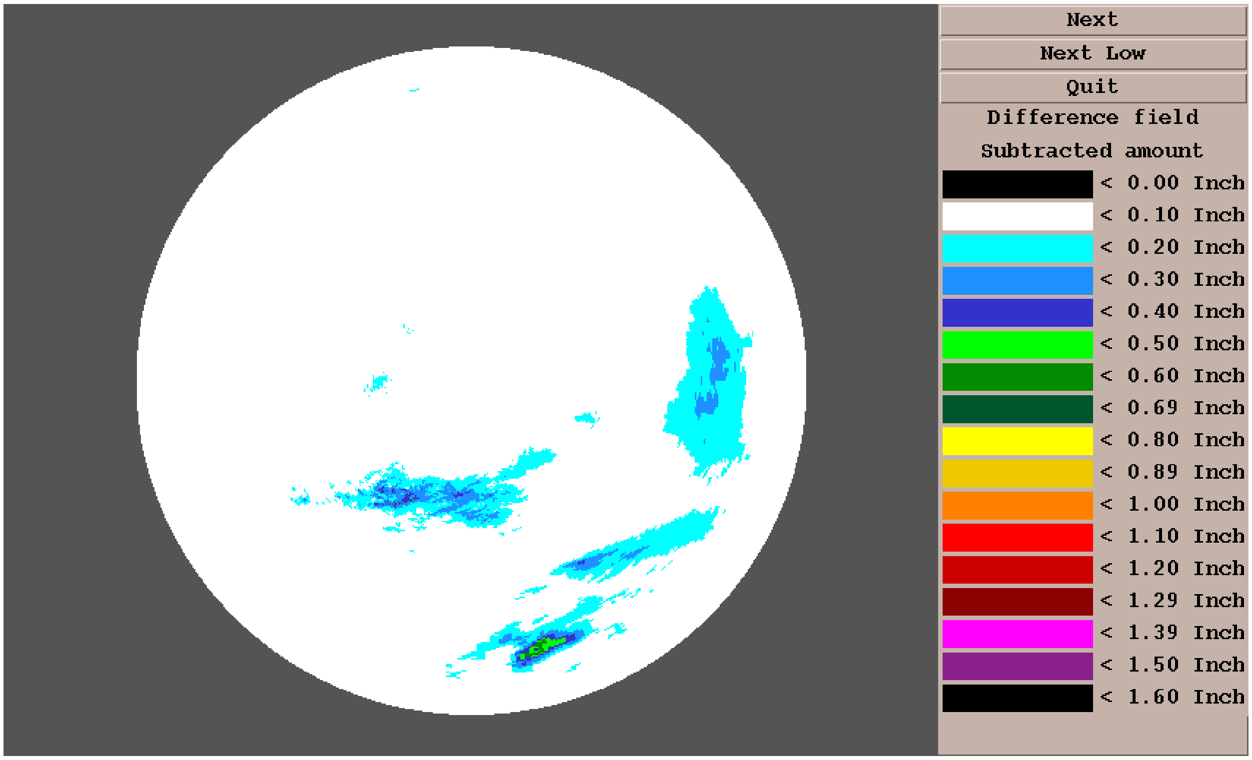

Figure 12. As in Fig. 10, except for CSSA/VIL-only.

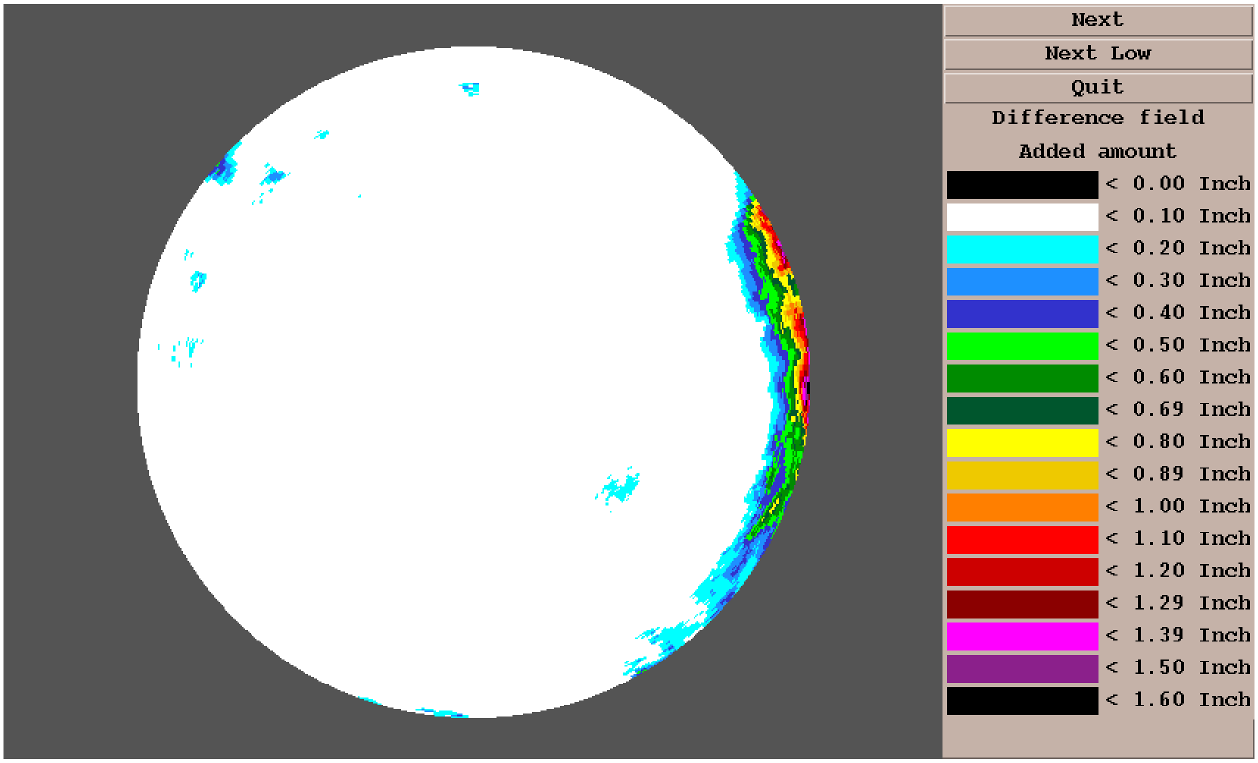

Figure 13. As in Fig. 11, except for RCA/VIL-only.

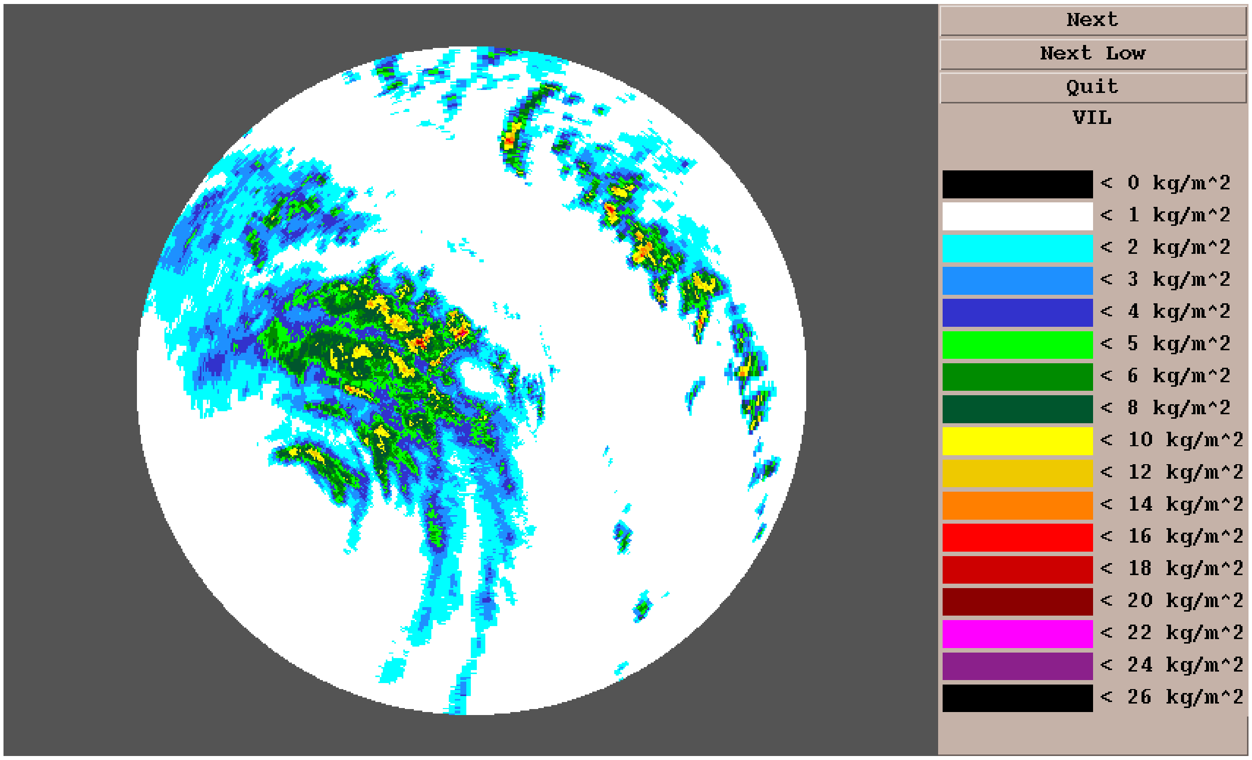

Figure 14. VIL field in KEVX umbrella, 4 October 1995.

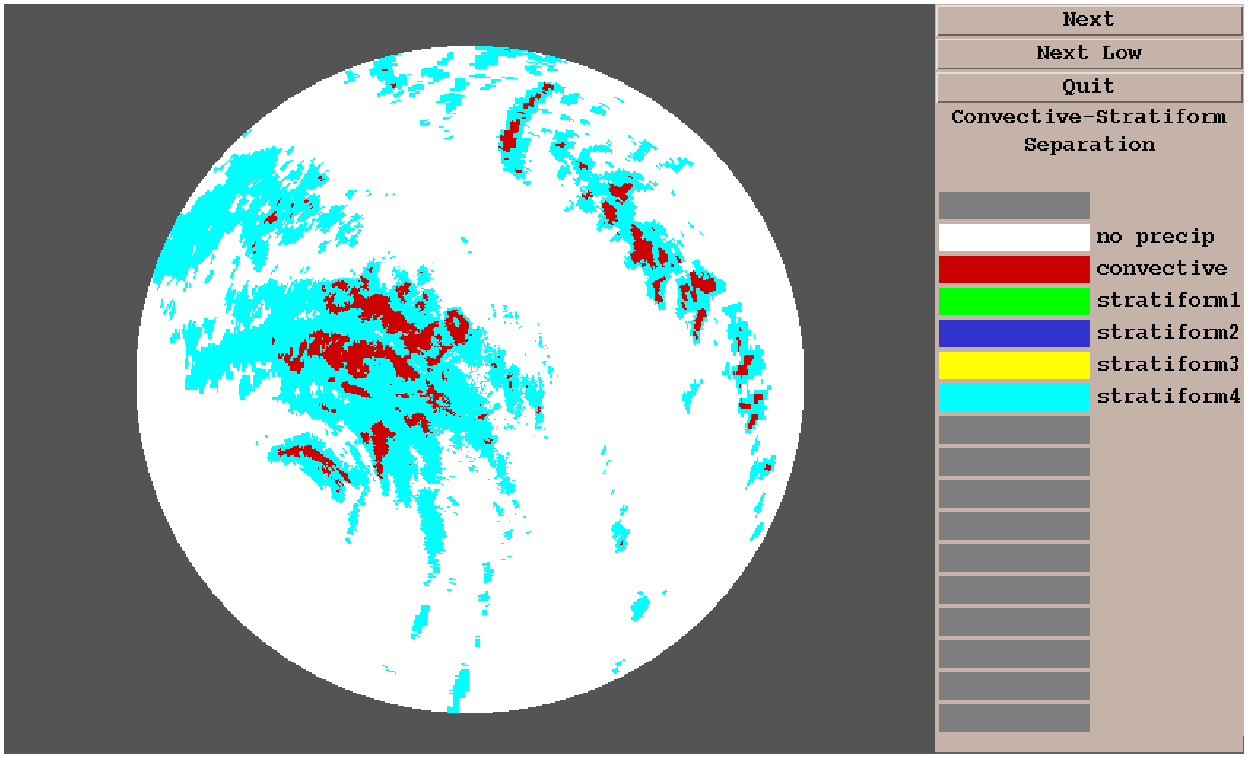

Figure 15. Output of CSSA/VIL-only, KEVX umbrella, 4 October 1995.

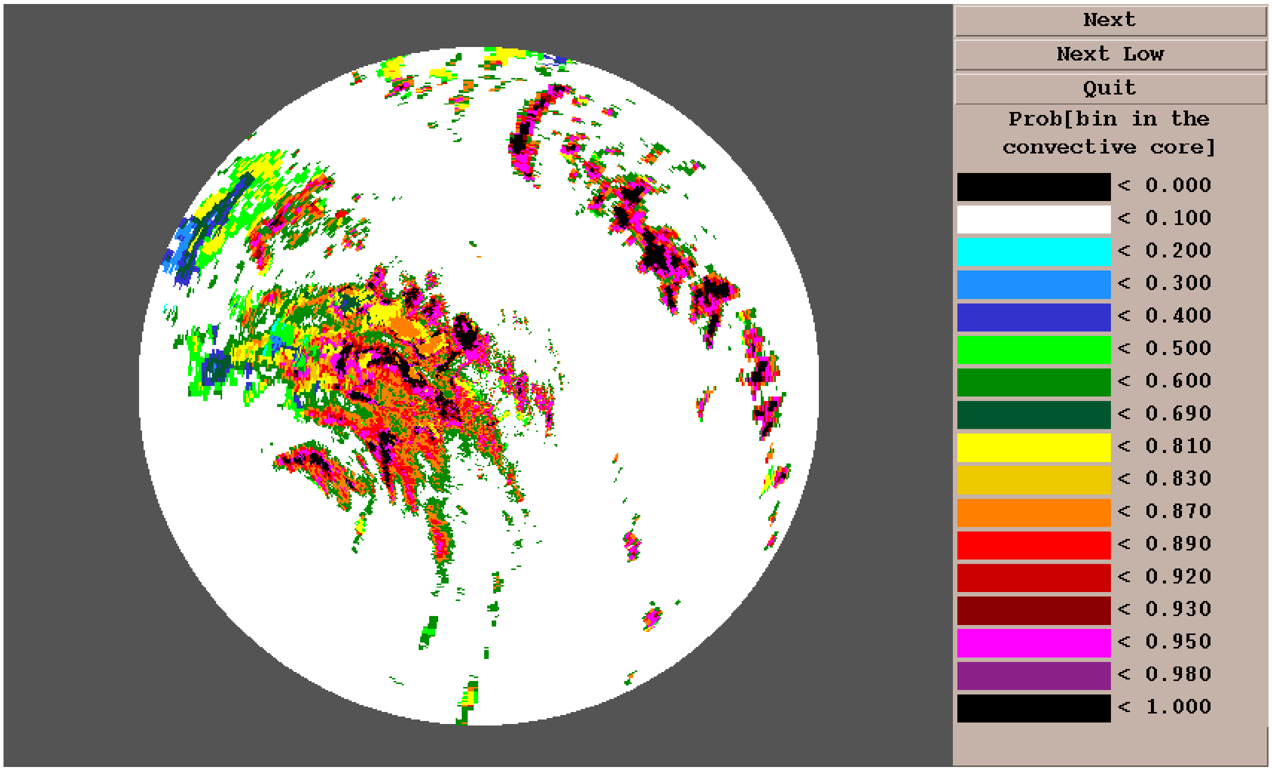

Figure 16. Output of full CSSA, KEVX umbrella, 4 October 1995.

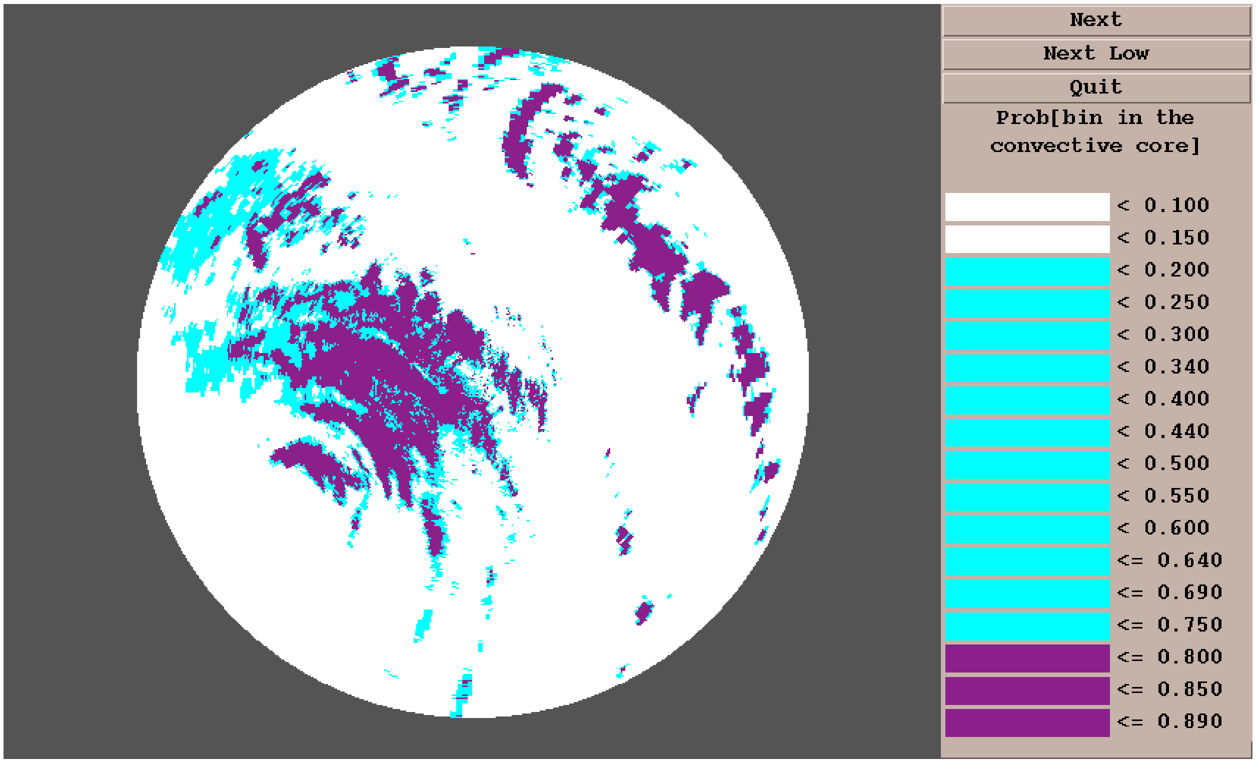

Figure 17. Full CSSA (categorical), KEVX umbrella.

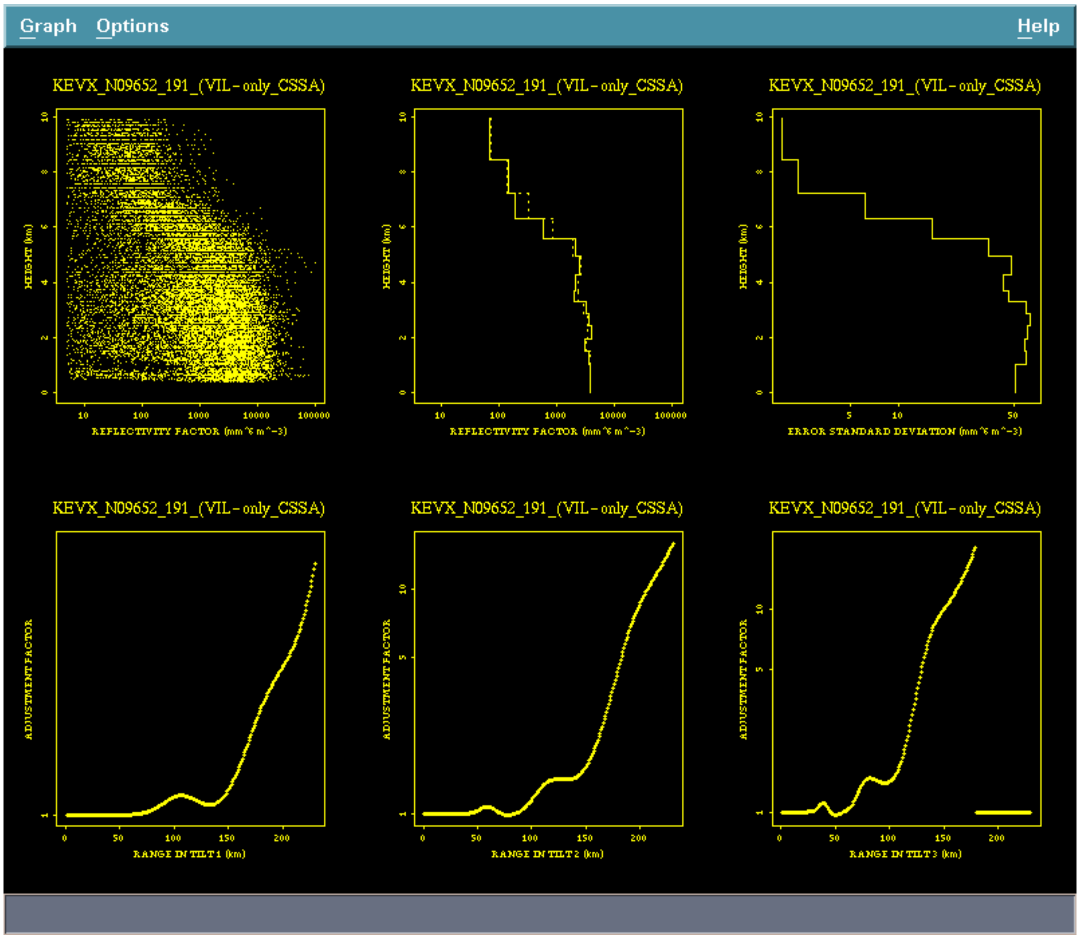

Figure 18. VPR and adjustment factor curves, KEVX umbrella, based on VIL-only CSSA.

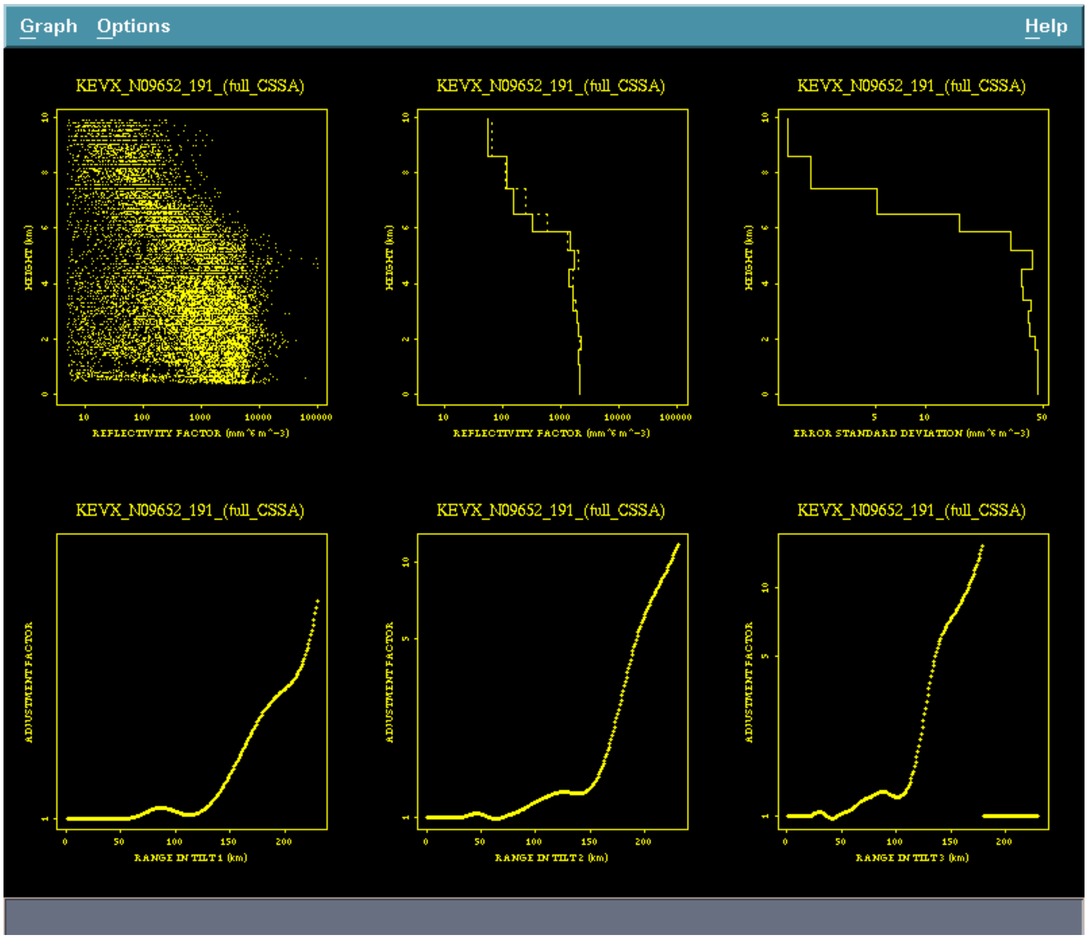

Figure 19. VPR and adjustment factor curves, KEVX umbrella, based on full CSSA.

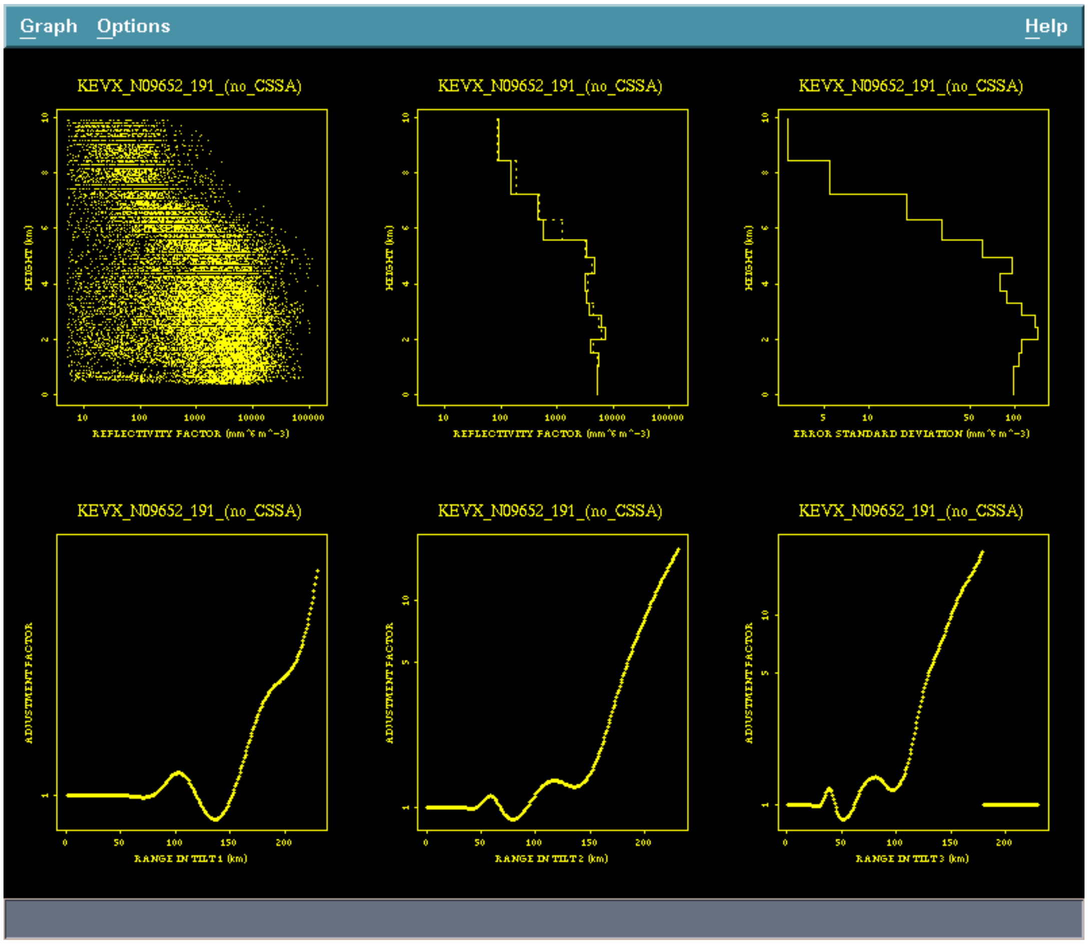

Figure 20. As in Figs. 18-19, except with no CSSA.

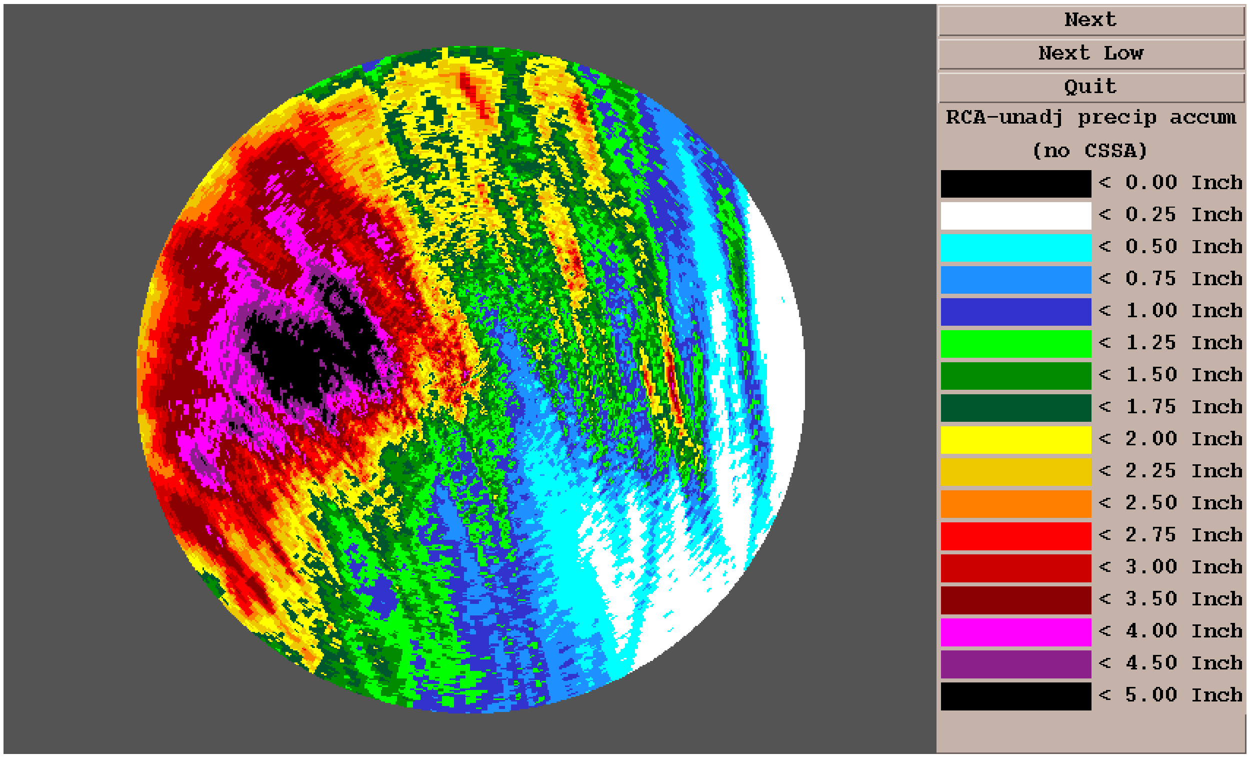

Figure 21. Rainfall over ~13.5 h, KEVX umbrella, with no range correction.

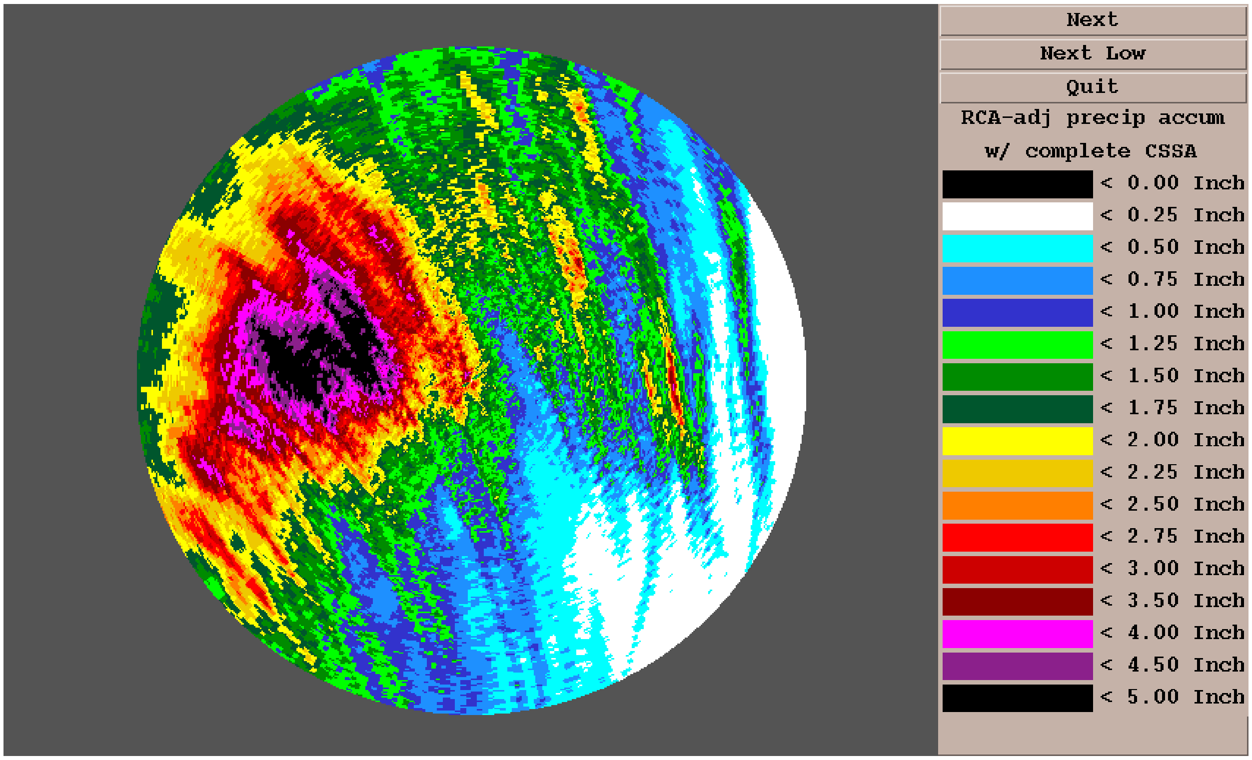

Figure 22. As in Fig. 21, except with RCA/full CSSA.

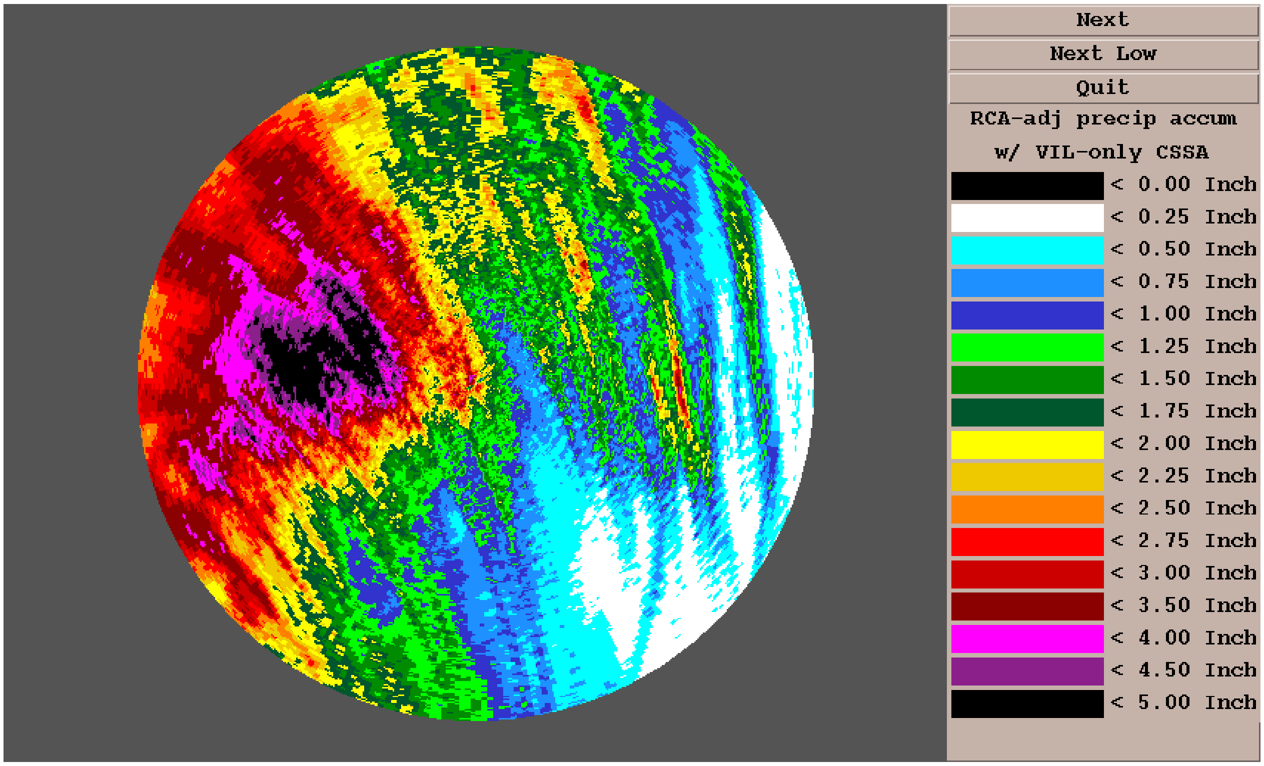

Figure 23. As in Fig. 21, except with RCA/ VIL-only CSSA.

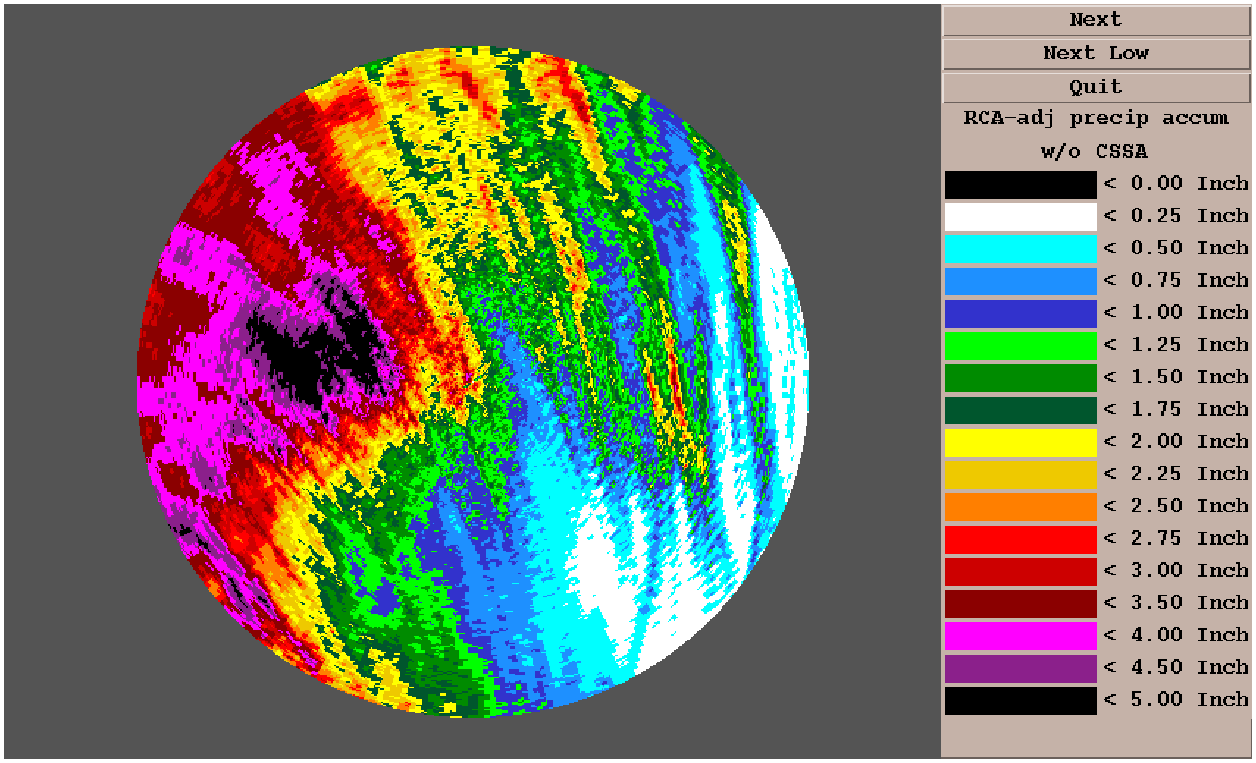

Figure 24. As in Figs. 22-23, except no CSSA used in range correction.

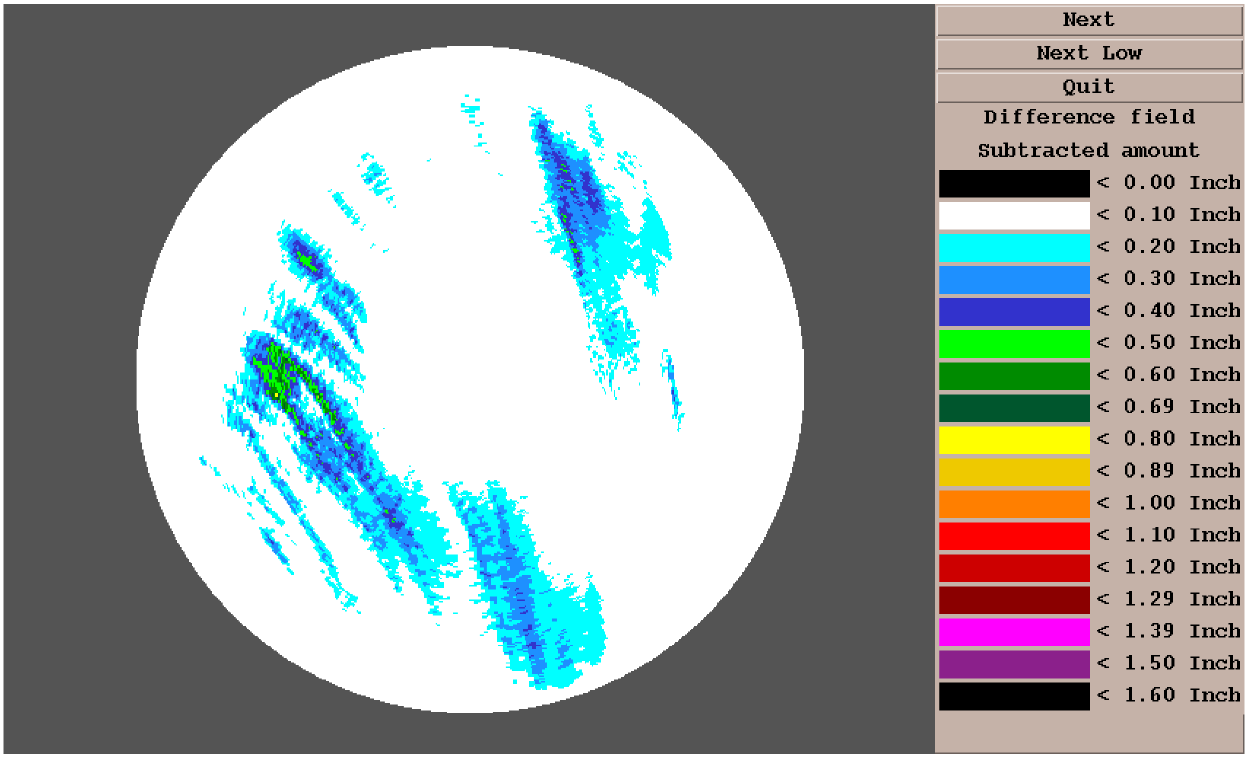

Figure 25. Rain amount apparently subtracted by RCA/no CSSA, corresponding to rainfall amounts in Figs. 21 and 24.

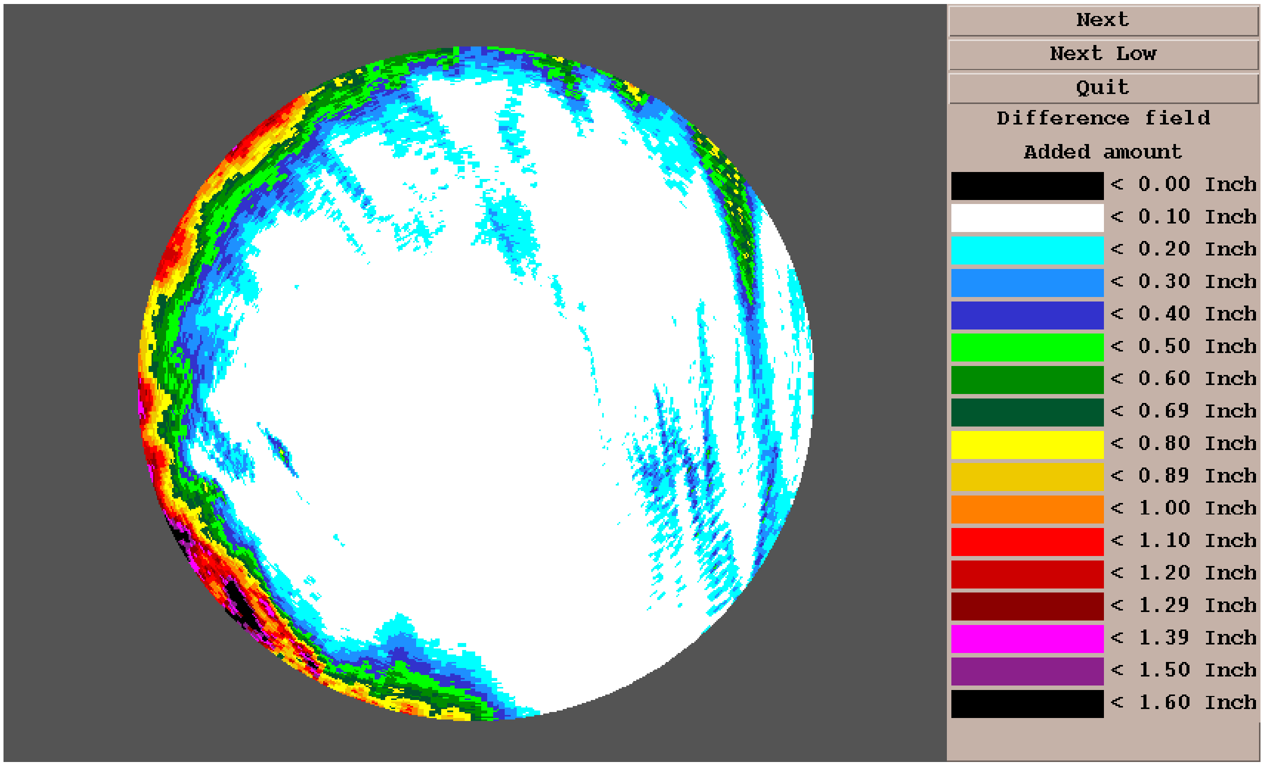

Figure 26. Rainfall apparently added by RCA/no CSSA, corresponding to rainfall in Figs. 21, 24.

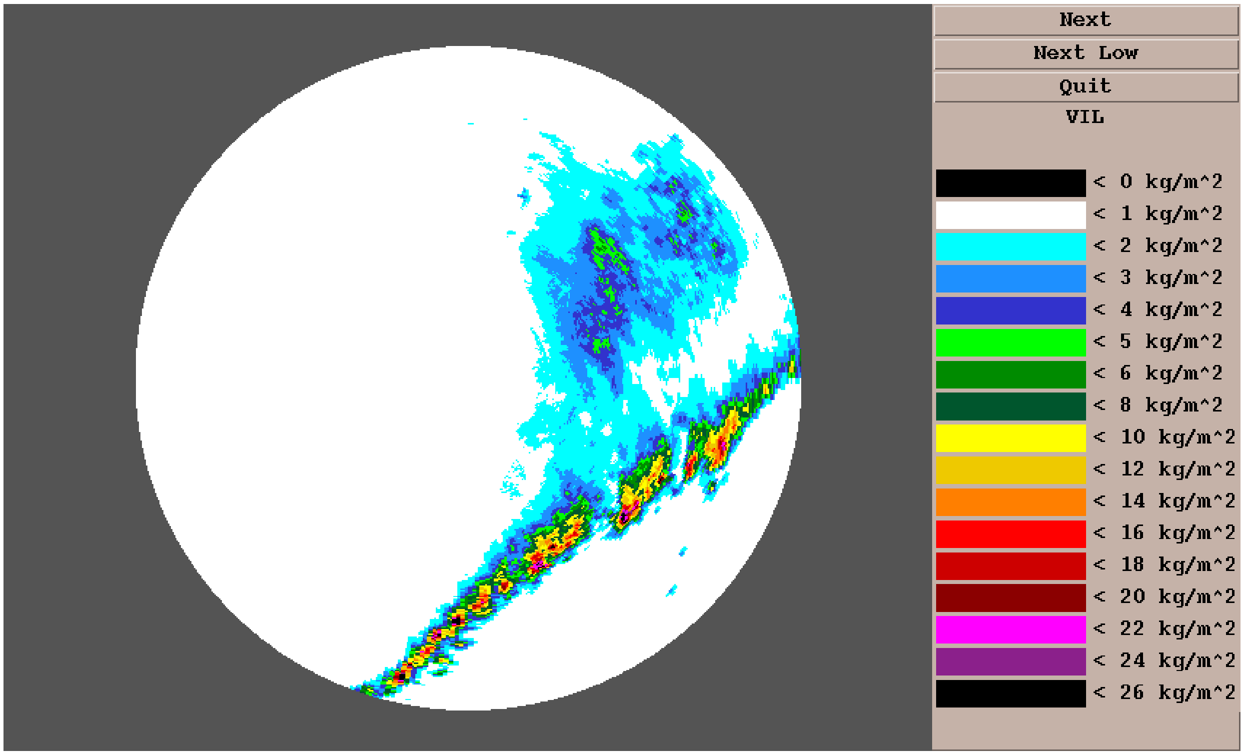

Figure 27. VIL field in KFDR umbrella, 9 May 1993.

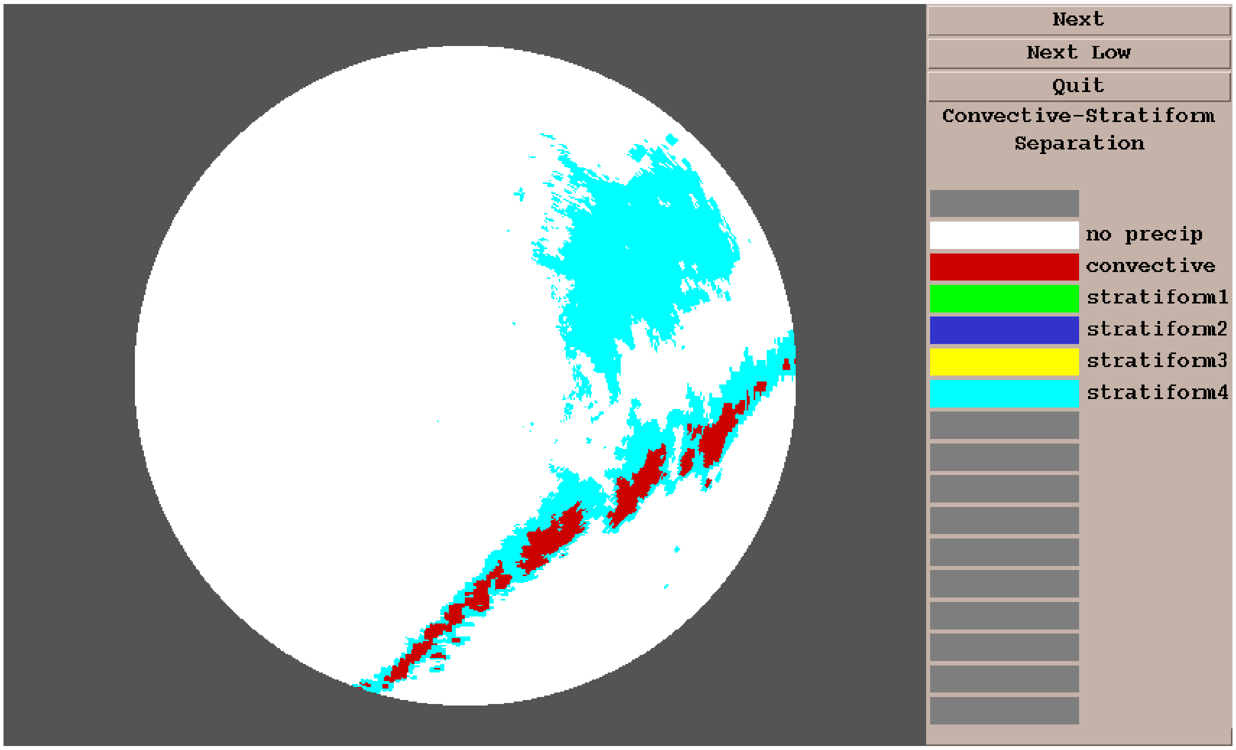

Figure 28. Output of CSSA/VIL-only, KFDR umbrella.

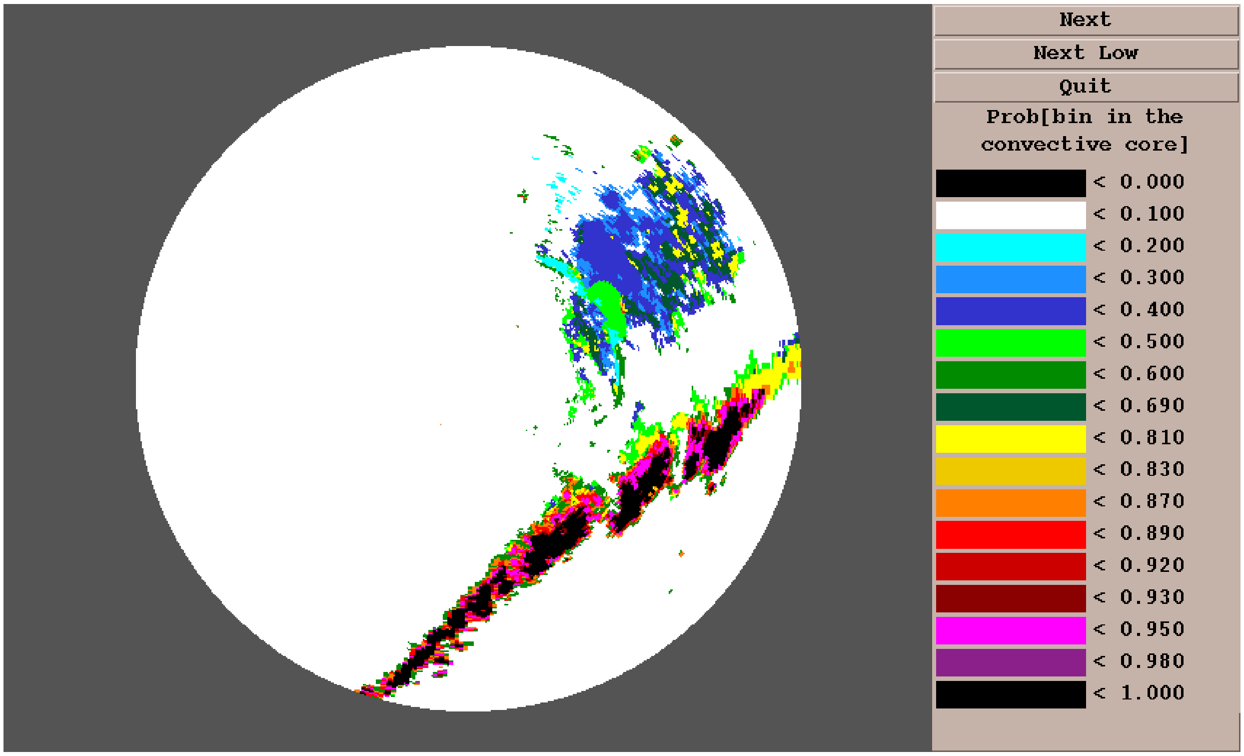

Figure 29. Output of full CSSA, KFDR umbrella.

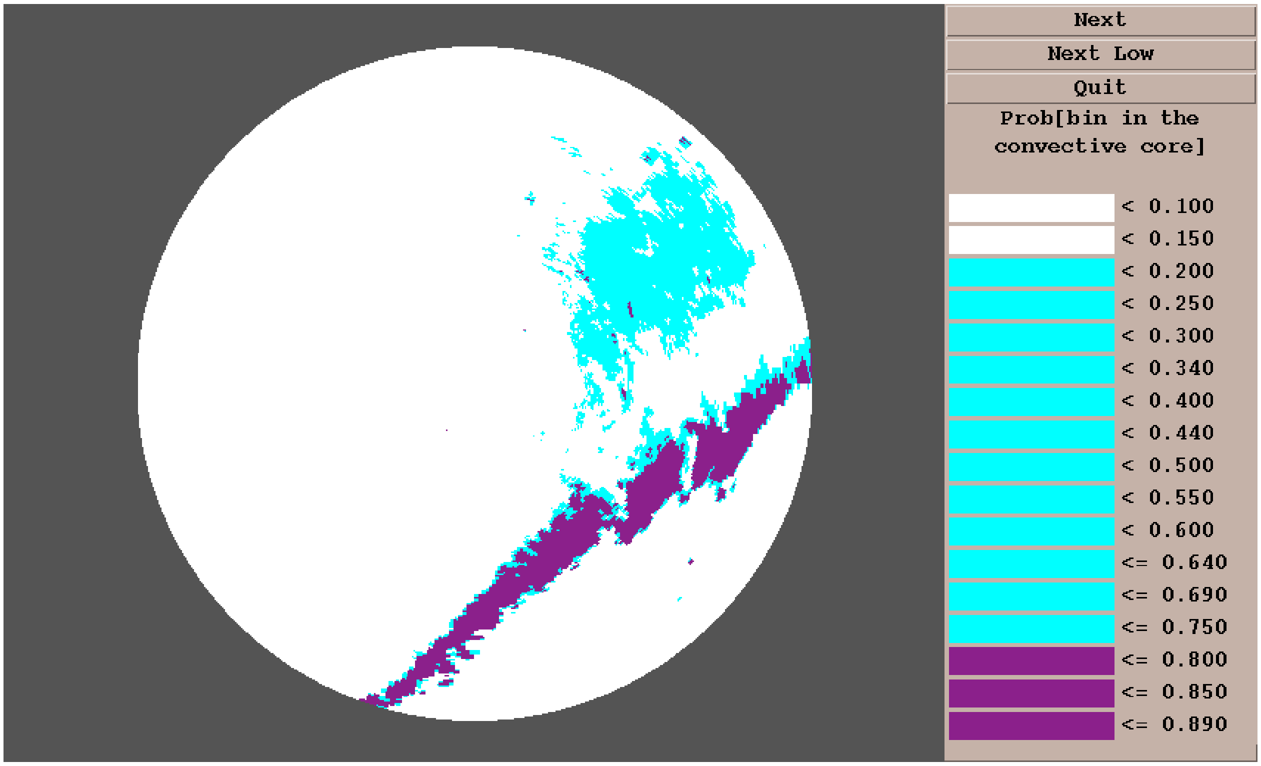

Figure 30. Full CSSA (categorical), KFDR umbrella.

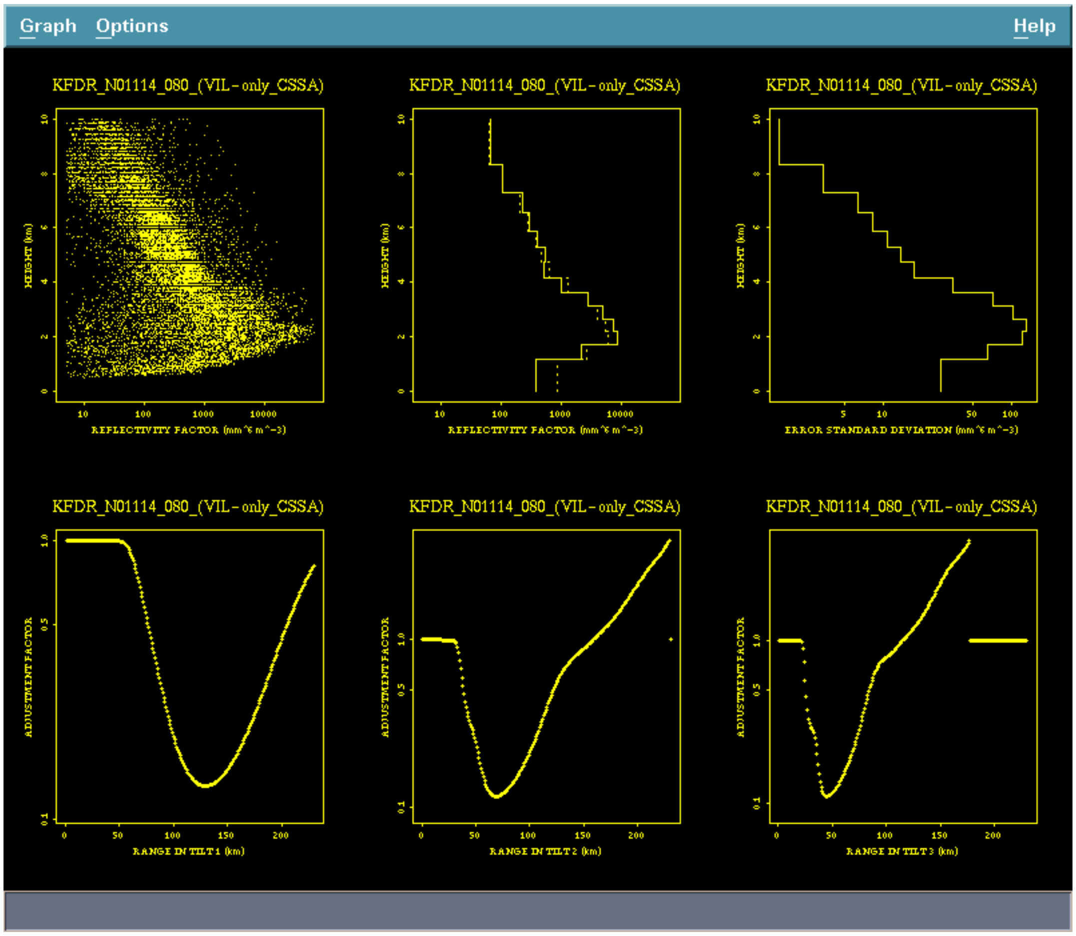

Figure 31. VPR and adjustment factor curves, from RCA/VIL-only CSSA.

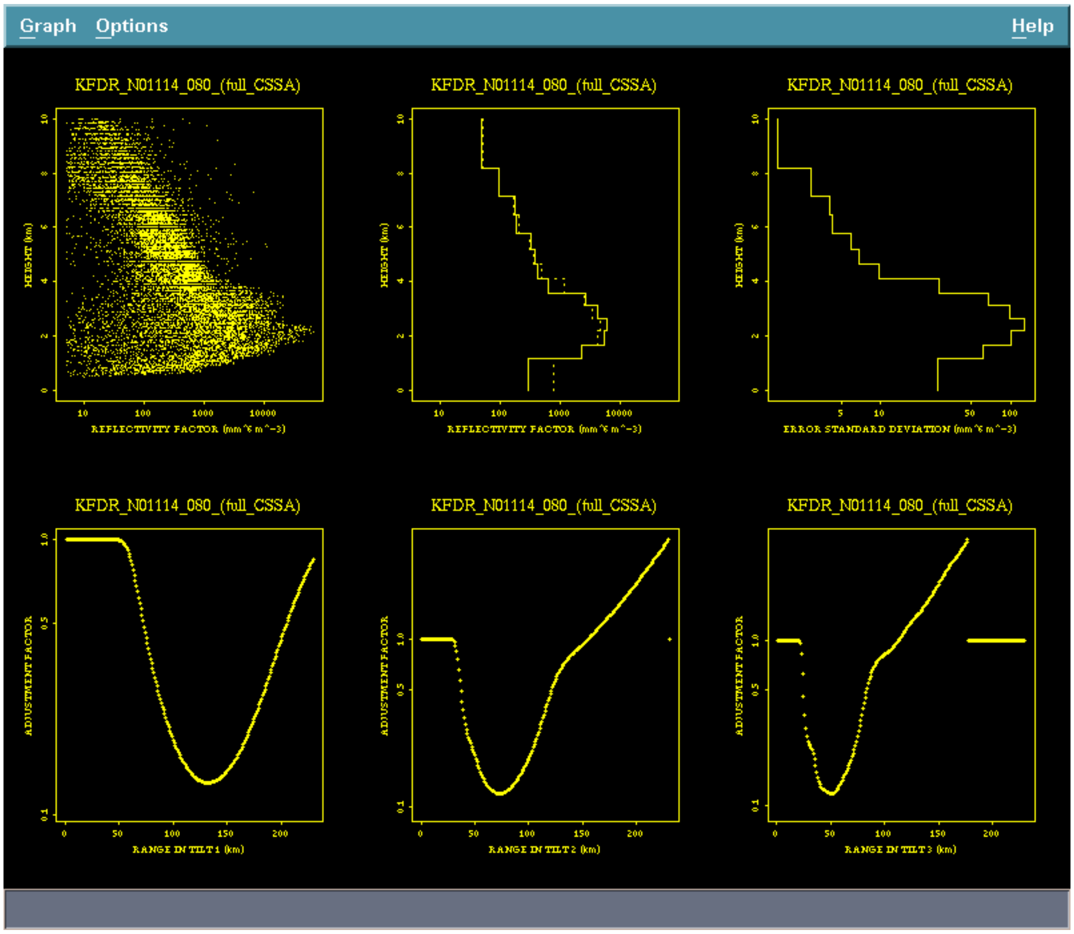

Figure 32. As in Fig. 31, except from RCA/full CSSA.

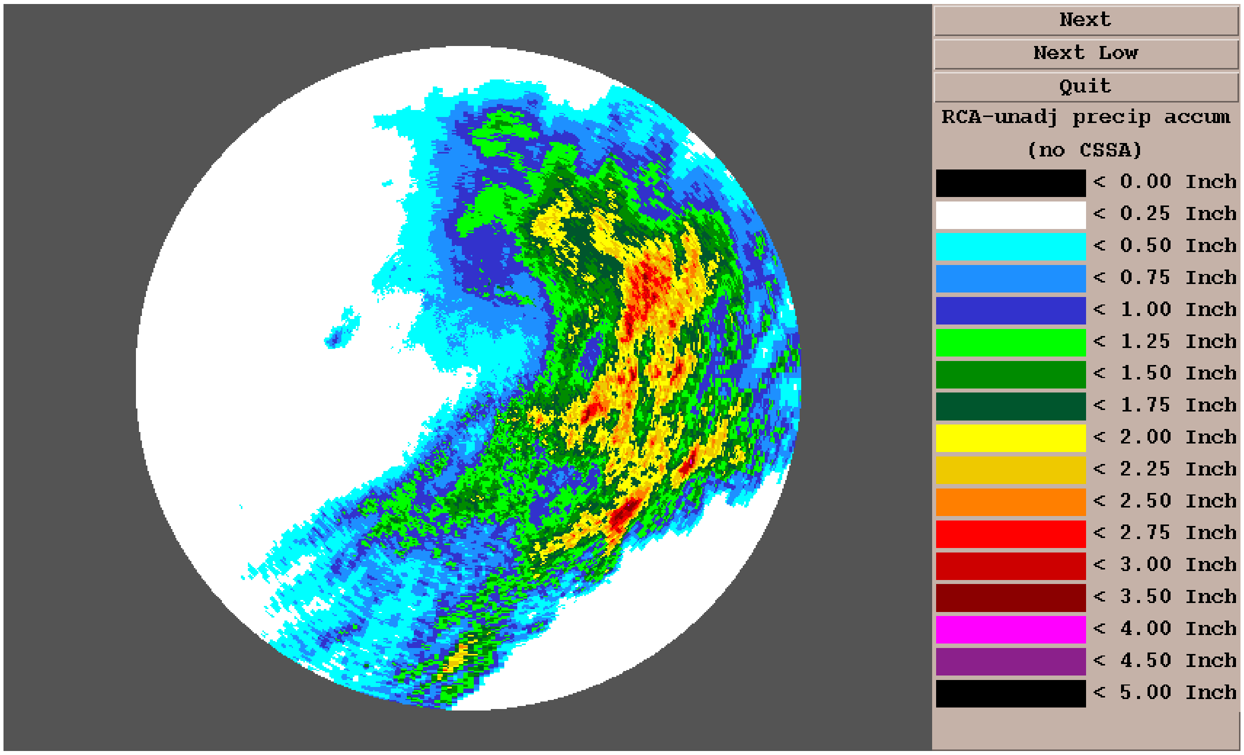

Figure 33. Rainfall over ~5.5 h, KFDR umbrella, no range correction.

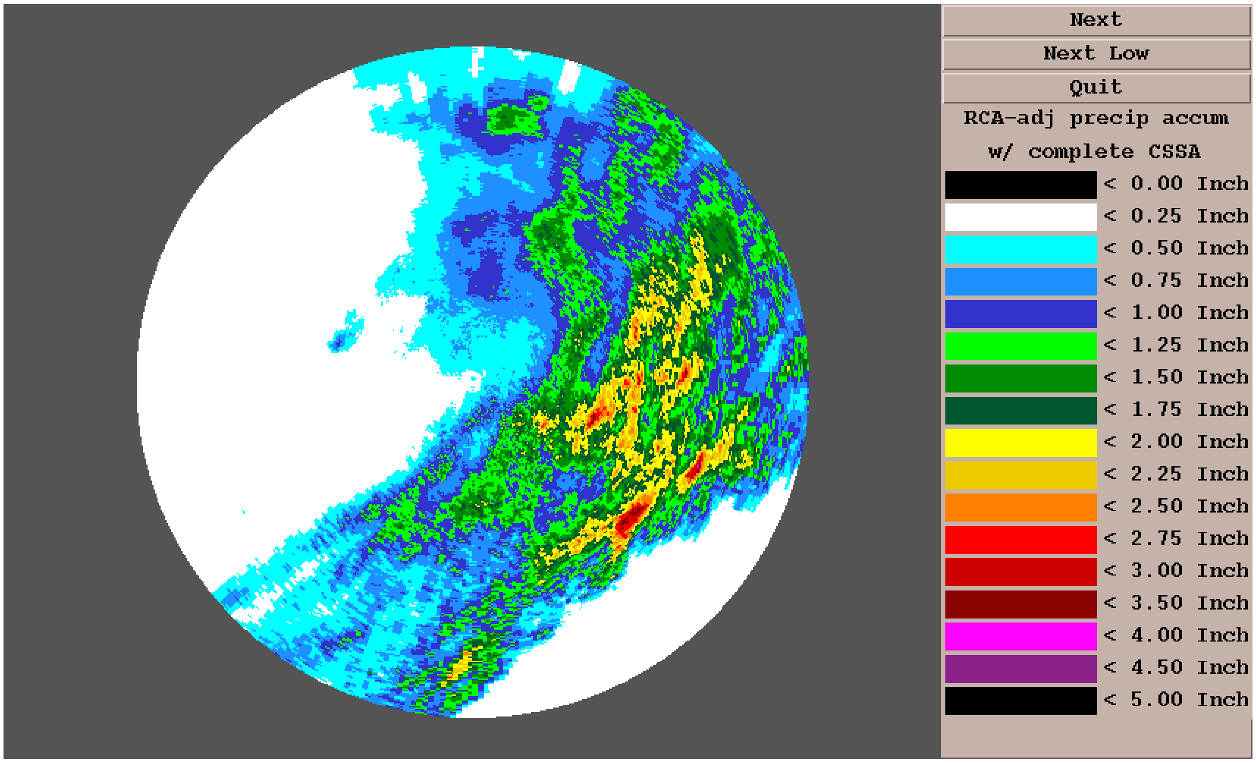

Figure 34. As in Fig. 33, except rainfall with RCA/full CSSA.

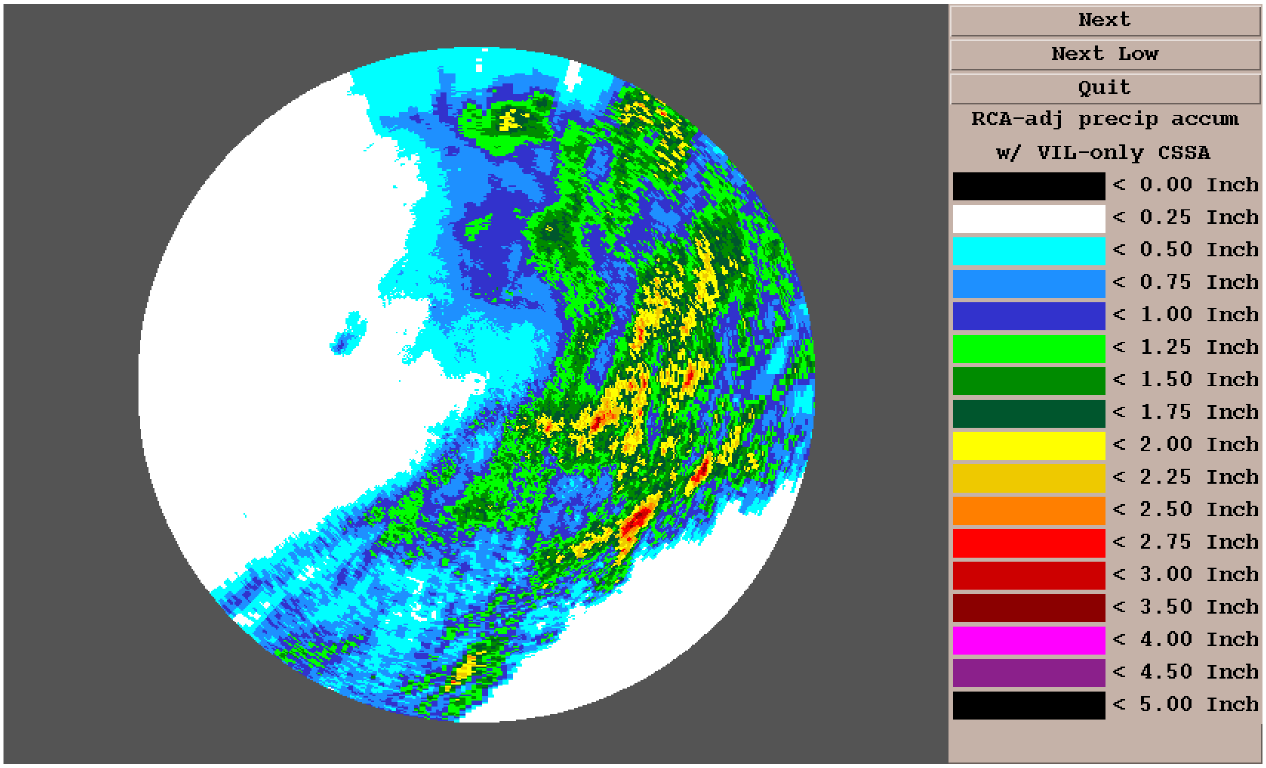

Figure 35. As in Fig. 33, except rainfall with RCA/VIL-only CSSA.

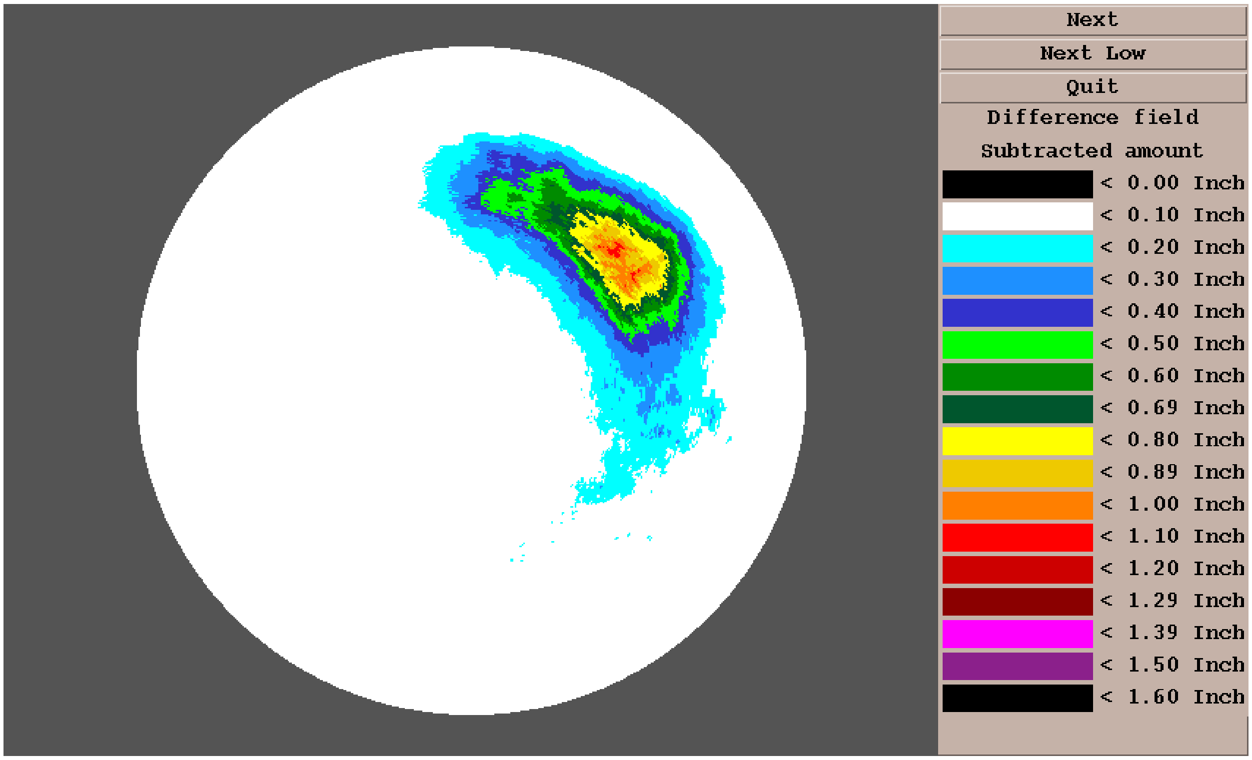

Figure 36. Rainfall apparently subtracted by RCA/full CSSA, corresponding to rainfall in Figs. 33 and 34.

:

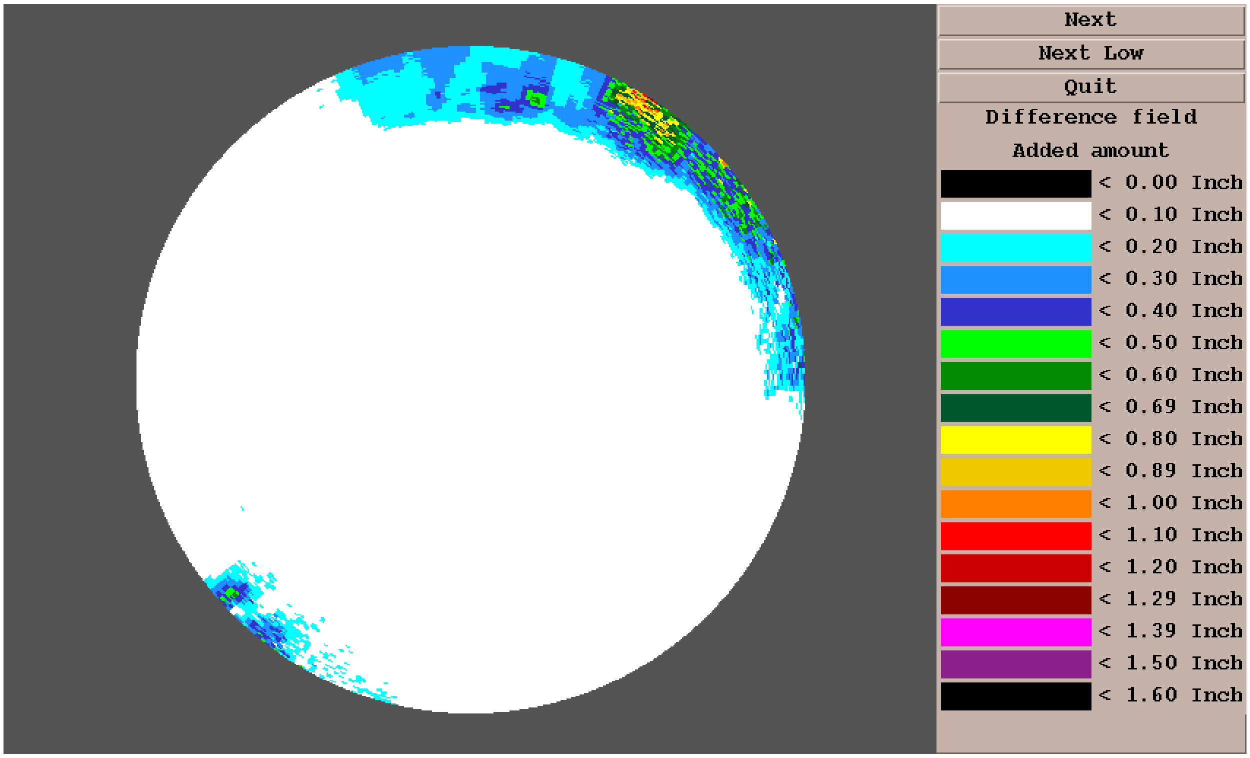

Figure 37. Rainfall apparently added by RCA/full CSSA, for KFDR case.

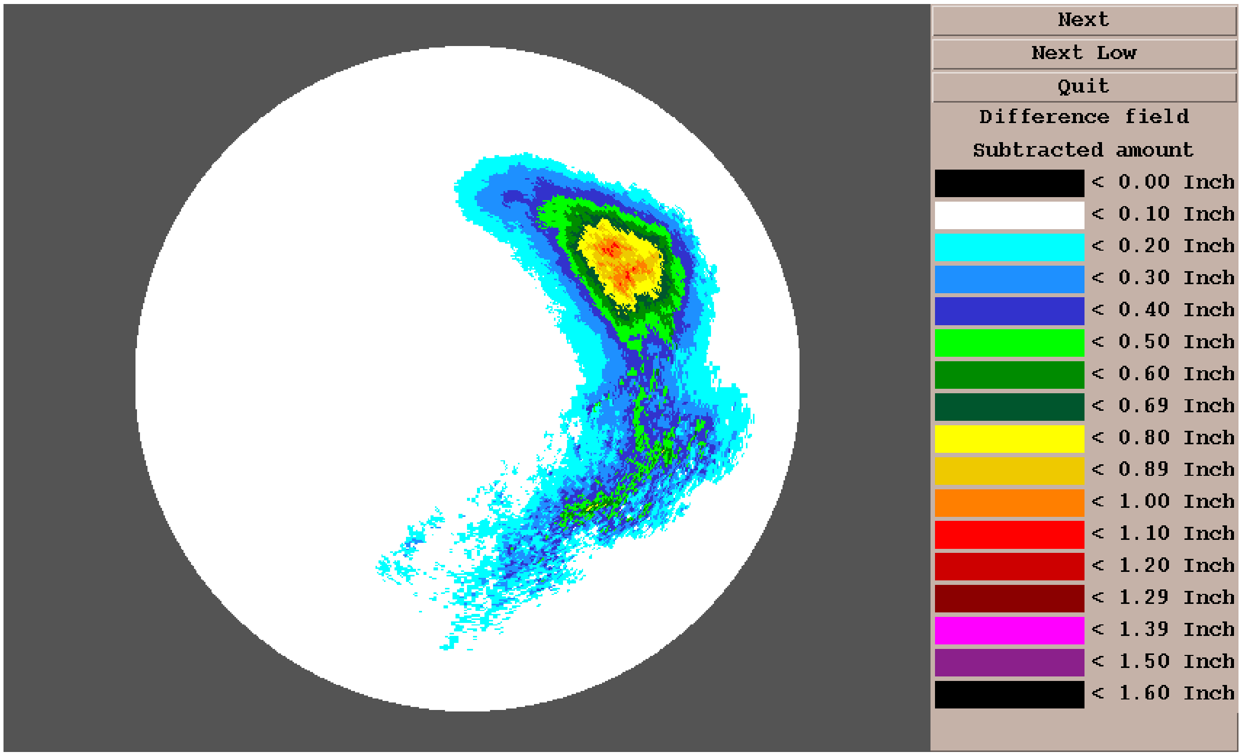

Figure 38. Rainfall apparently subtracted by RCA/VIL-only CSSA, for KFDR case.

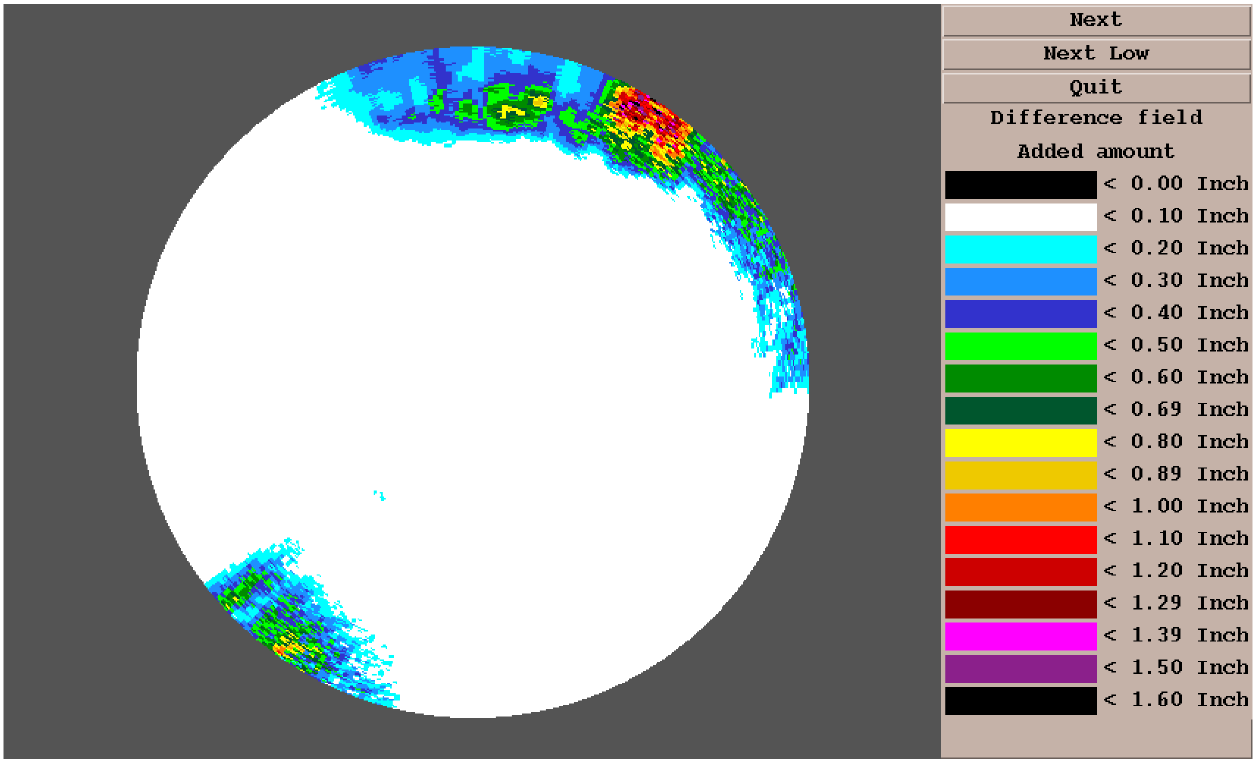

Figure 39. Rainfall apparently added by RCA/VIL-only CSSA, KFDR case.

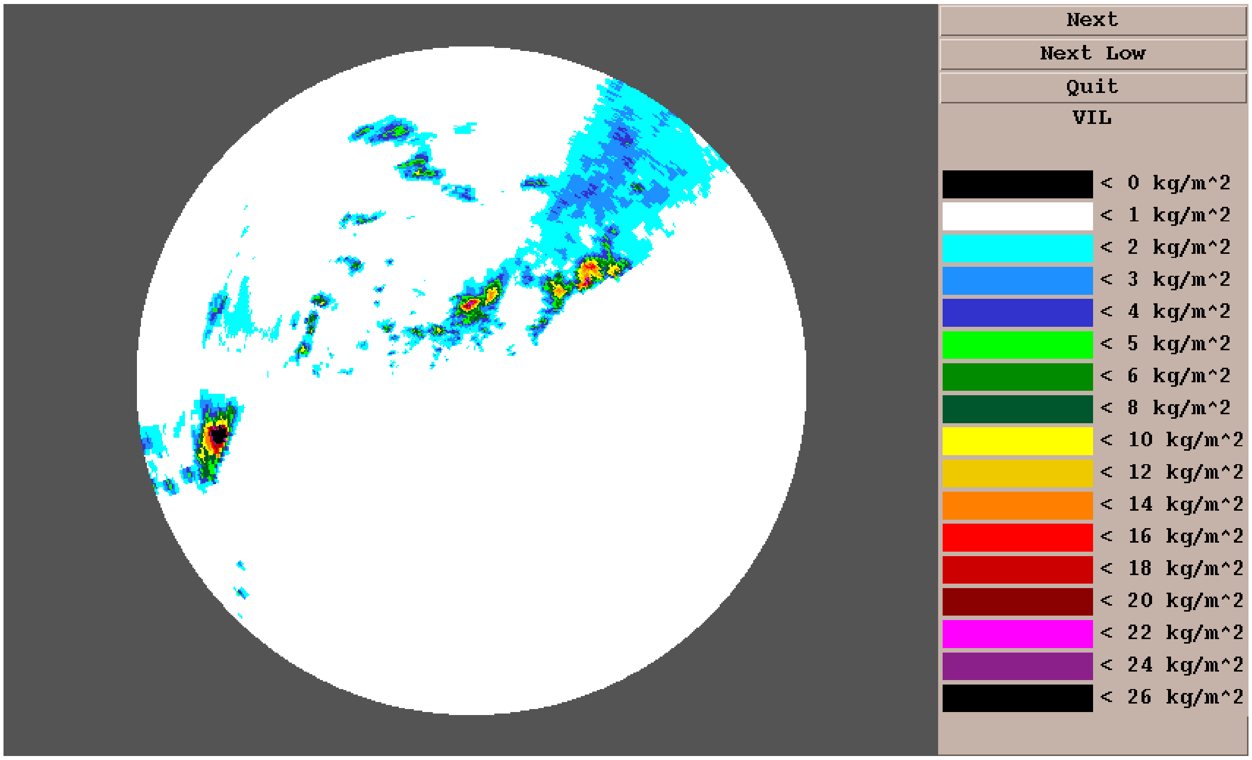

Figure 40. VIL field in KHGX umbrella, 17 October 1994.

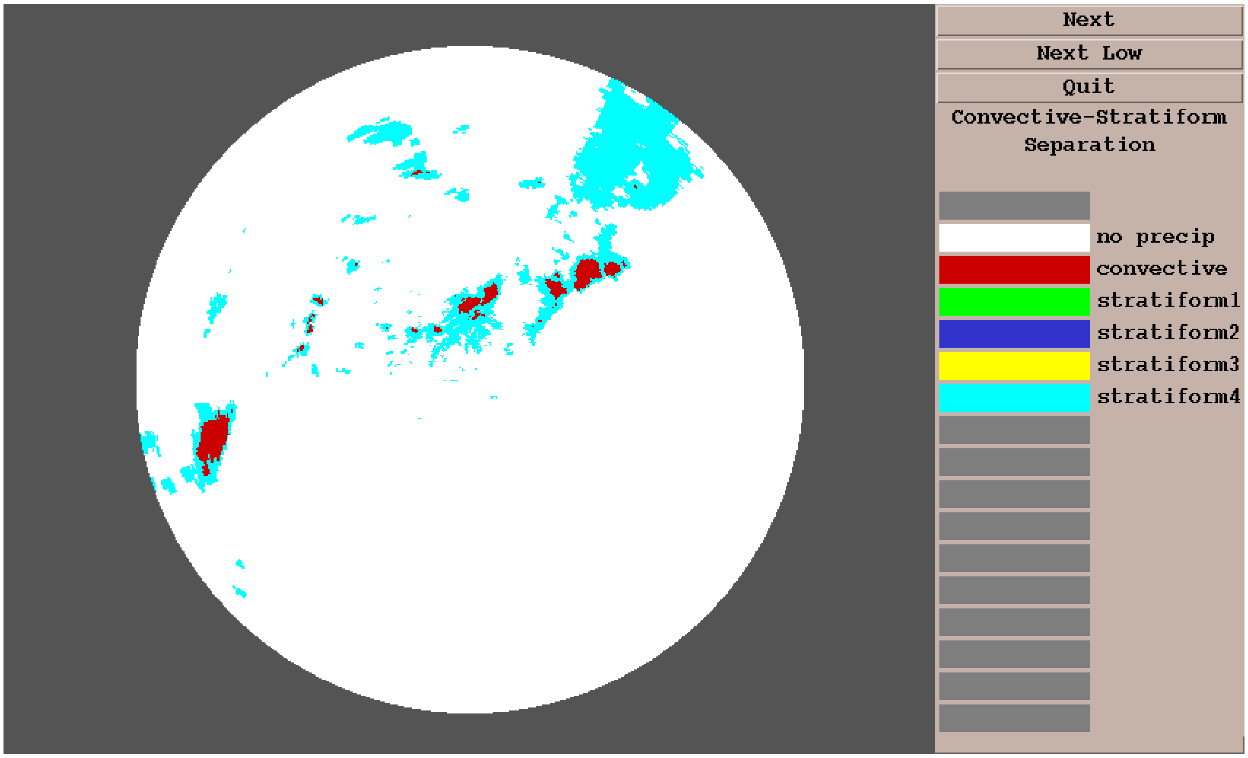

Figure 41. Output of CSSA/VIL-only, KHGX umbrella.

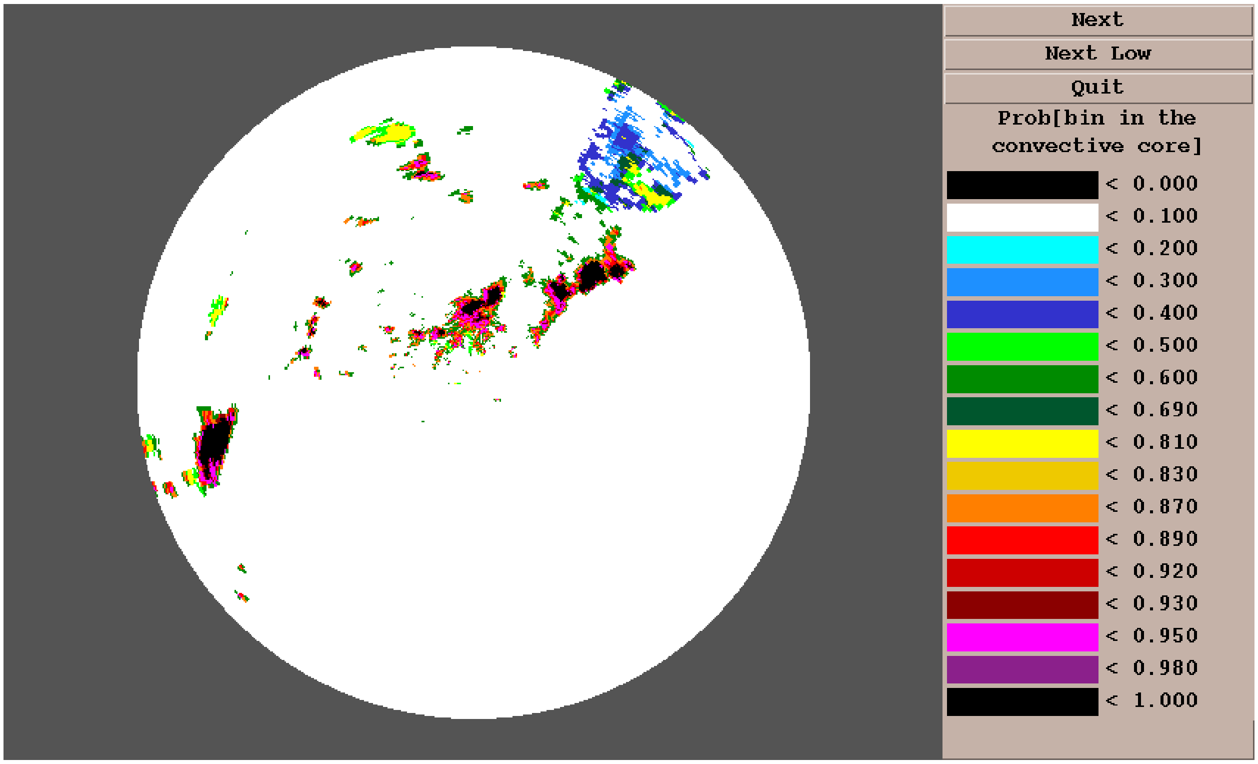

Figure 42. Output of full CSSA, KHGX umbrella.

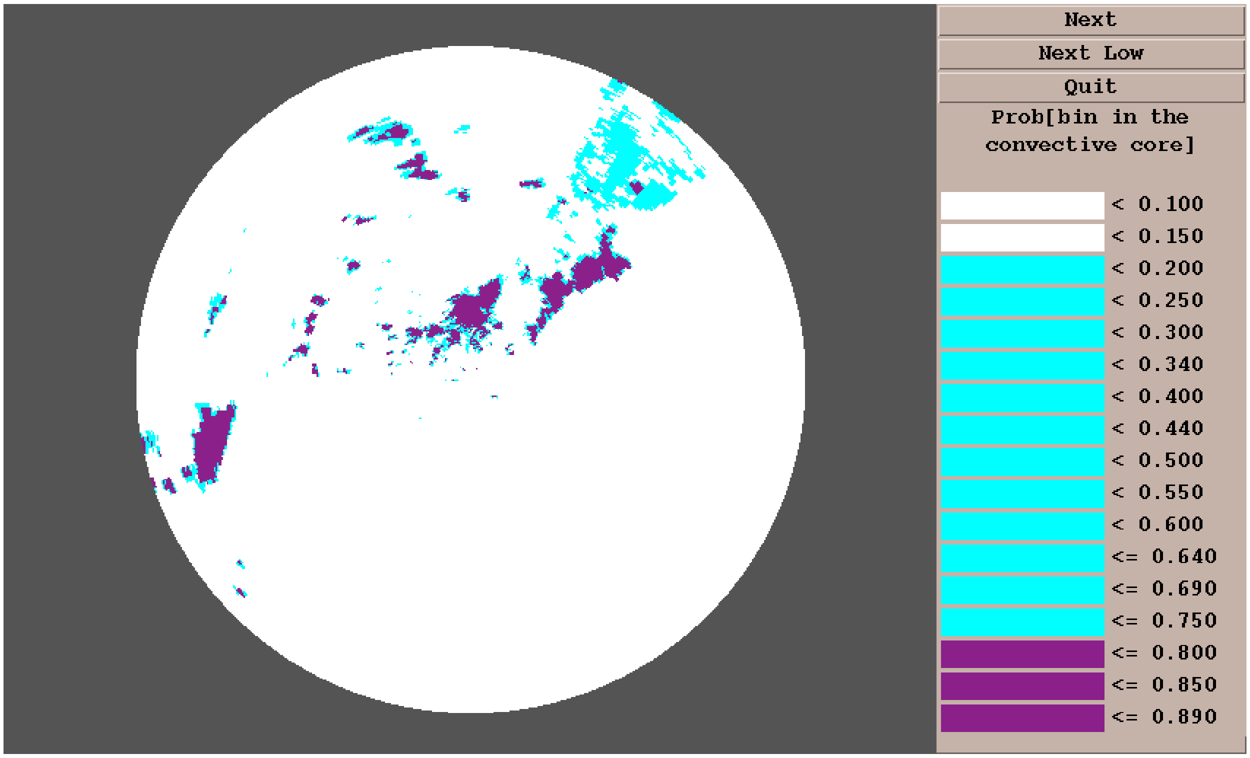

Figure 43. Full CSSA (categorical), KHGX umbrella.

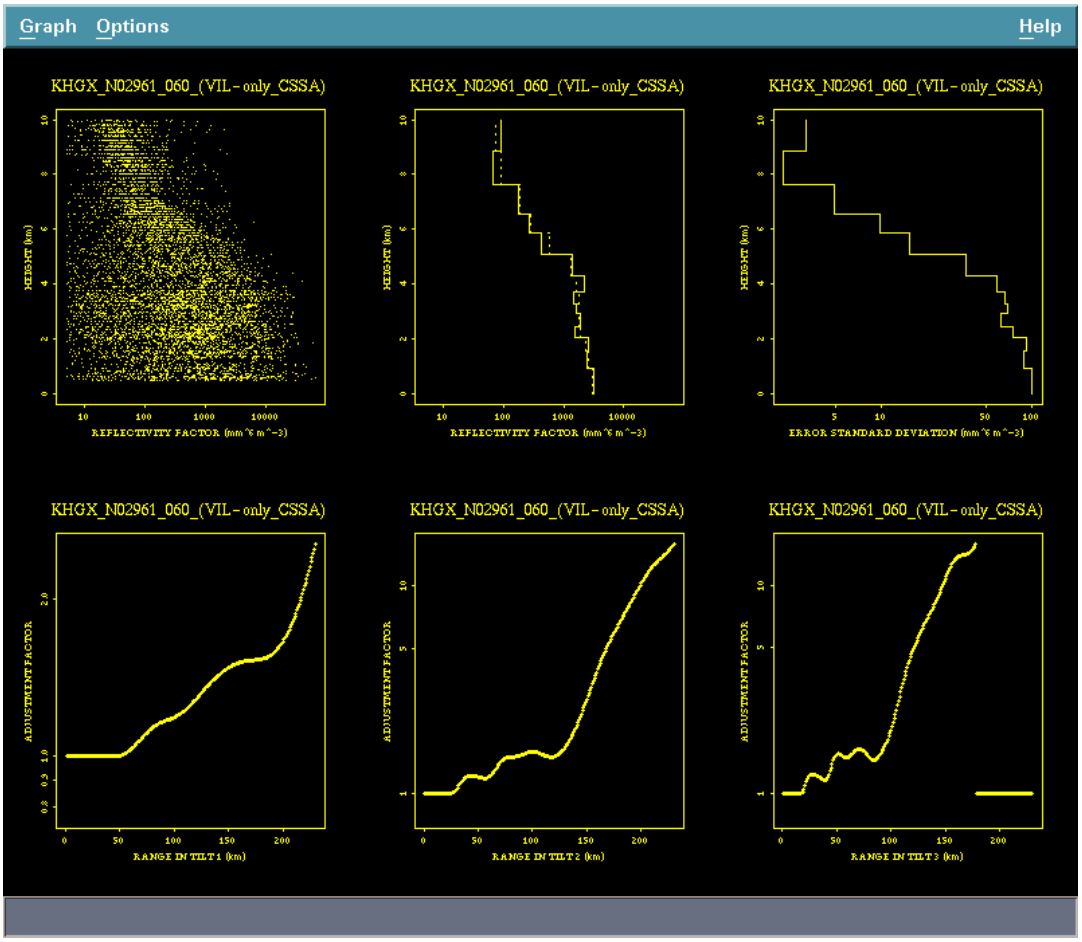

Figure 44. VPR and adjustment factor curves from RCA/VIL-only CSSA, KHGX umbrella.

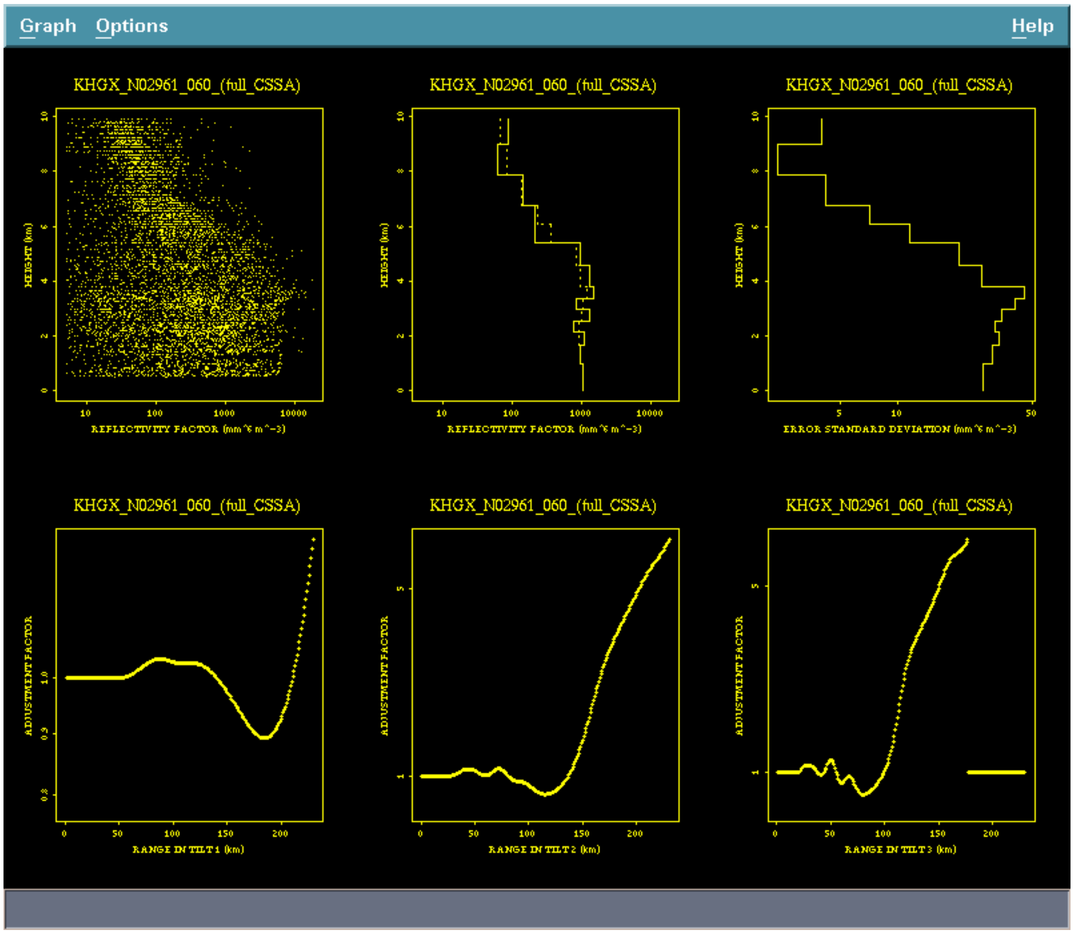

Figure 45. As in Fig. 44, except for RCA/full CSSA.

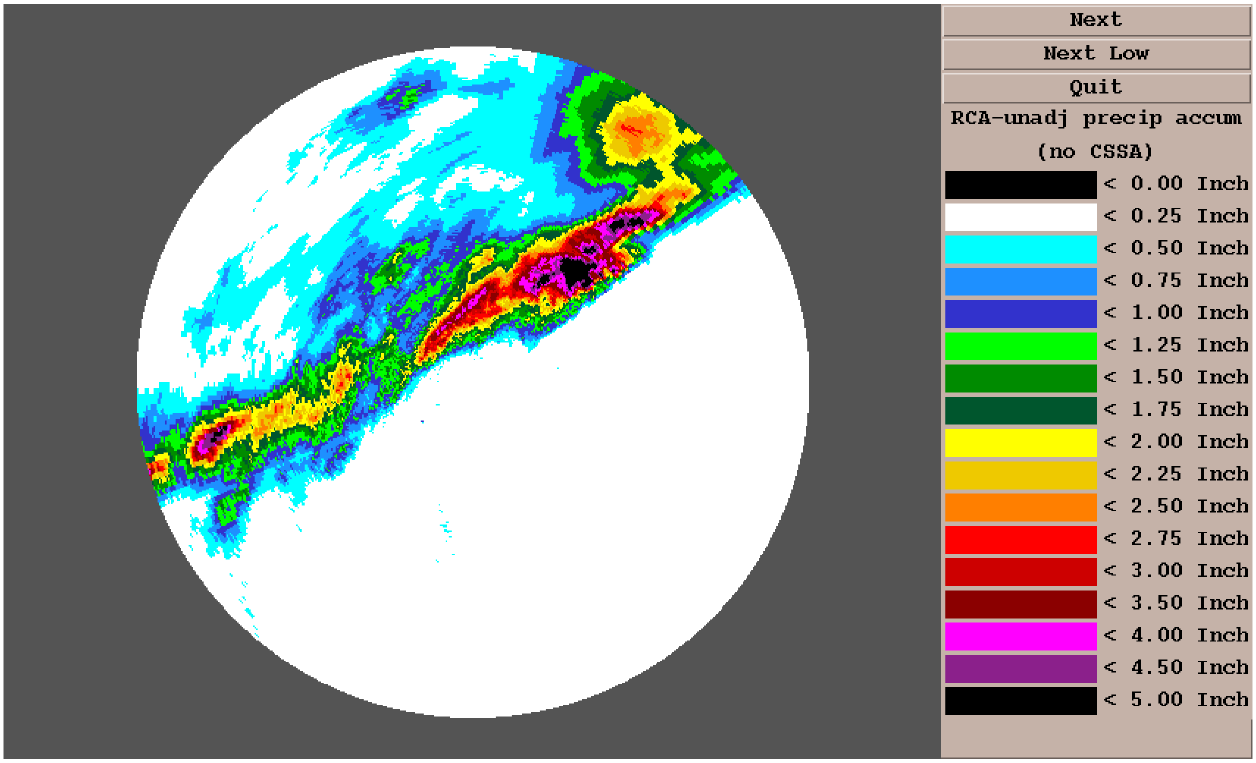

Figure 46. Rainfall over ~9 h in KHGX umbrella, without range correction.

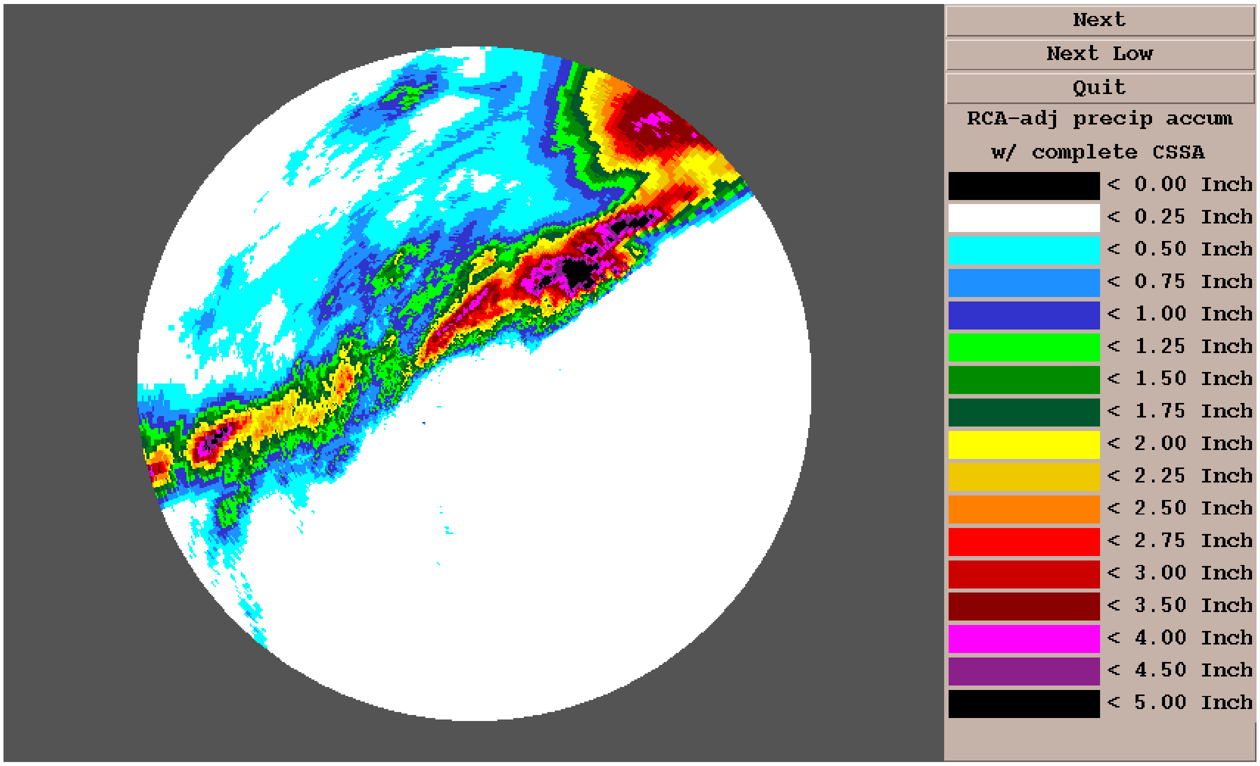

Figure 47. As in Fig. 46, except with RCA/full CSSA.

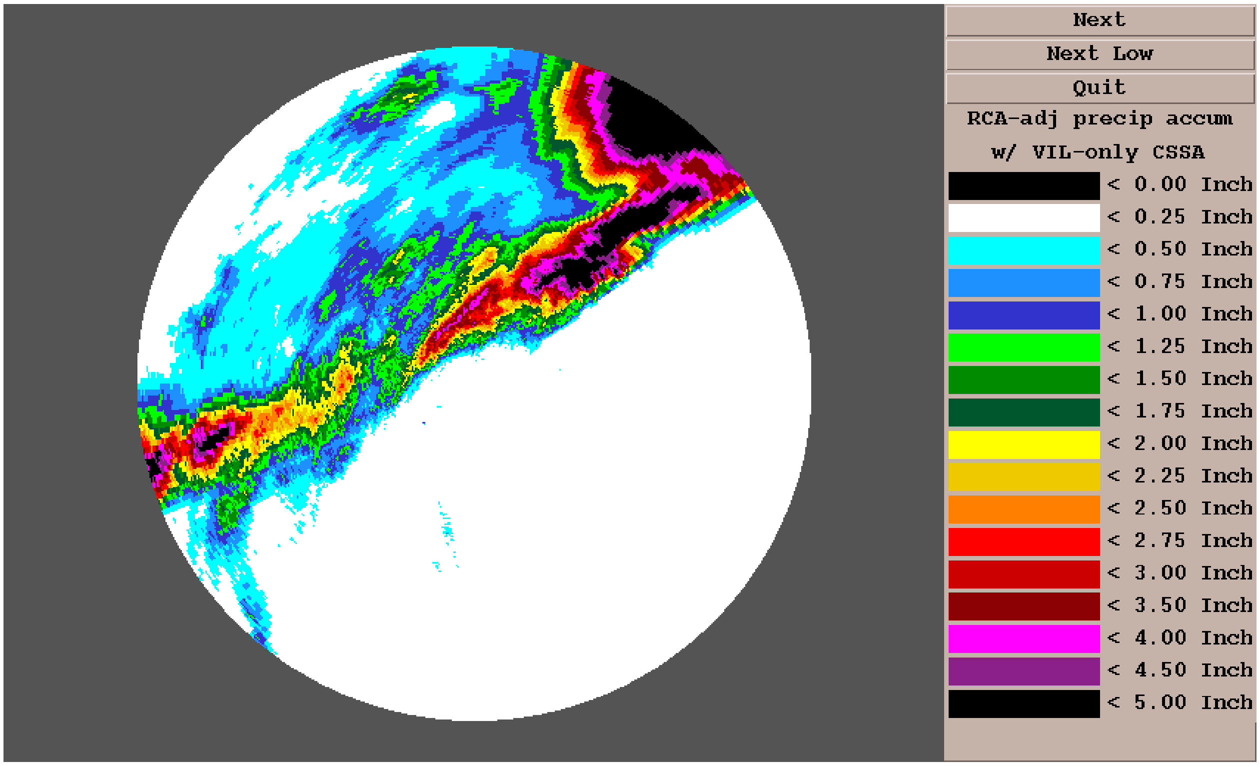

Figure 48. As in Fig. 46, except with RCA/VIL-only CSSA.

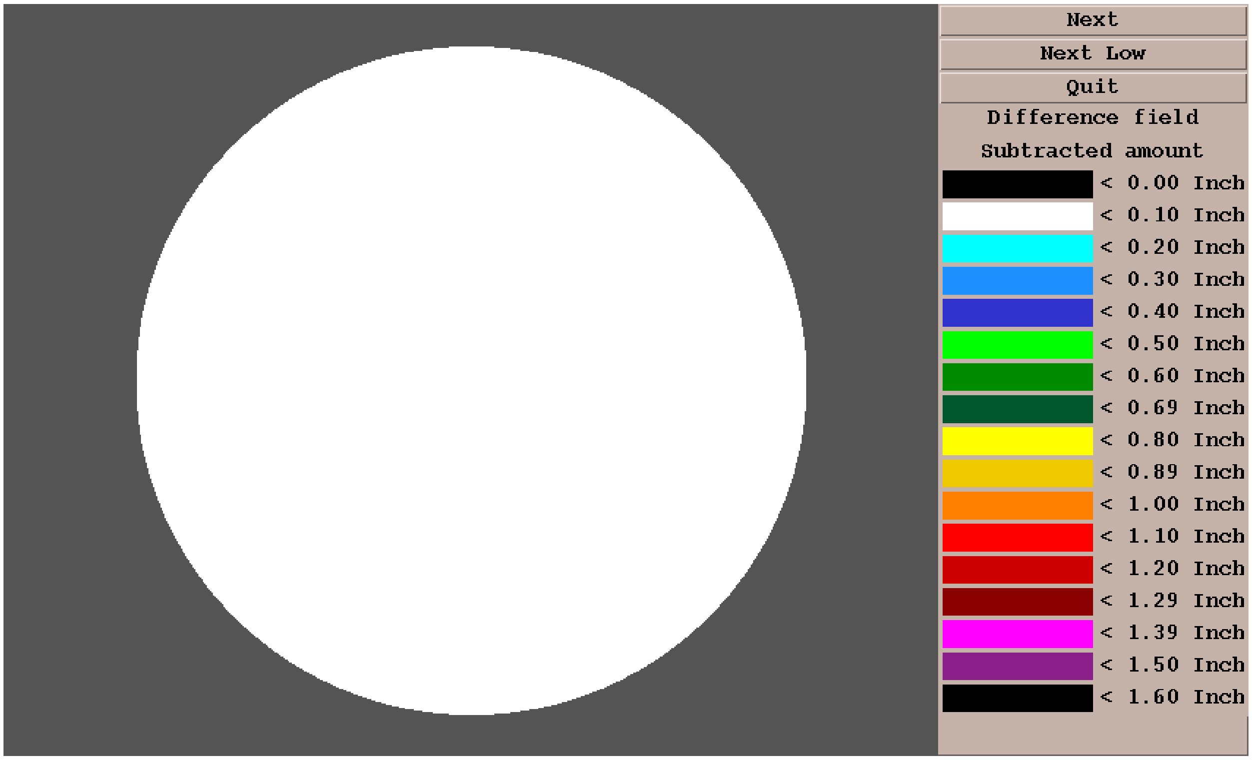

Figure 49. Rainfall apparently subtracted by RCA/full CSSA, KHGX umbrella.

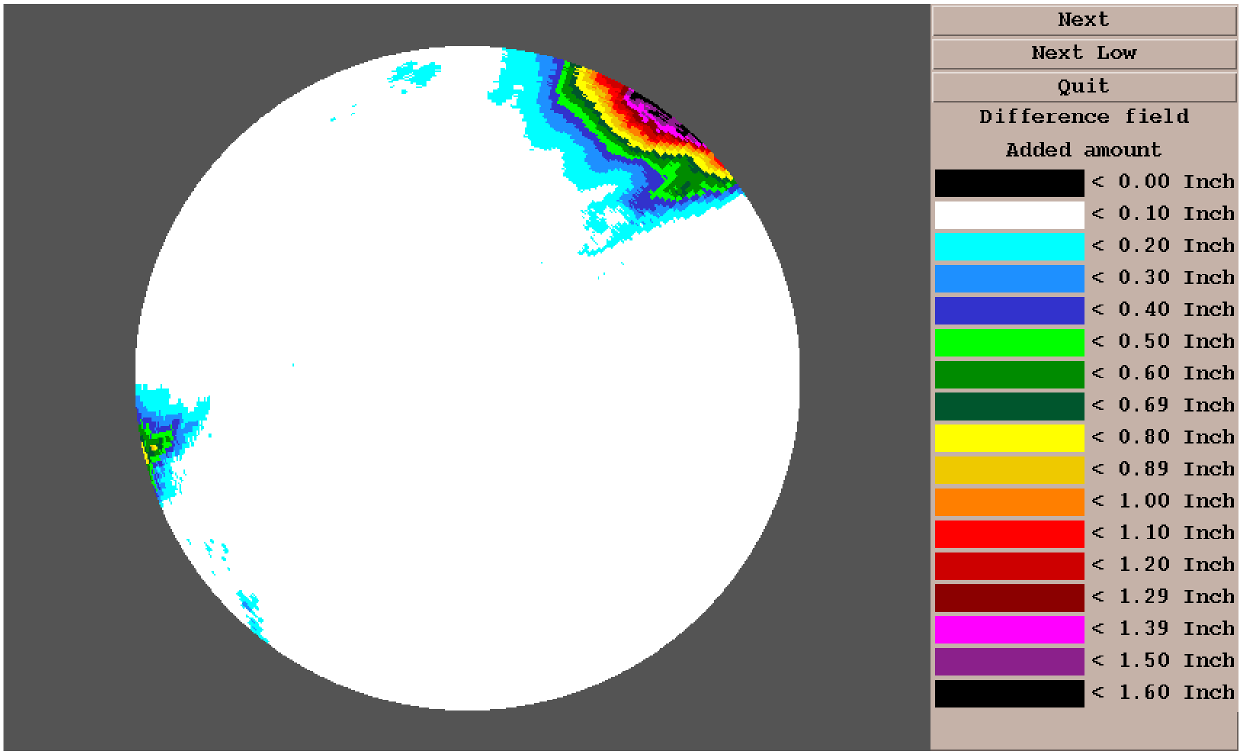

Figure 50. Rainfall apparently added by RCA/full CSSA, KHGX case.

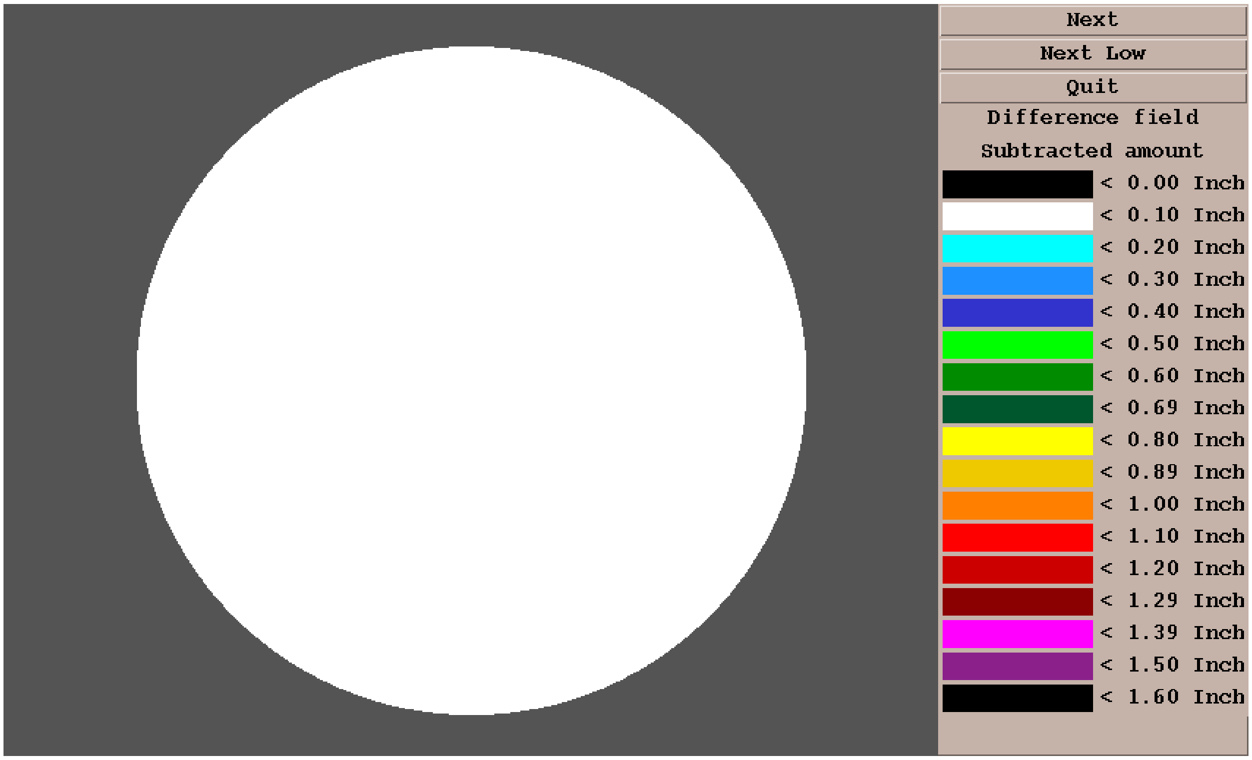

Figure 51. Rainfall apparently subtracted by RCA/VIL-only CSSA, KHGX case.

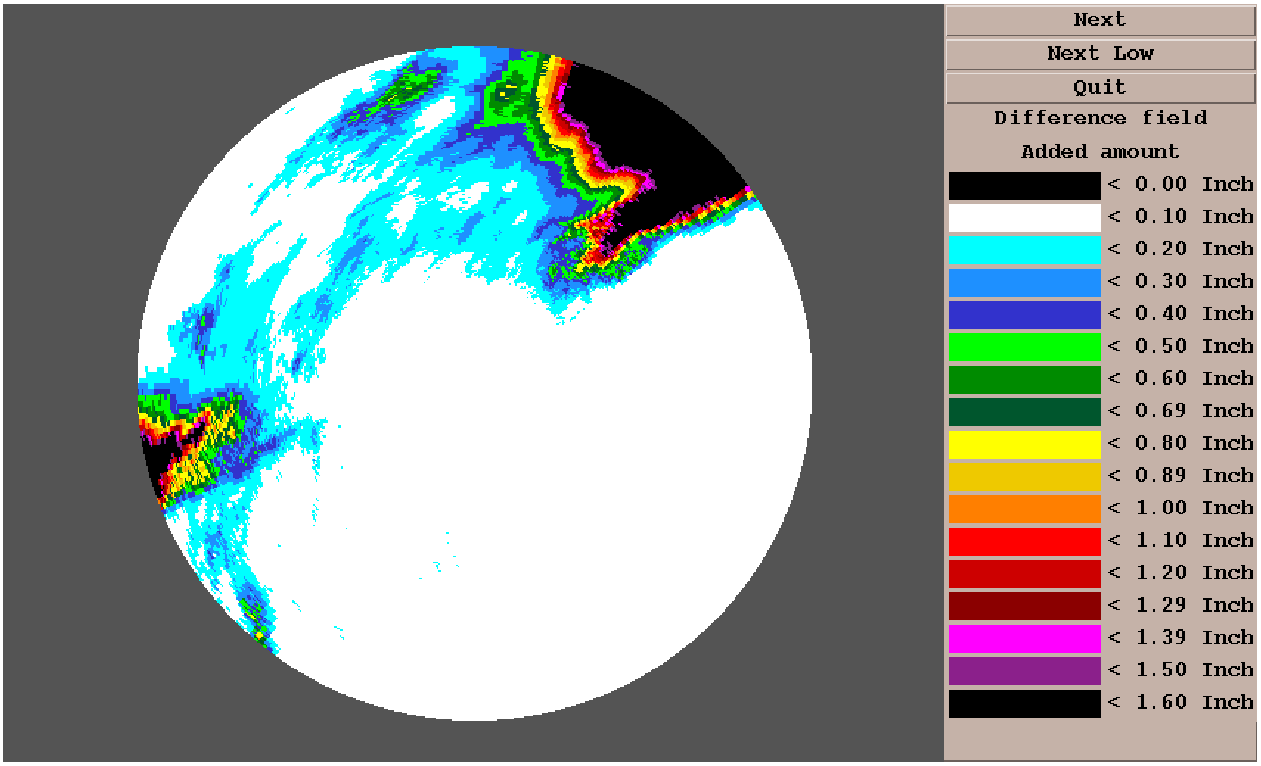

Figure 52. Rainfall apparently added by RCA/VIL-only CSSA, KHGX case.

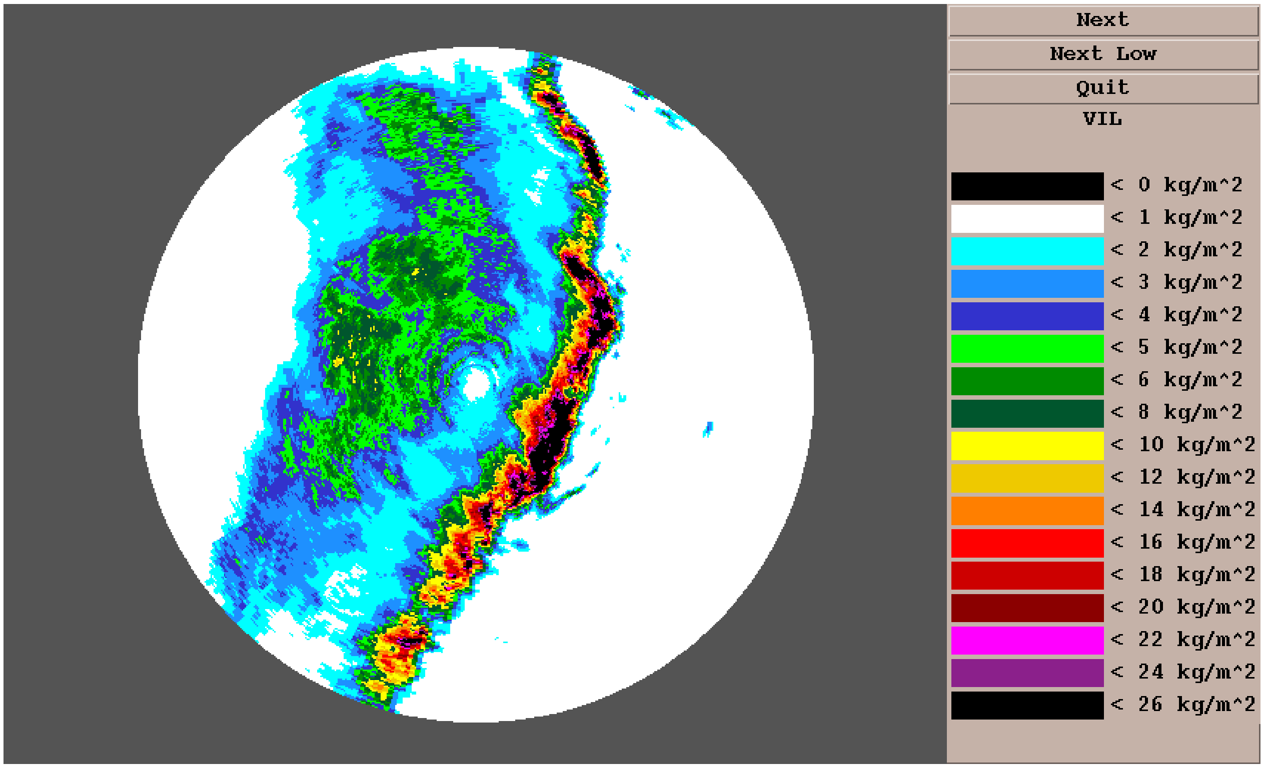

Figure 53. VIL field in KINX umbrella, 5 August 1995.

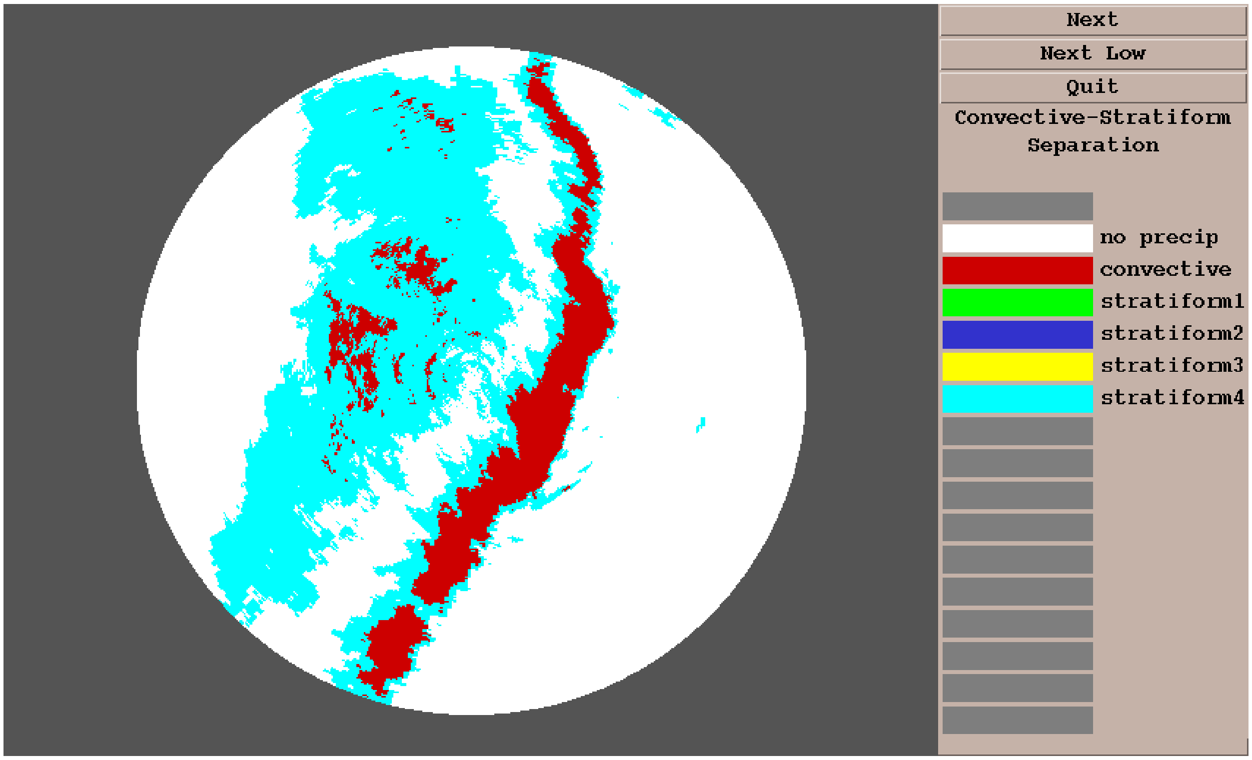

Figure 54. Output of VIL-only CSSA, corresponding to KINX VIL field in Fig. 53.

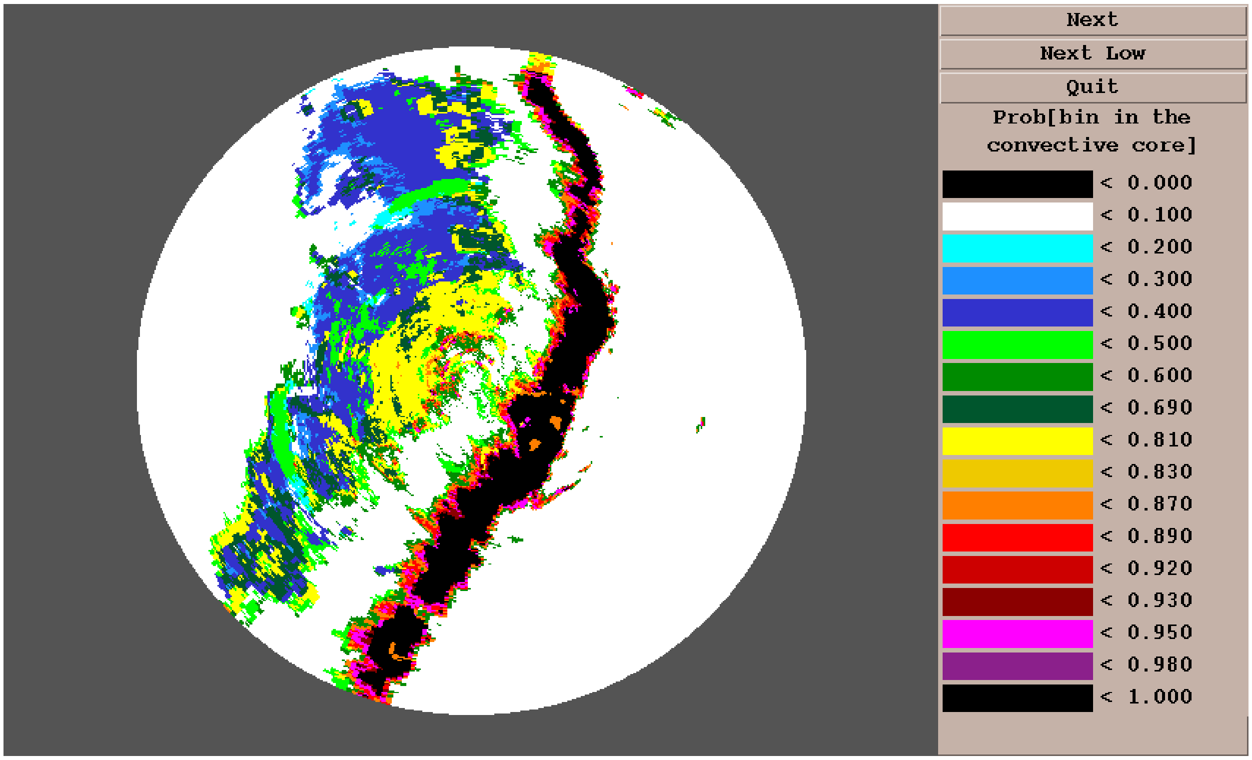

Figure 55. Output of full CSSA, KINX umbrella, corresponding to Fig. 53.

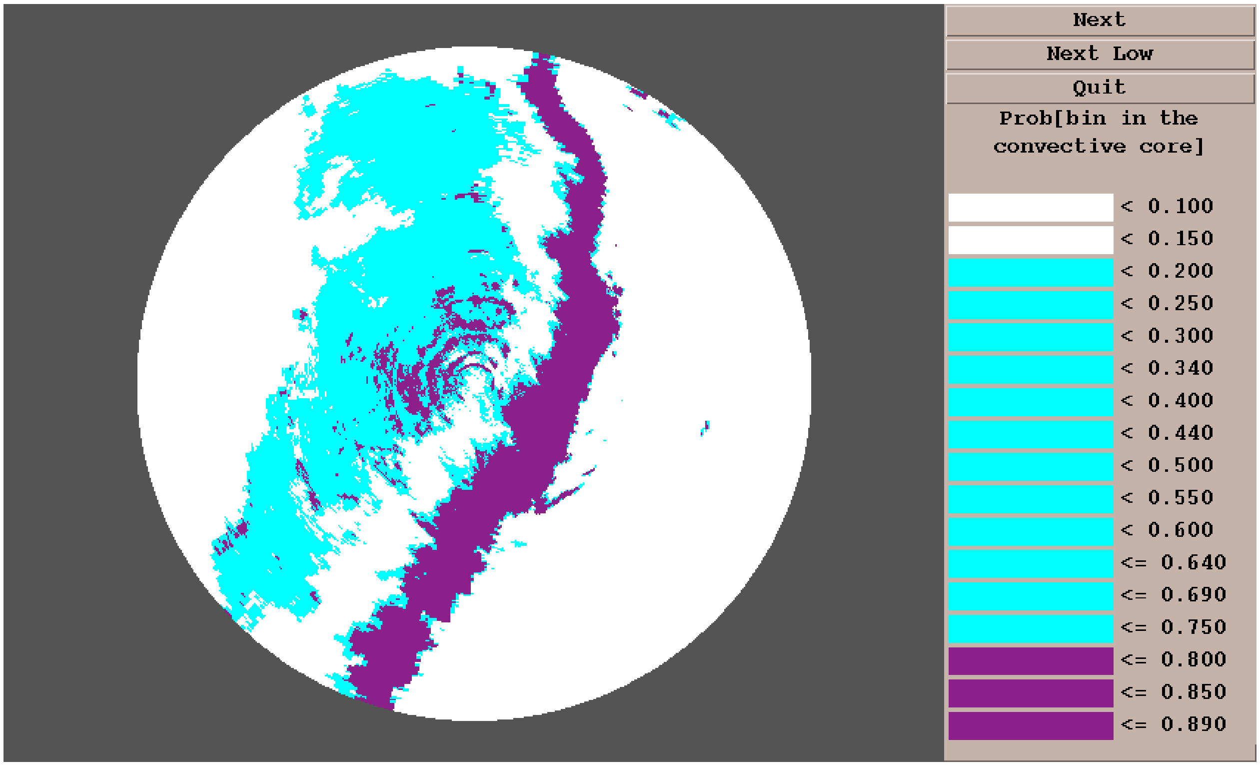

Figure 56. As in Fig. 55, except categorical CSSA, KINX umbrella.

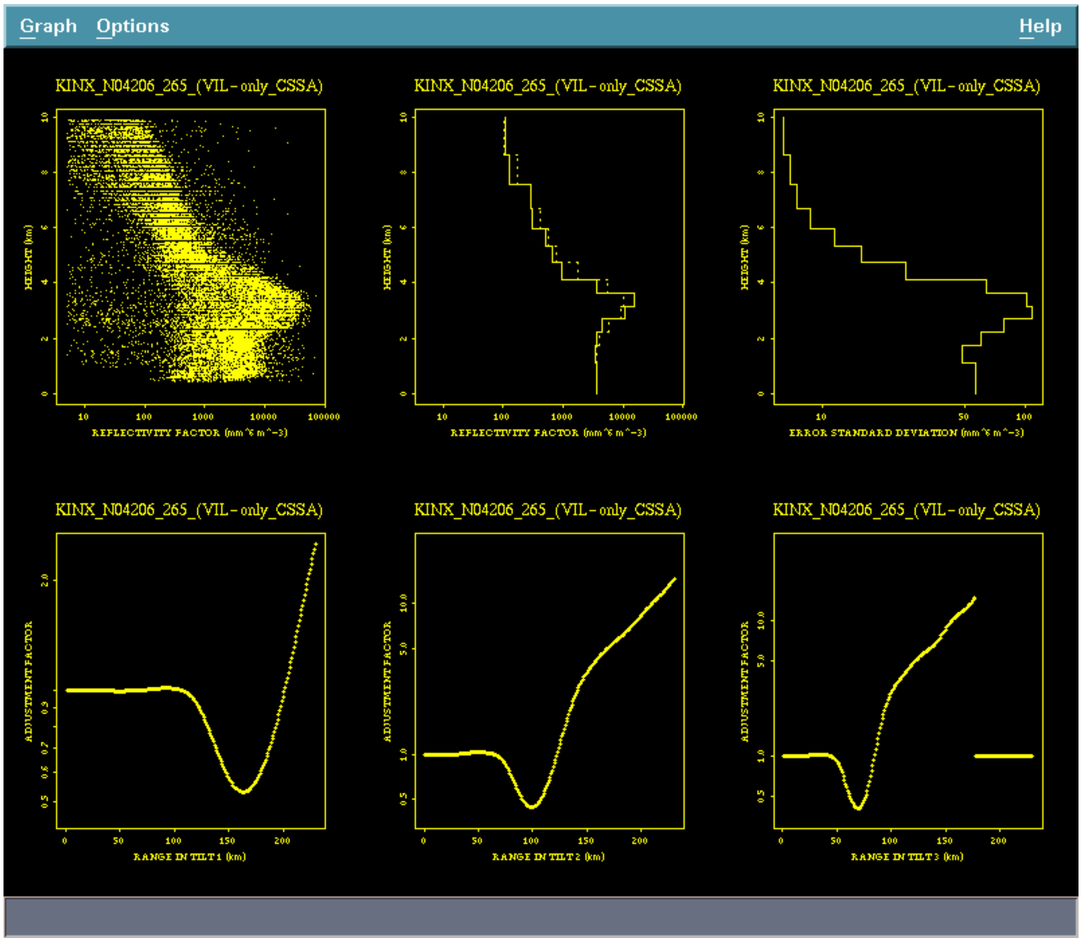

Figure 57. VPR and adjustment factor curves for KINX case, based on RCA/VIL-only CSSA.

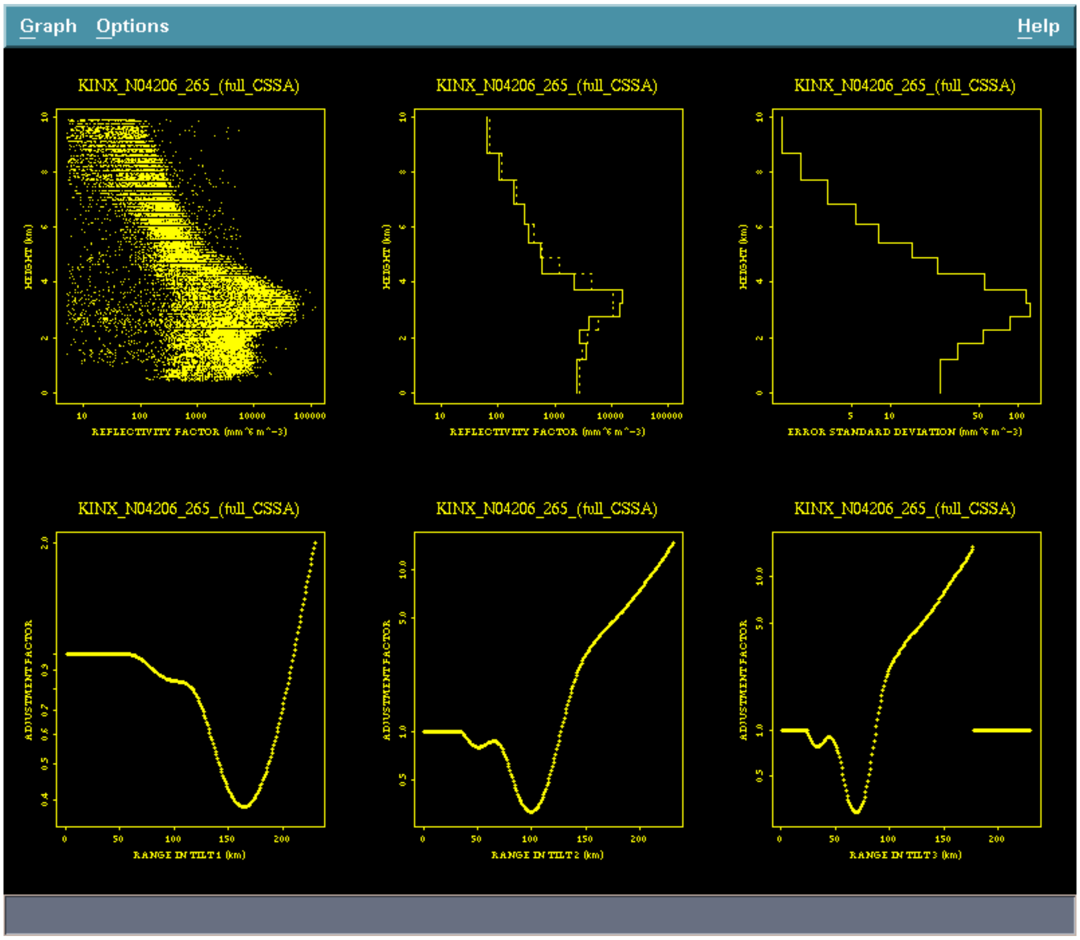

Figure 58. As in Fig. 57, except for RCA/full CSSA.

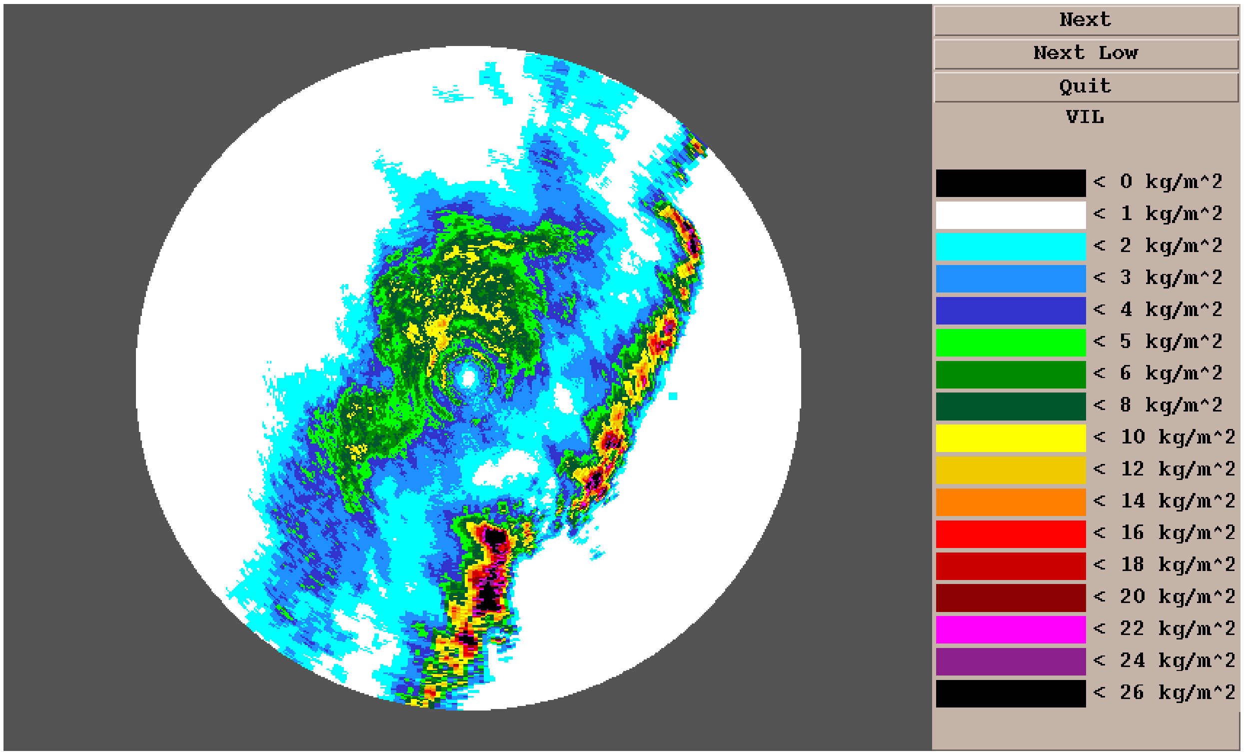

Figure 59. VIL field in KINX umbrella, 5 August 1995. Observations are later than those in Fig. 53.

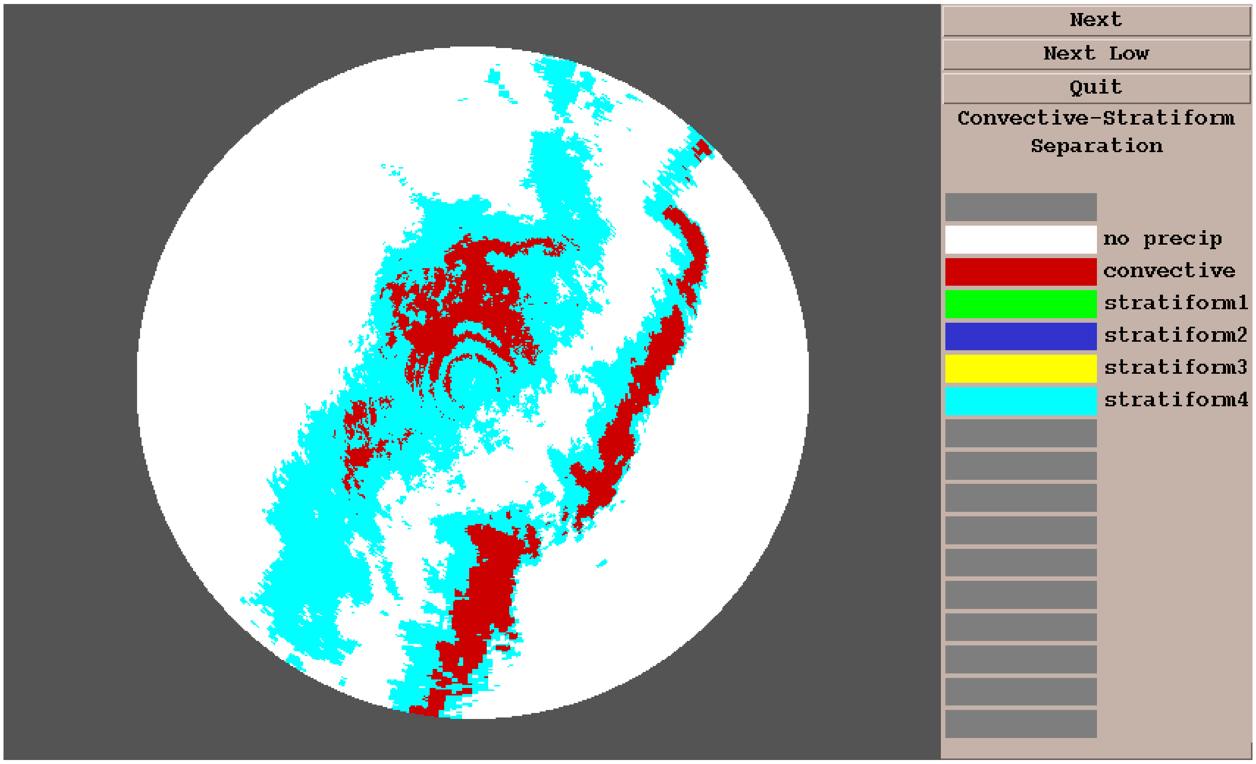

Figure 60. Output of VIL-only CSSA, KINX umbrella, corresponding to VIL field in Fig. 59.

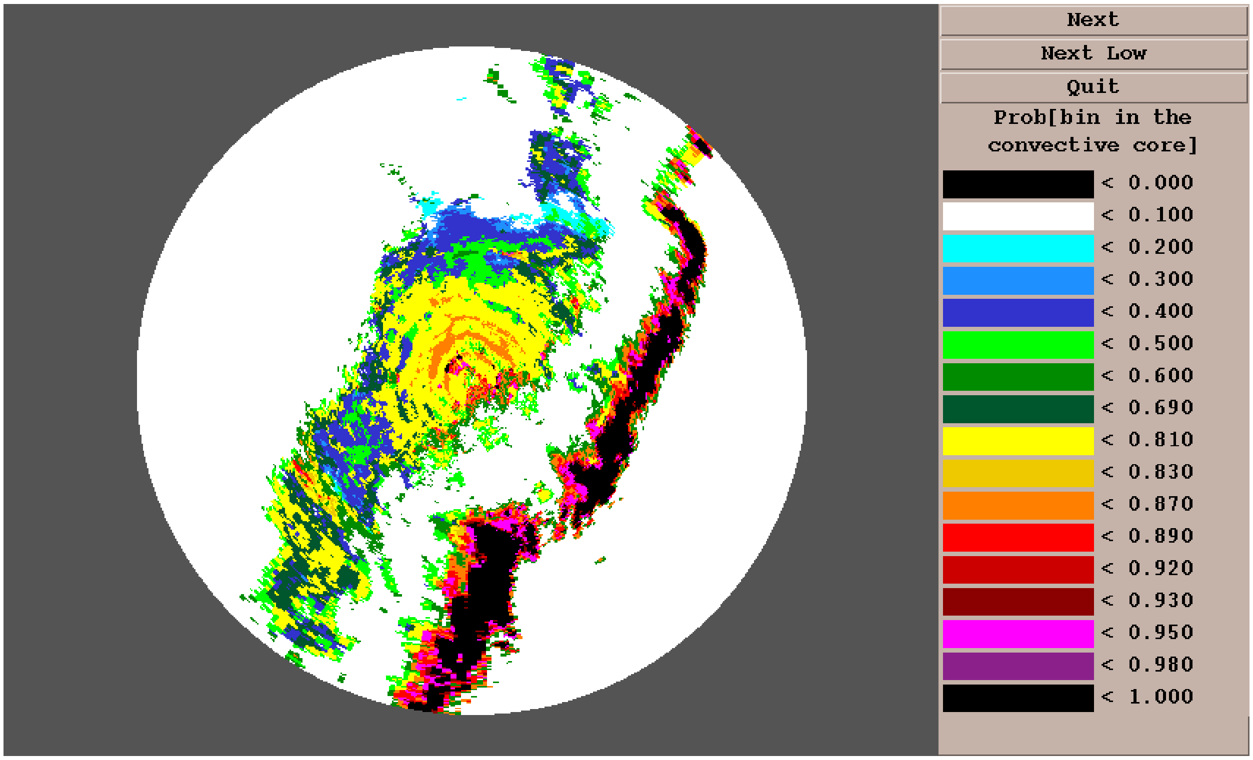

Figure 61. Output of full CSSA, KINX umbrella, corresponding to Fig. 59.

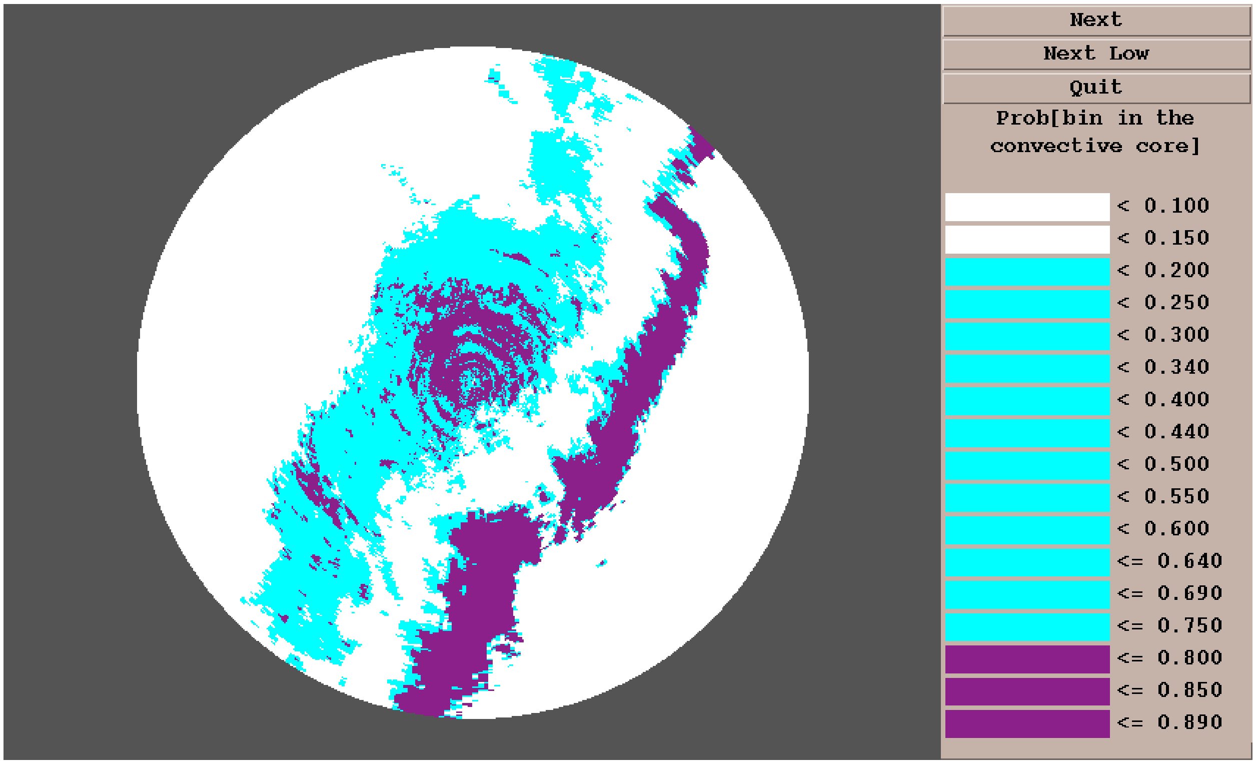

Figure 62. Categorical CSSA, KINX umbrella, corresponding to Figs. 61 and 59.

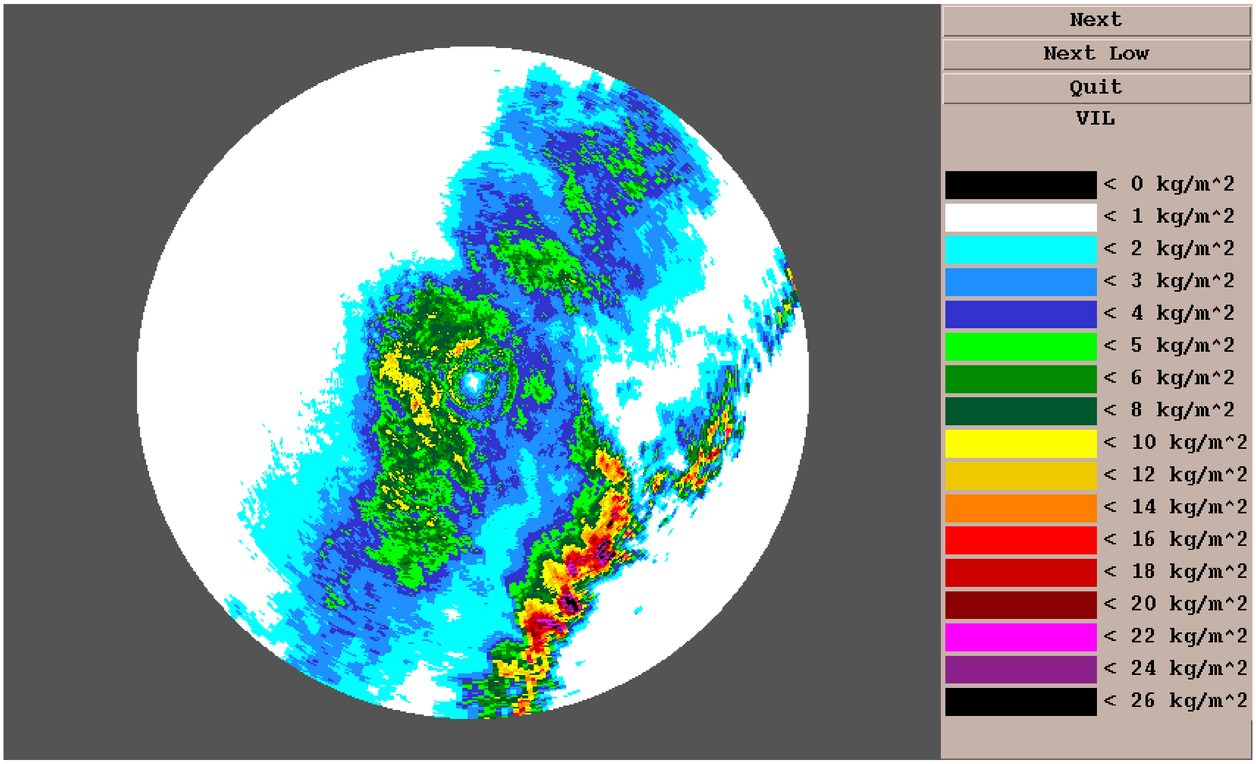

Figure 63. VIL field, KINX umbrella, 5 August 1995. Observations are later than those in Fig. 53.

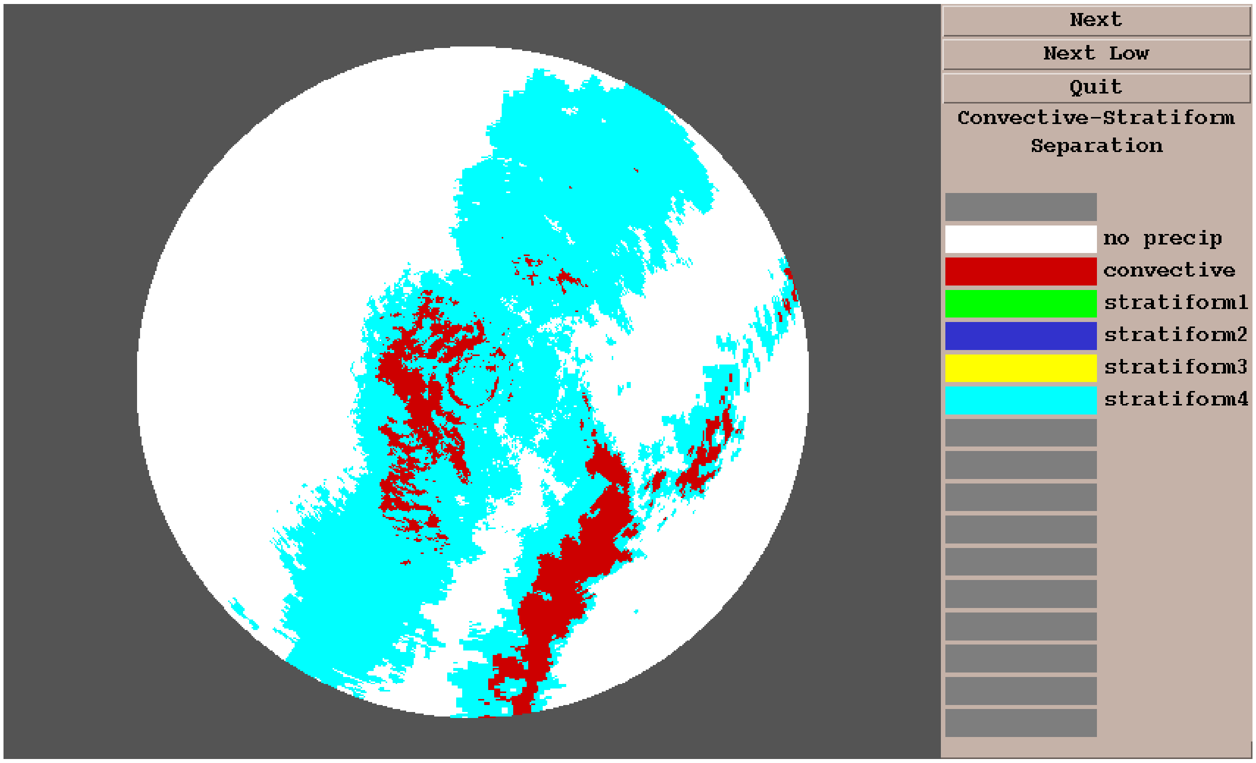

Figure 64. Output of VIL-only CSSA, KINX umbrella, corresponding to Fig. 63.

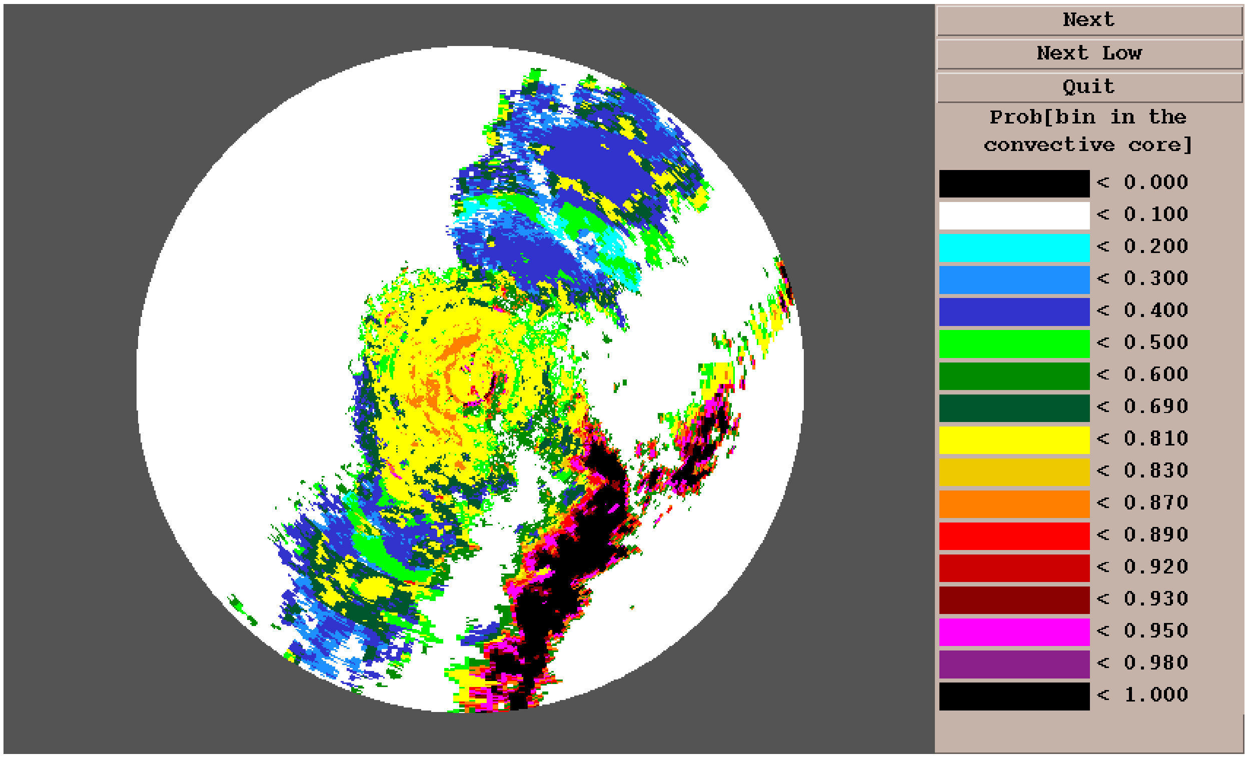

Figure 65. Output of full CSSA, KINX umbrella, corresponding to Fig. 63.

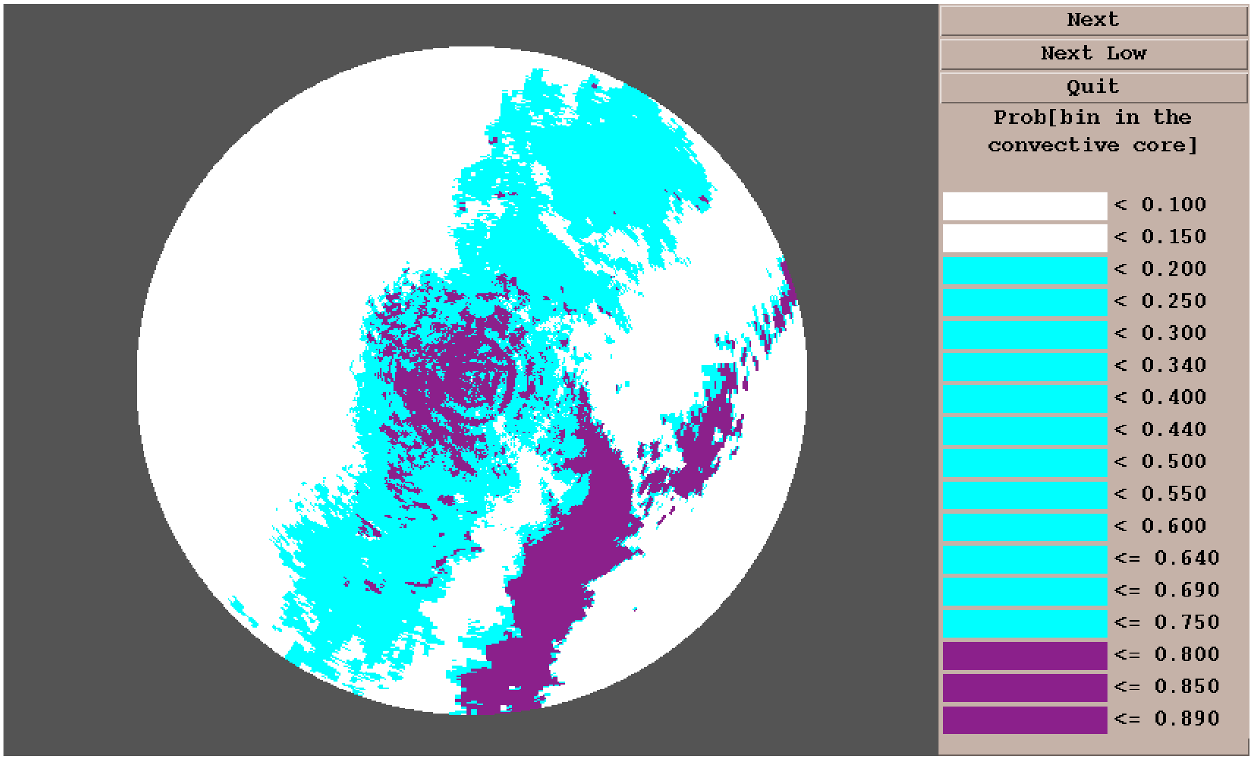

Figure 66. Categorical CSSA, KINX umbrella, corresponding to Fig. 63.

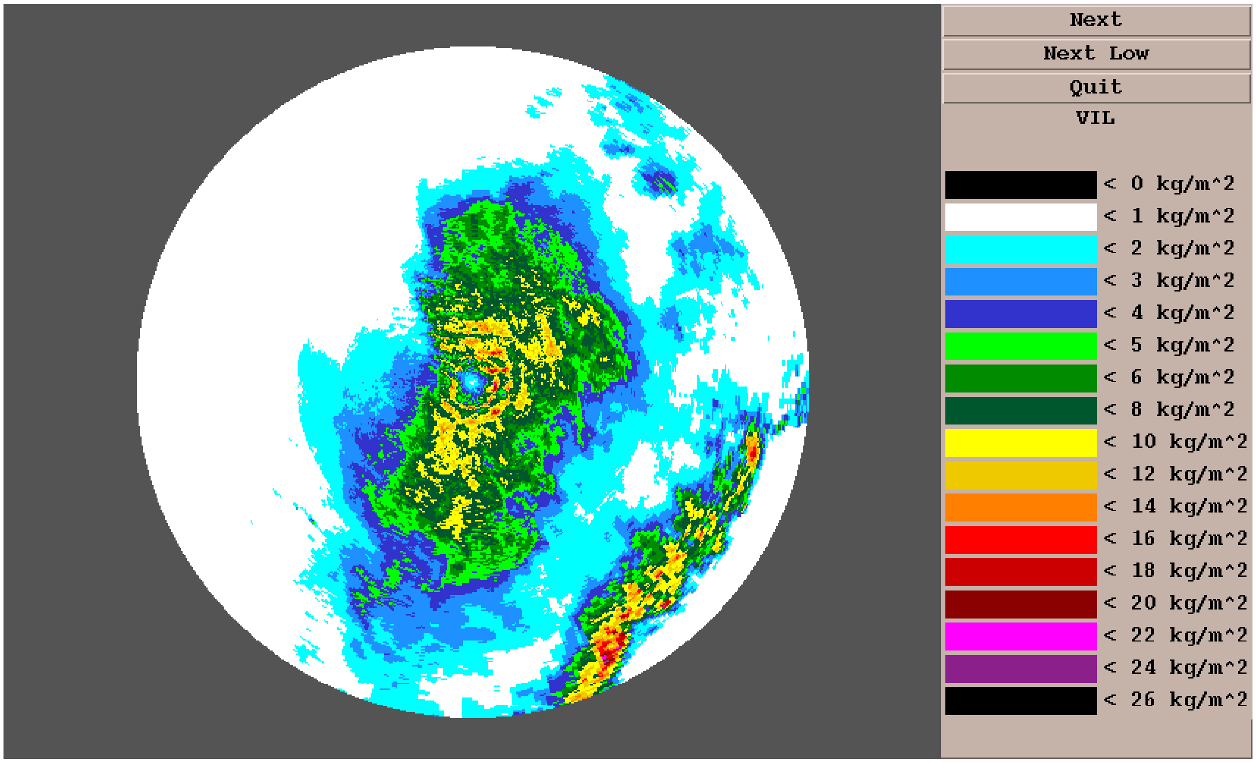

Figure 67. VIL field in KINX umbrella, 5 August 1995. Observations are later than those in Fig. 63.

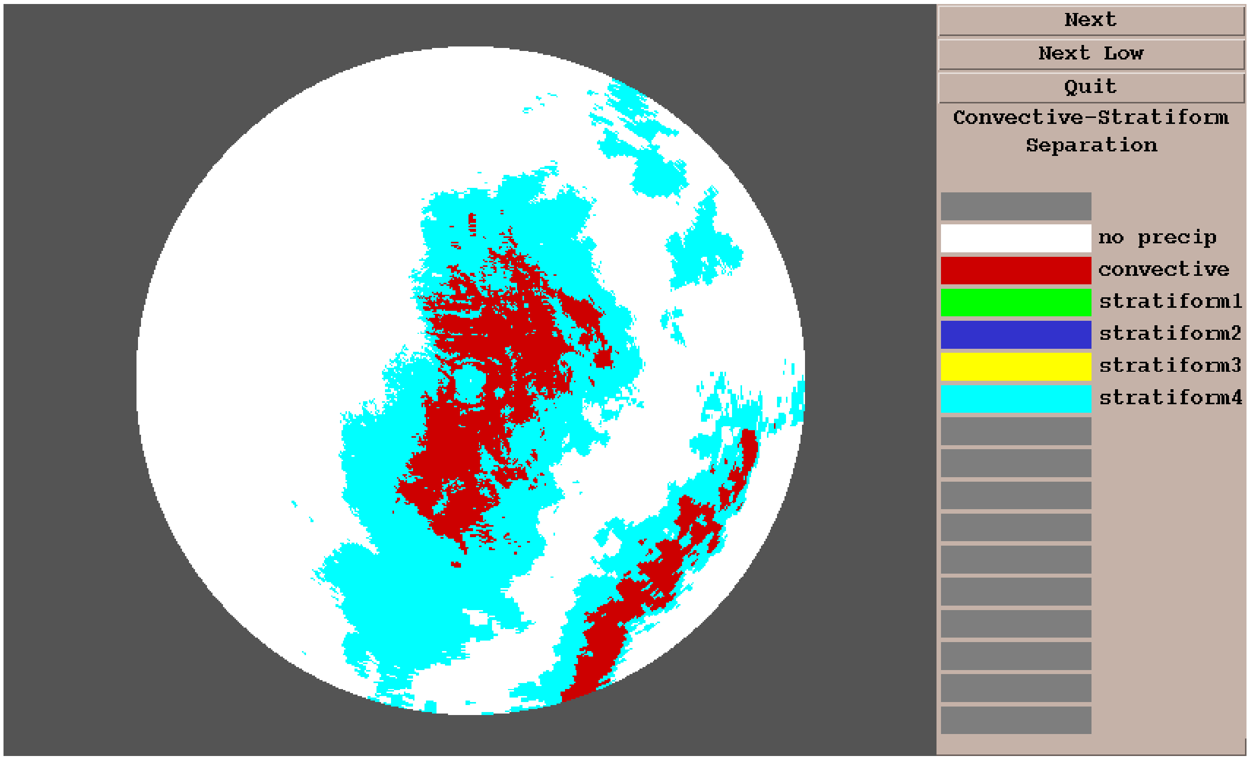

Figure 68. VIL-only CSSA, KINX umbrella, for VIL field in Fig. 67.

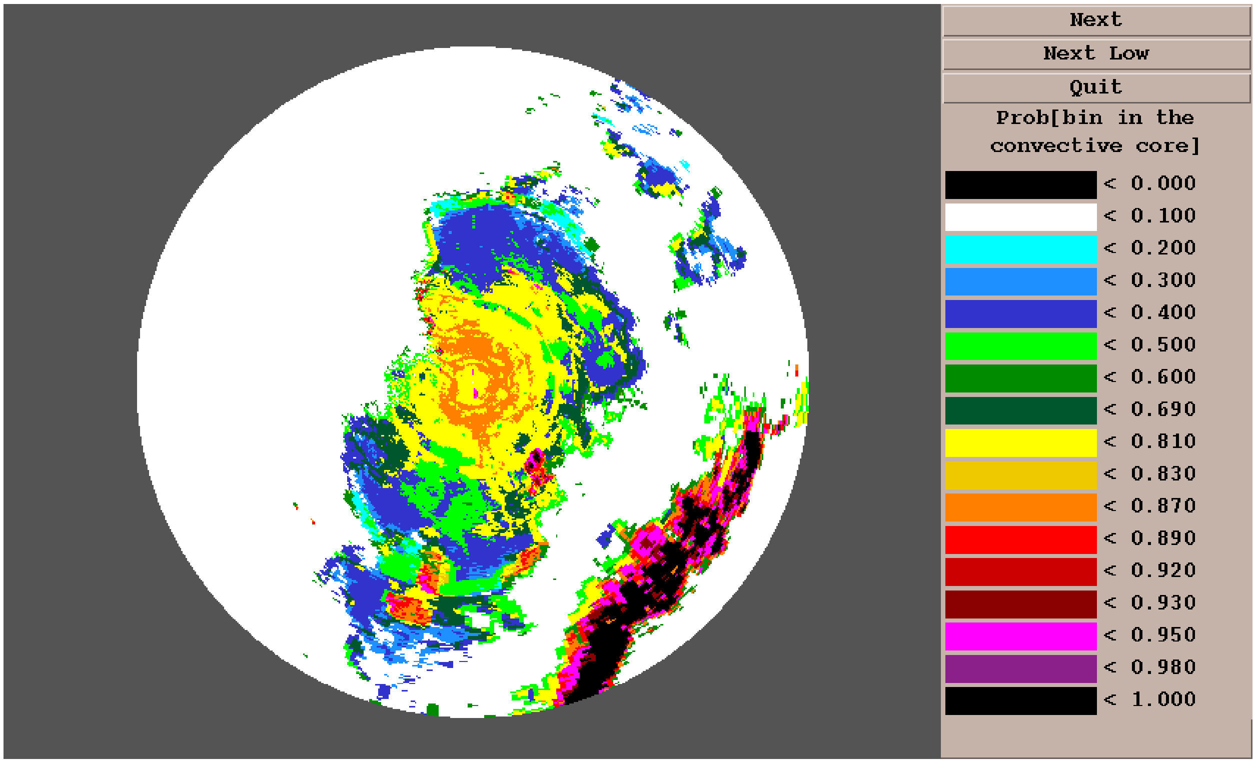

Figure 69. Output of full CSSA, KINX umbrella, for corresponding to field in Fig. 67.

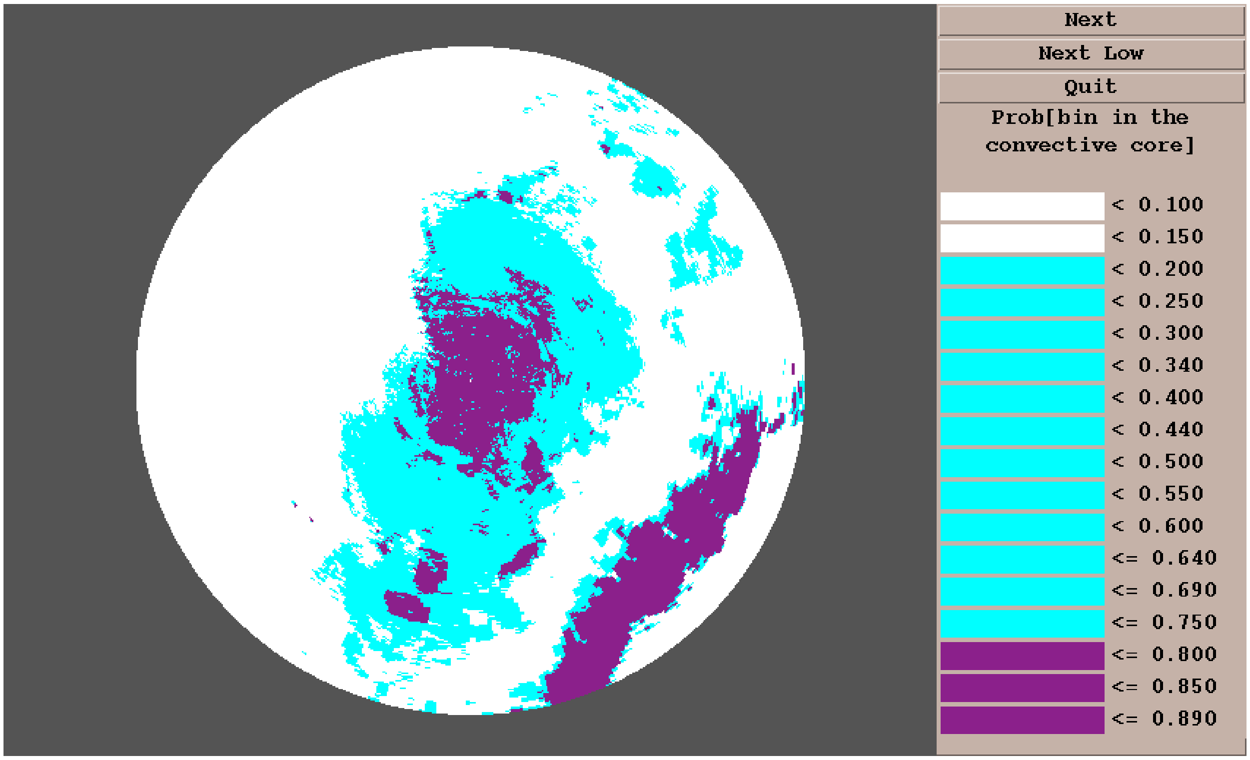

Figure 70. Categorical CSSA, KINX umbrella, corresponding to Fig. 69.

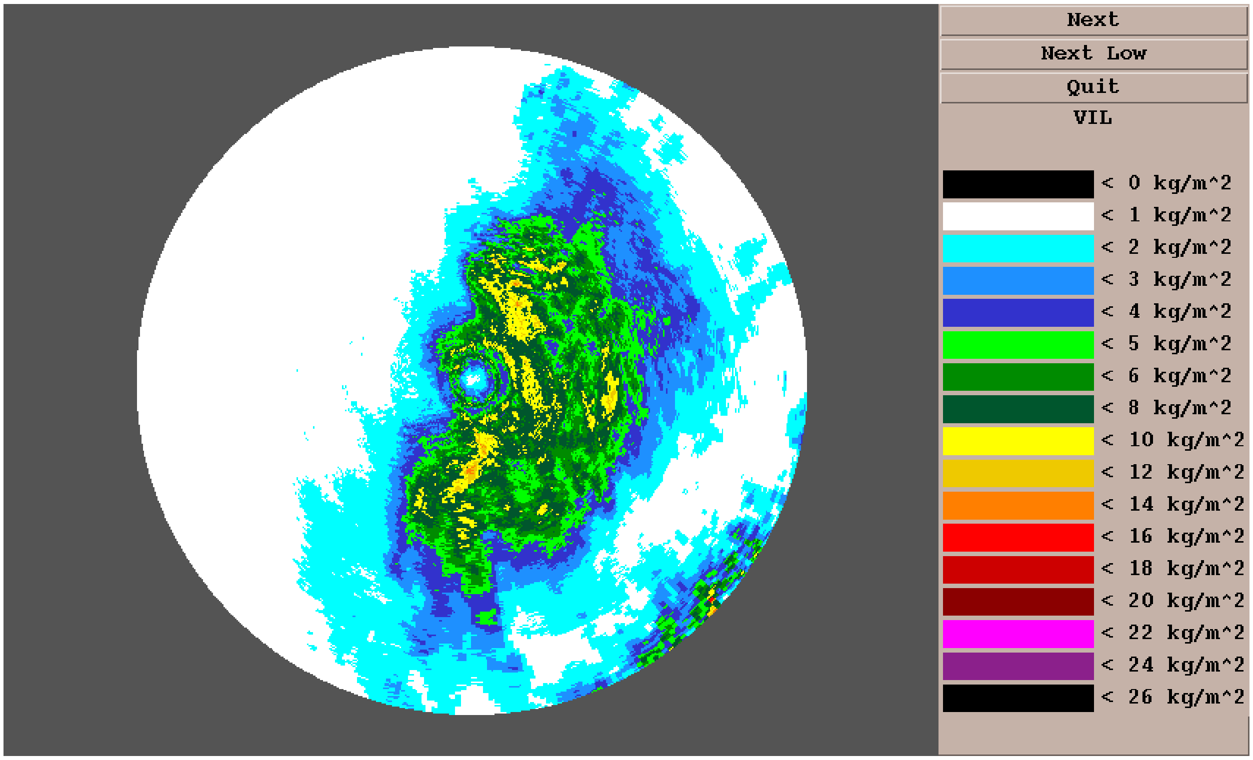

Figure 71. VIL field, KINX umbrella, 5 August 1995. Observations are later than those in Fig. 67.

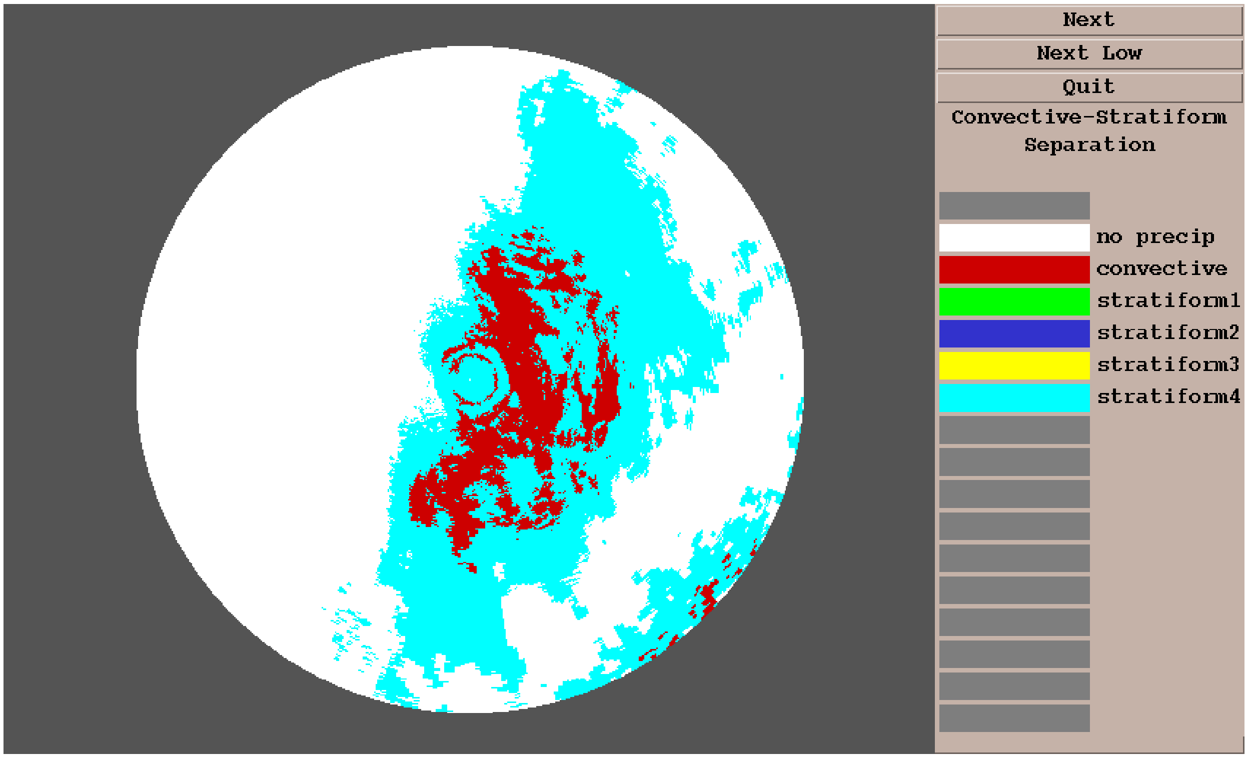

Figure 72. VIL-only CSSA, KINX umbrella, corresponding to Fig. 71.

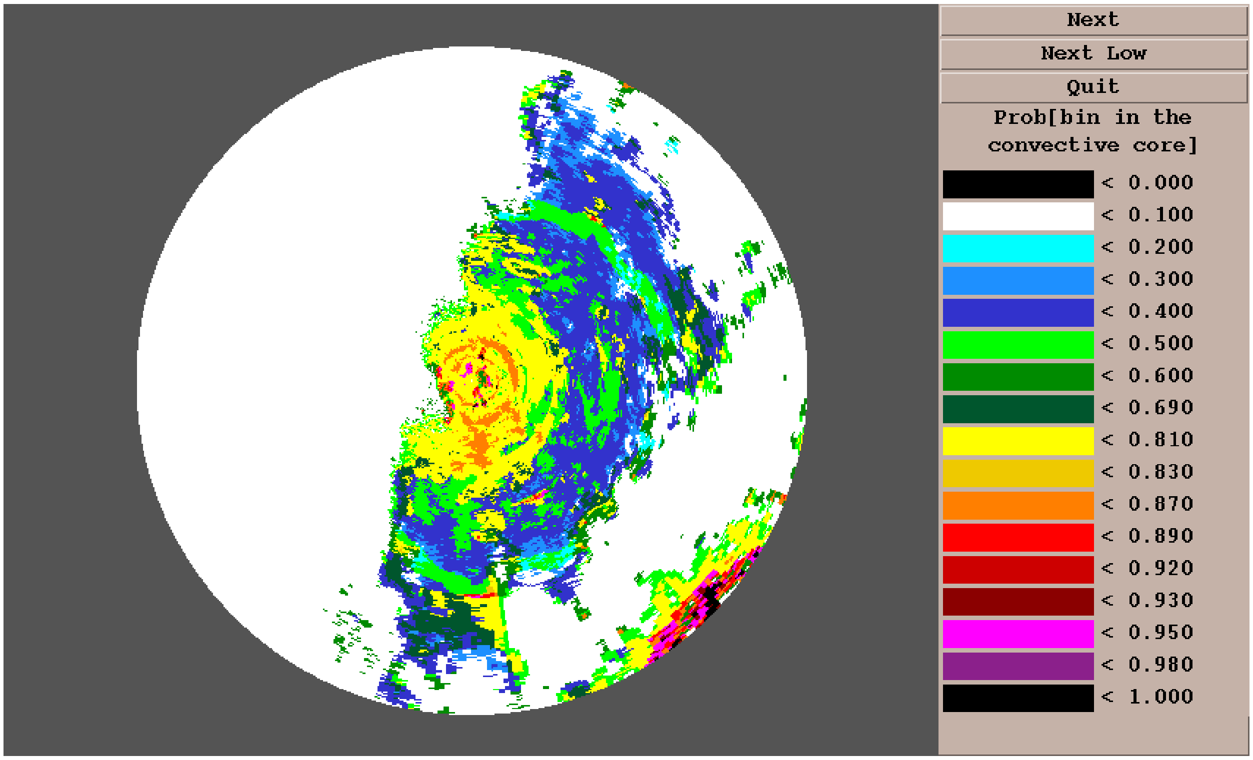

Figure 73. Output of full CSSA, KINX umbrella, corresponding to Fig. 71.

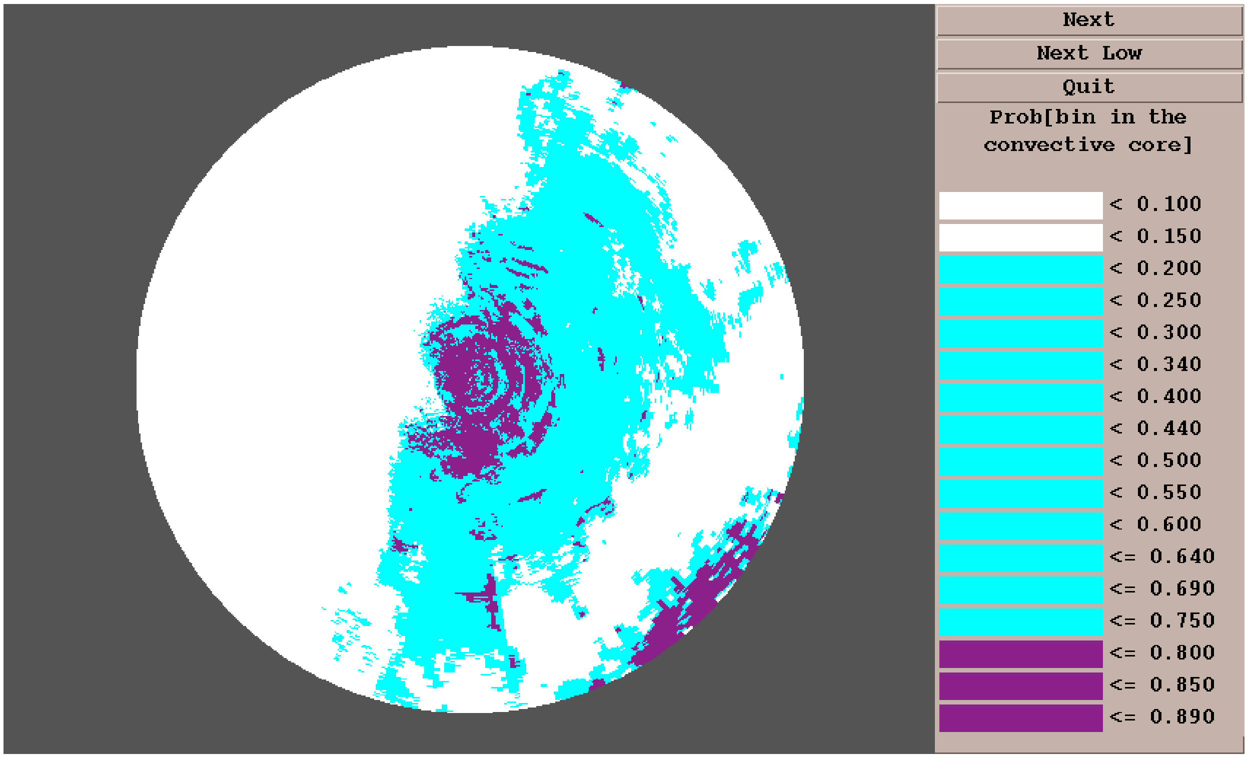

Figure 74. Categorical CSSA, KINX umbrella, corresponding to Fig. 73.

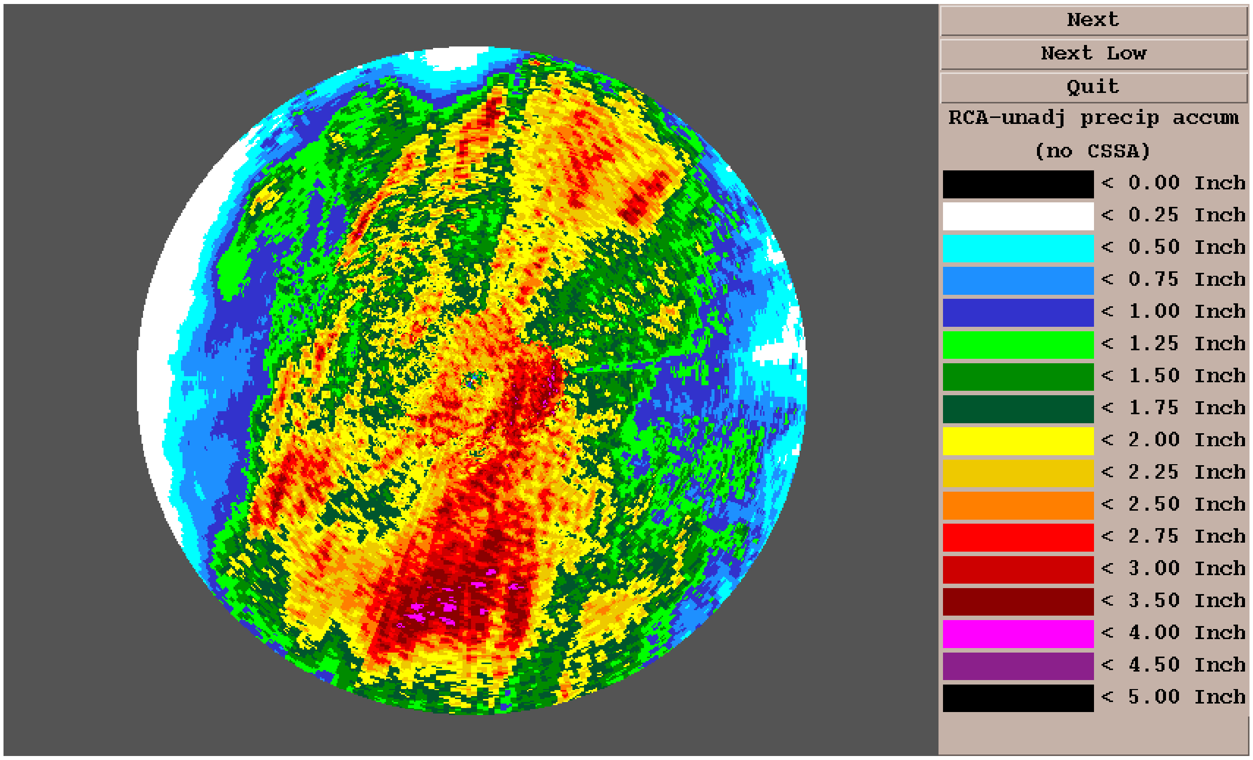

Figure 75. Rainfall over ~7.5 h, KINX umbrella, no range correction.

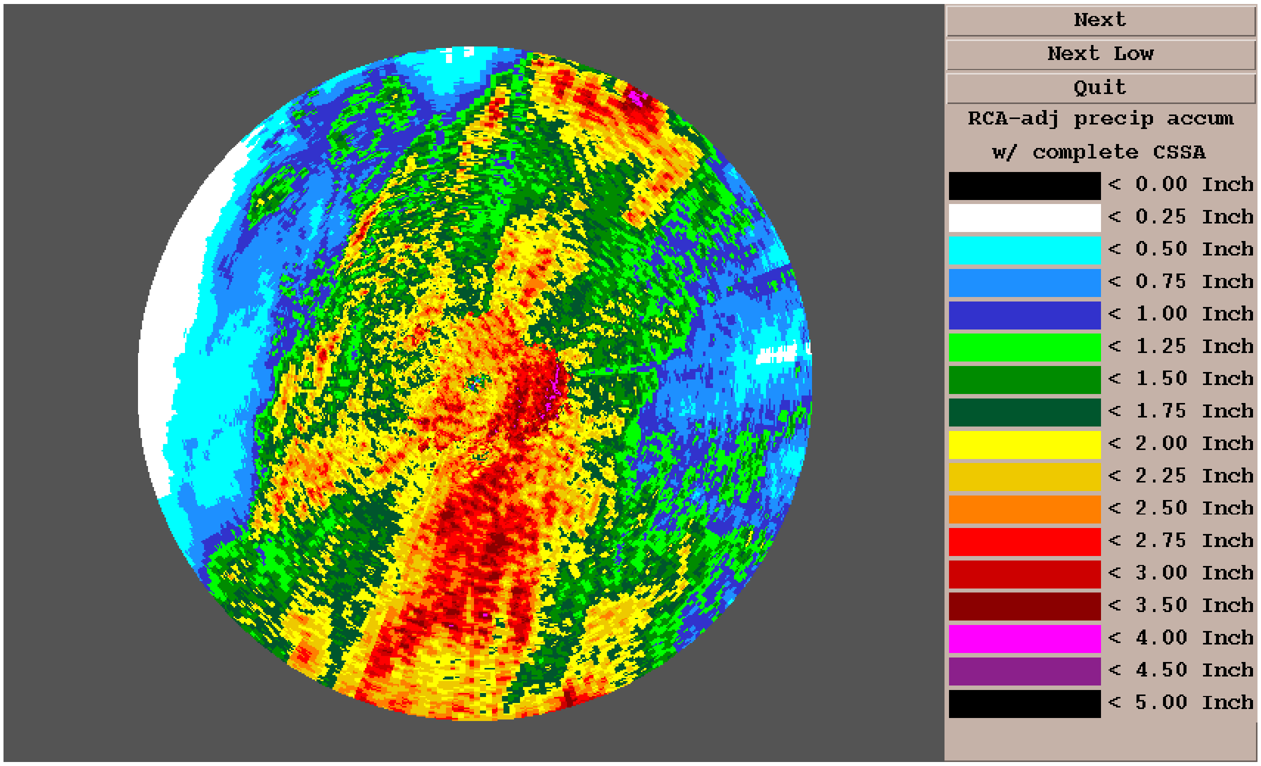

Figure 76. As in Fig. 75., except with RCA/full CSSA.

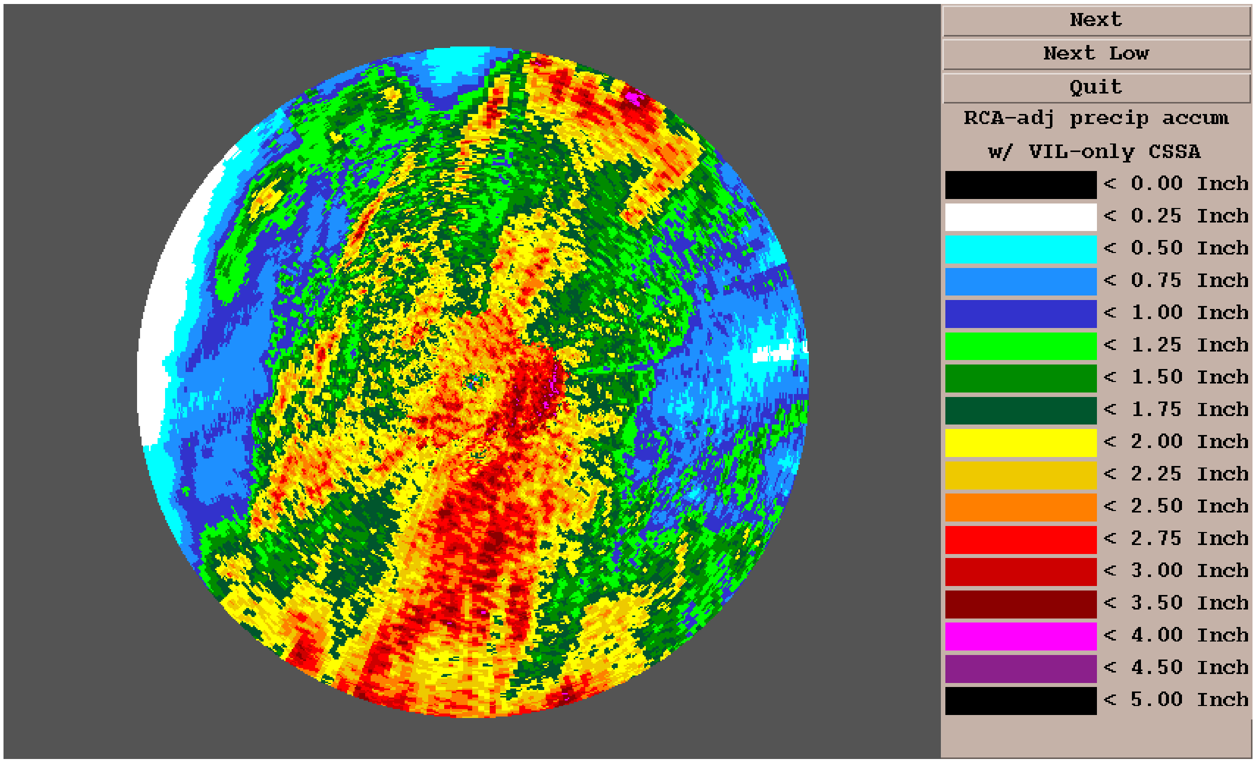

Figure 77. As in Fig. 75, except with RCA/VIL-only CSSA.

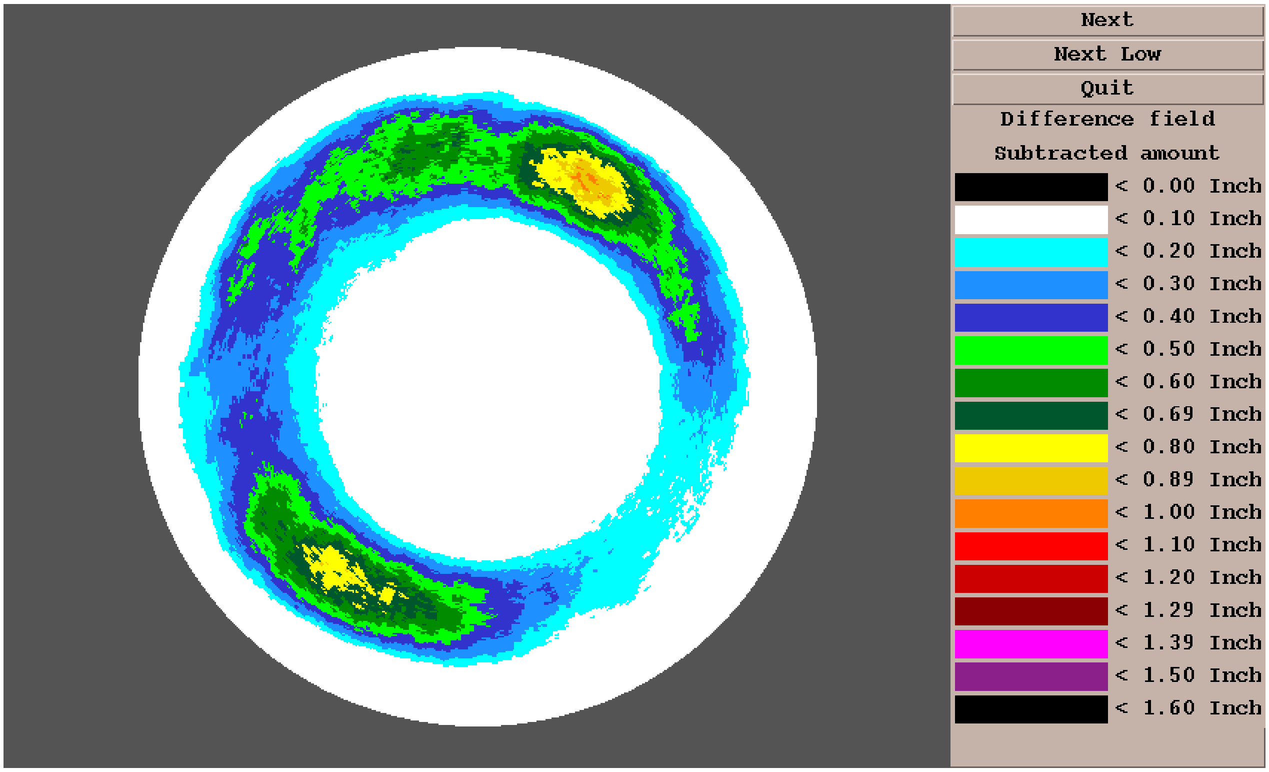

Figure 78. Rainfall apparently subtracted by RCA/full CSSA, corresponding to rainfall in Figs. 75 and 76.

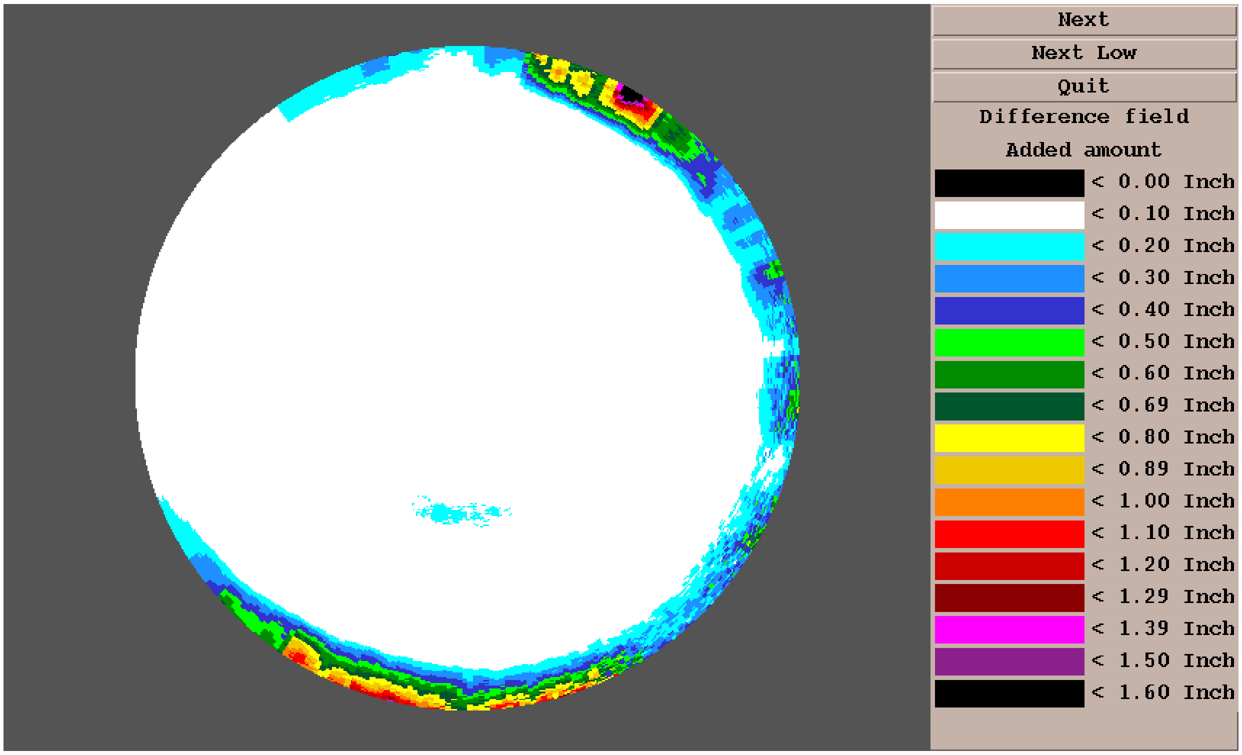

Figure 79. Rainfall apparently added by RCA/full CSSA, corresponding to rainfall in Figs. 75 and 76

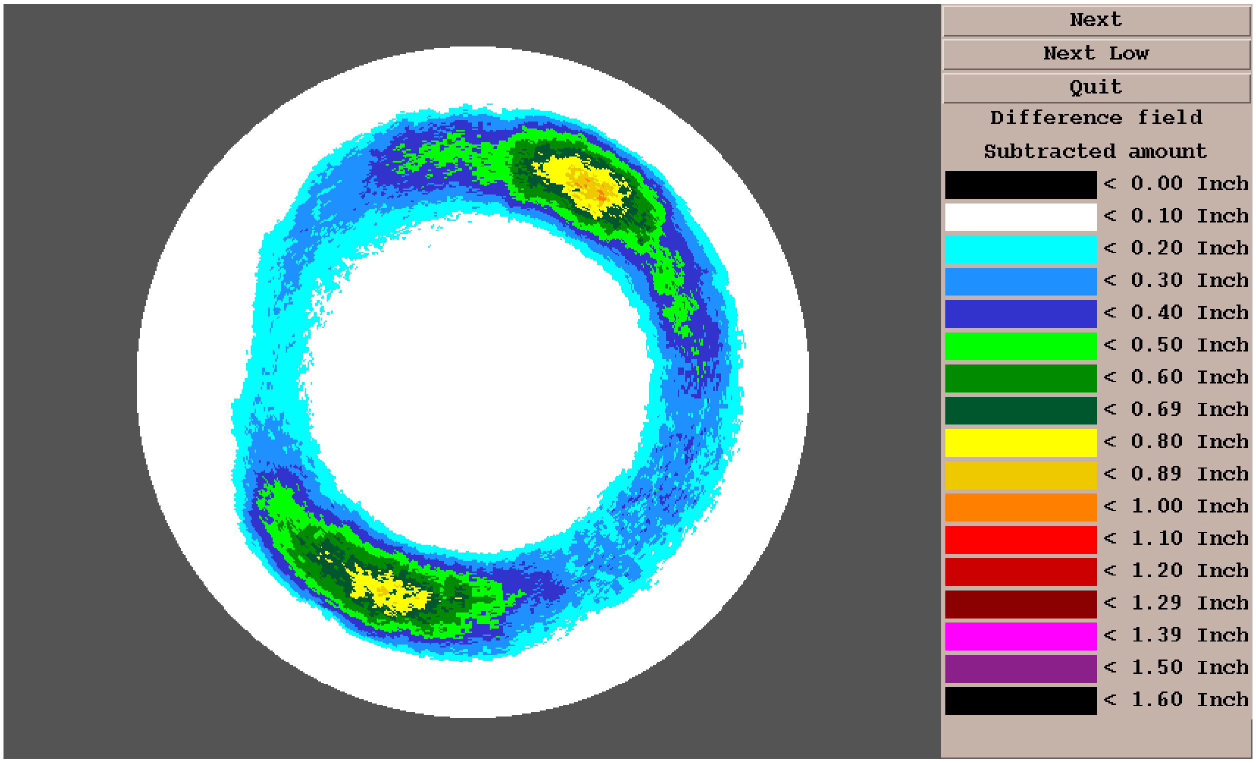

Figure 80. Rainfall apparently subtracted by RCA/VIL-only CSSA, corresponding to rainfall in Figs. 75 and 77.

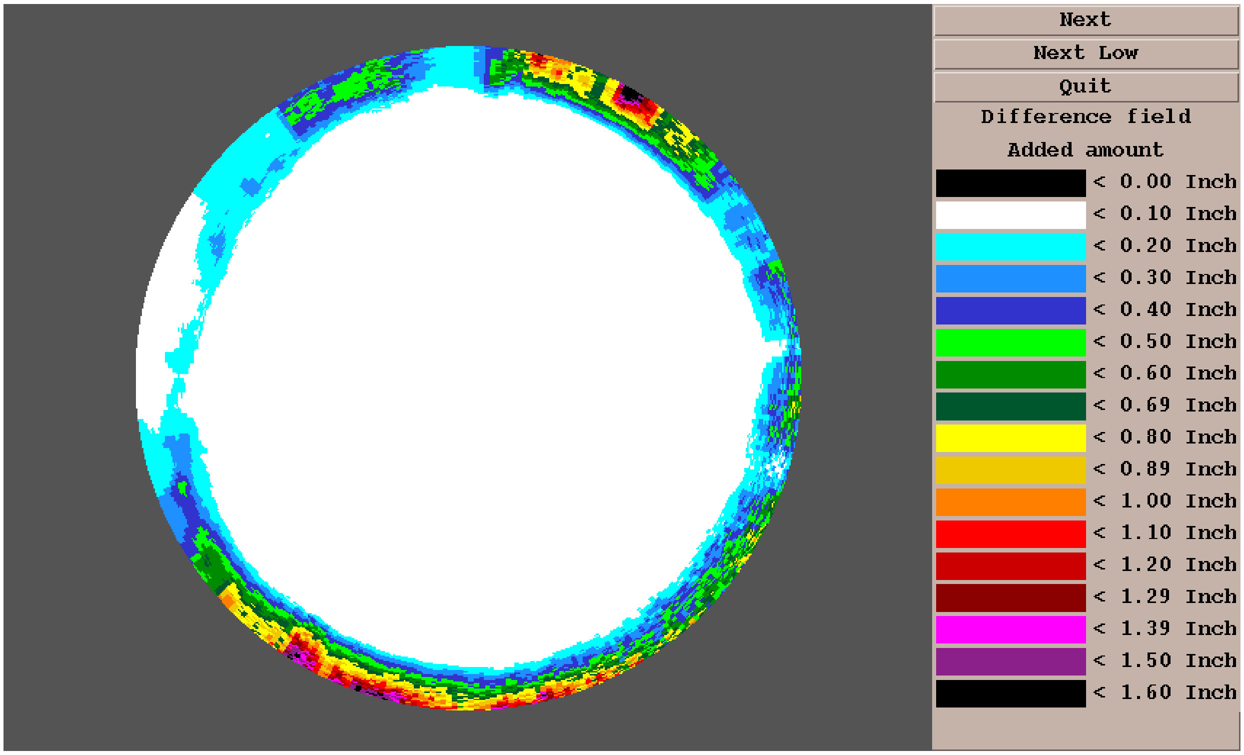

Figure 81. Rainfall apparently added by RCA/VIL-only CSSA, corresponding to rainfall in Figs. 75 and 77.

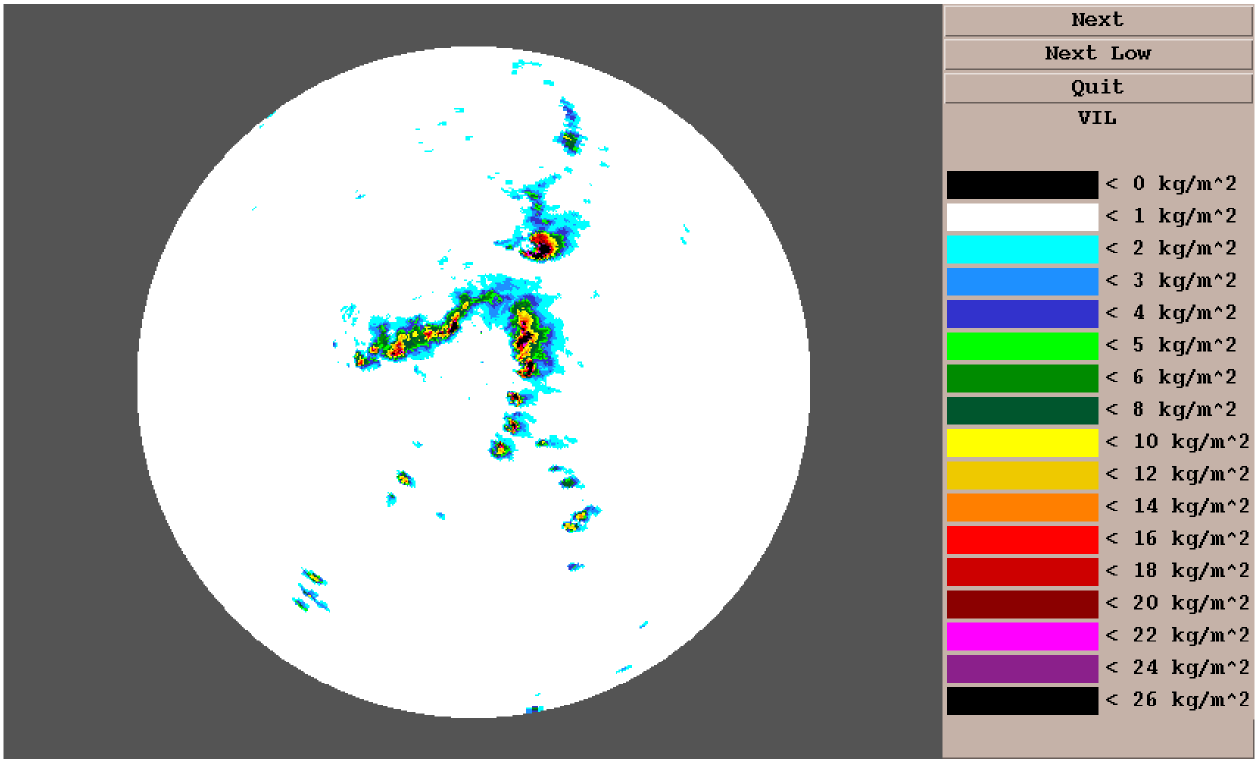

Figure 82. VIL field in KMLB umbrella, 25 March 1992.

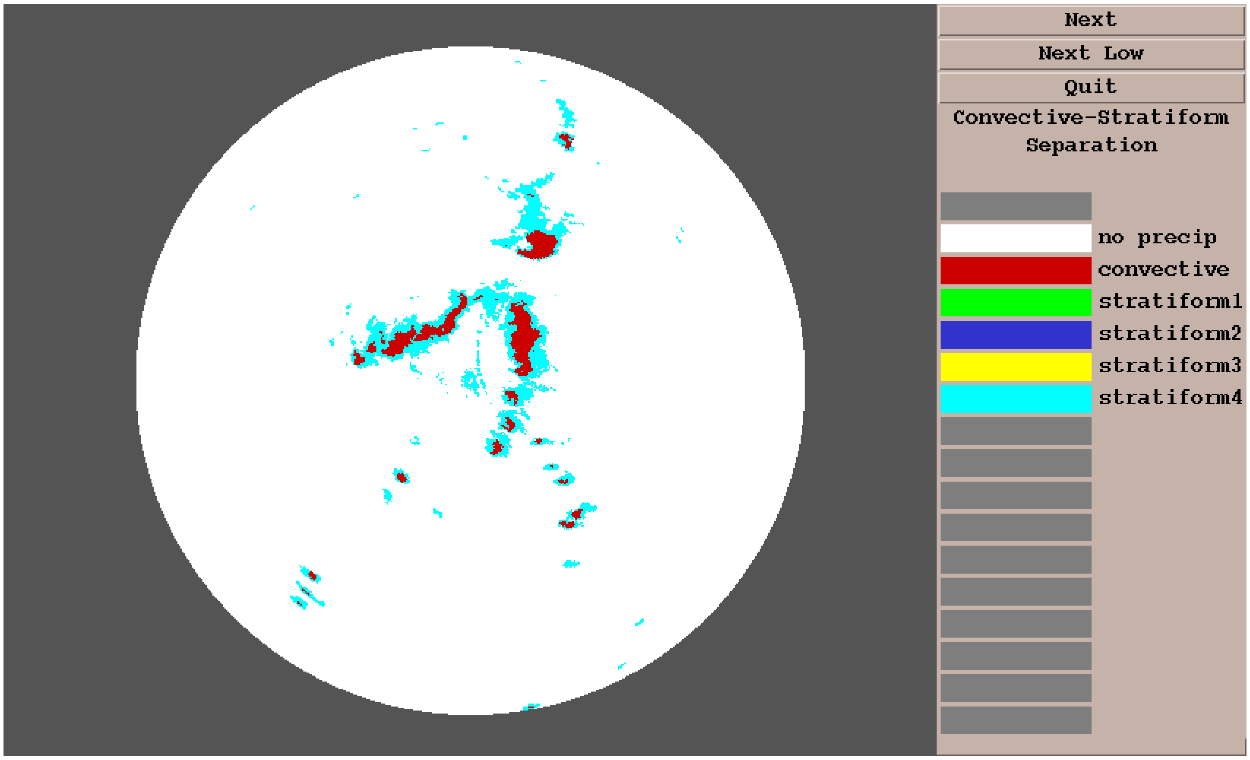

Figure 83. Output of VIL-only CSSA, KMLB umbrella.

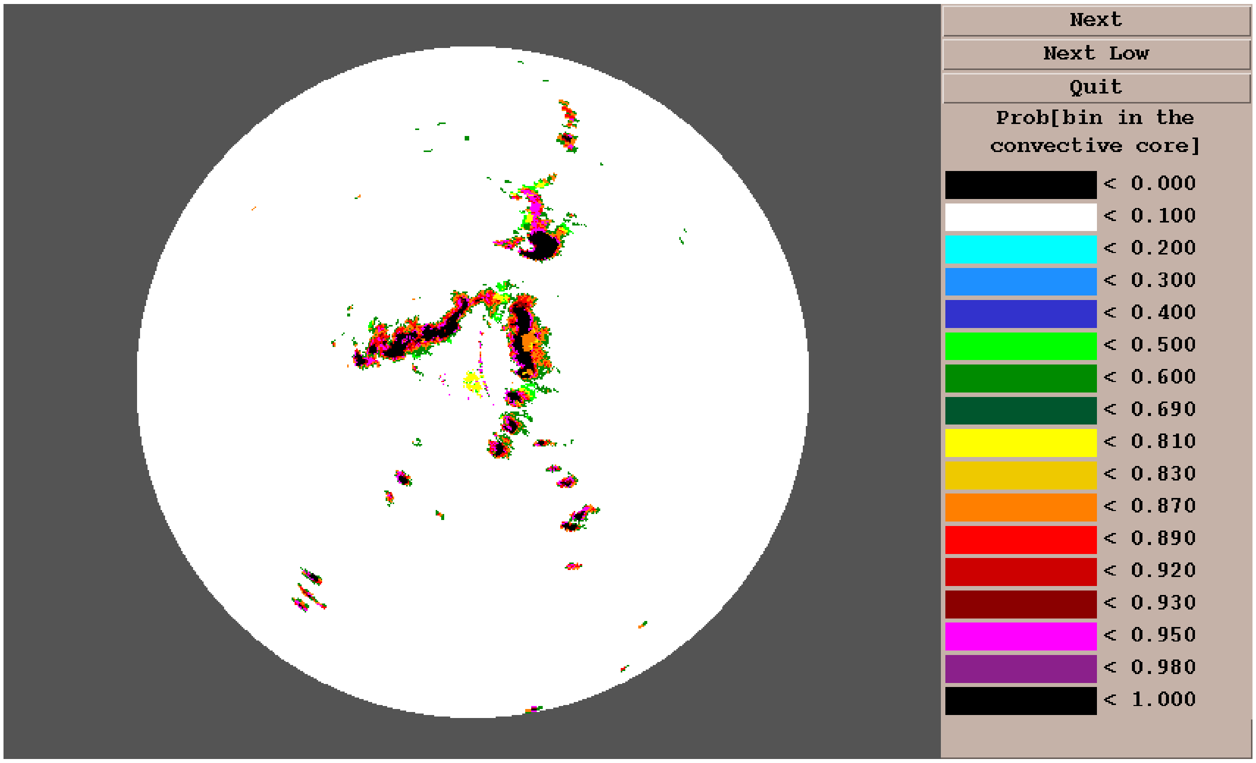

Figure 84. Output of full CSSA, KMLB umbrella.

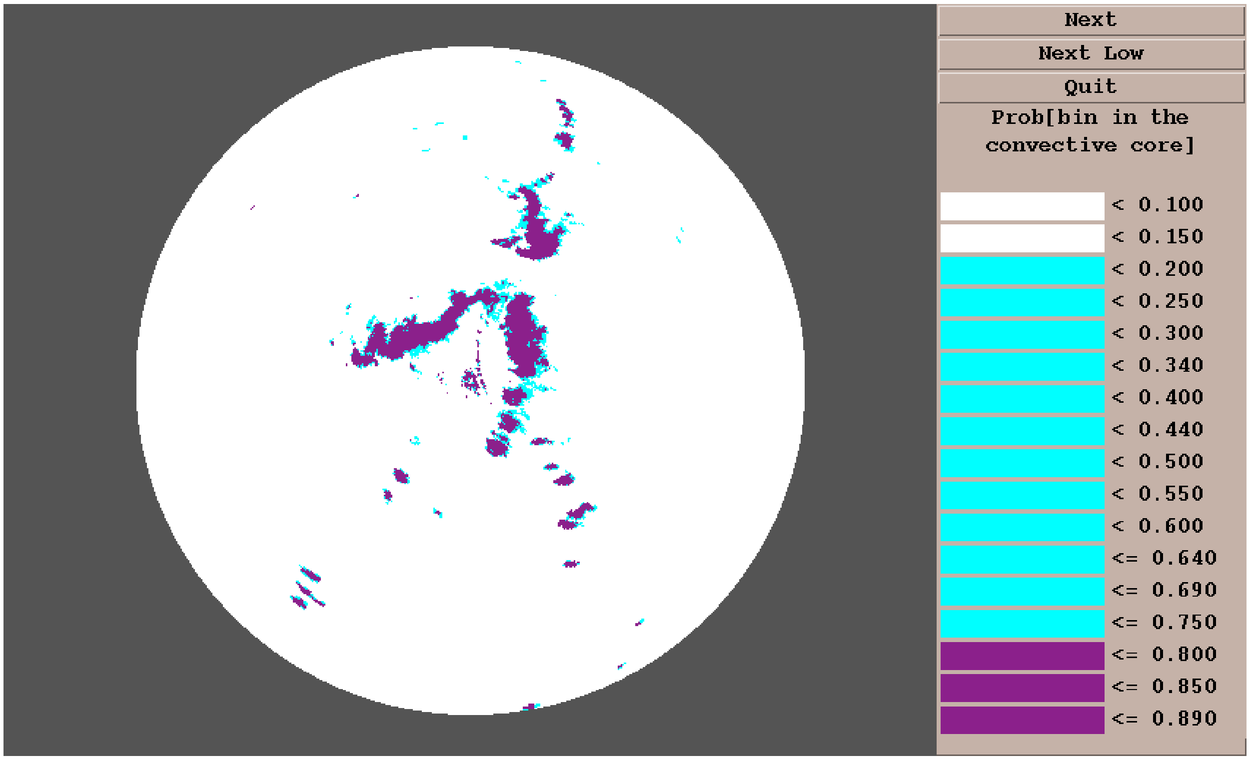

Figure 85. Categorical CSSA corresponding to output in Fig. 84.

:

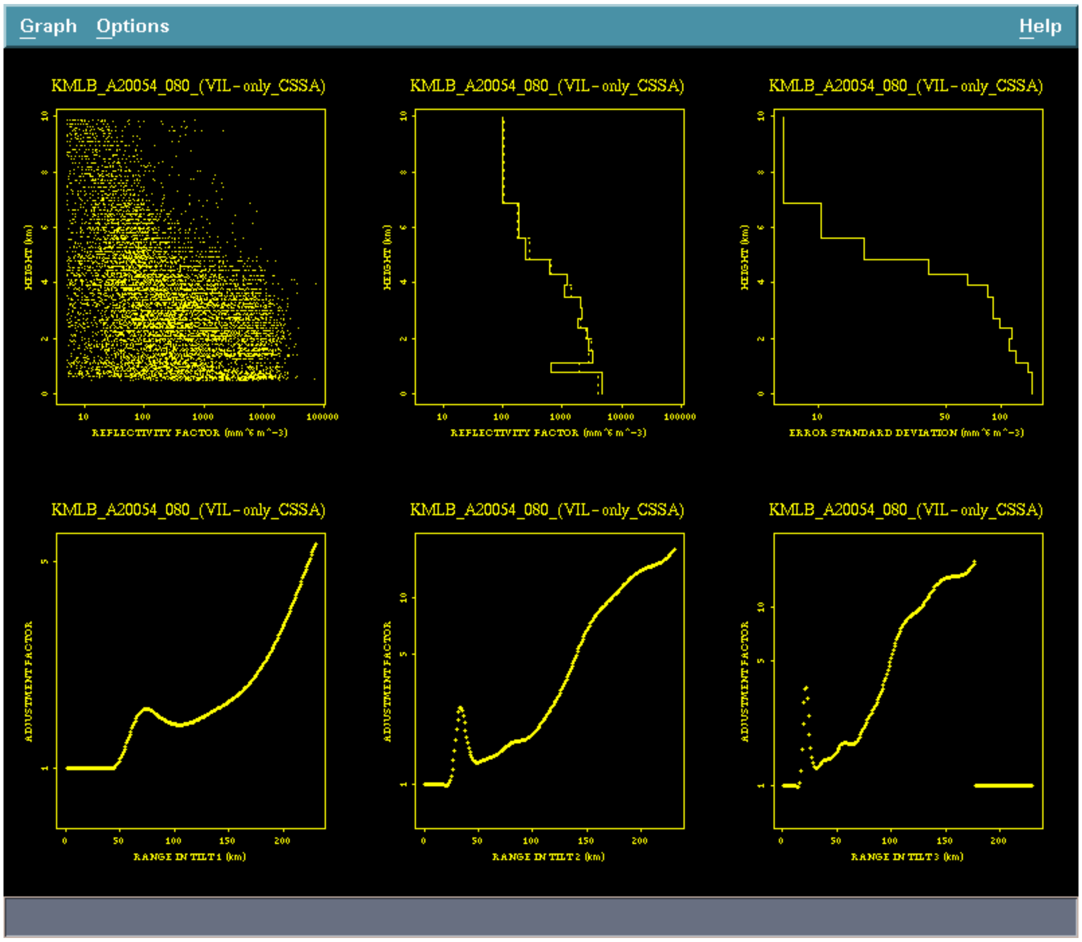

Figure 86. VPR and adjustment factors from RCA/VIL-only CSSA for KMLB case.

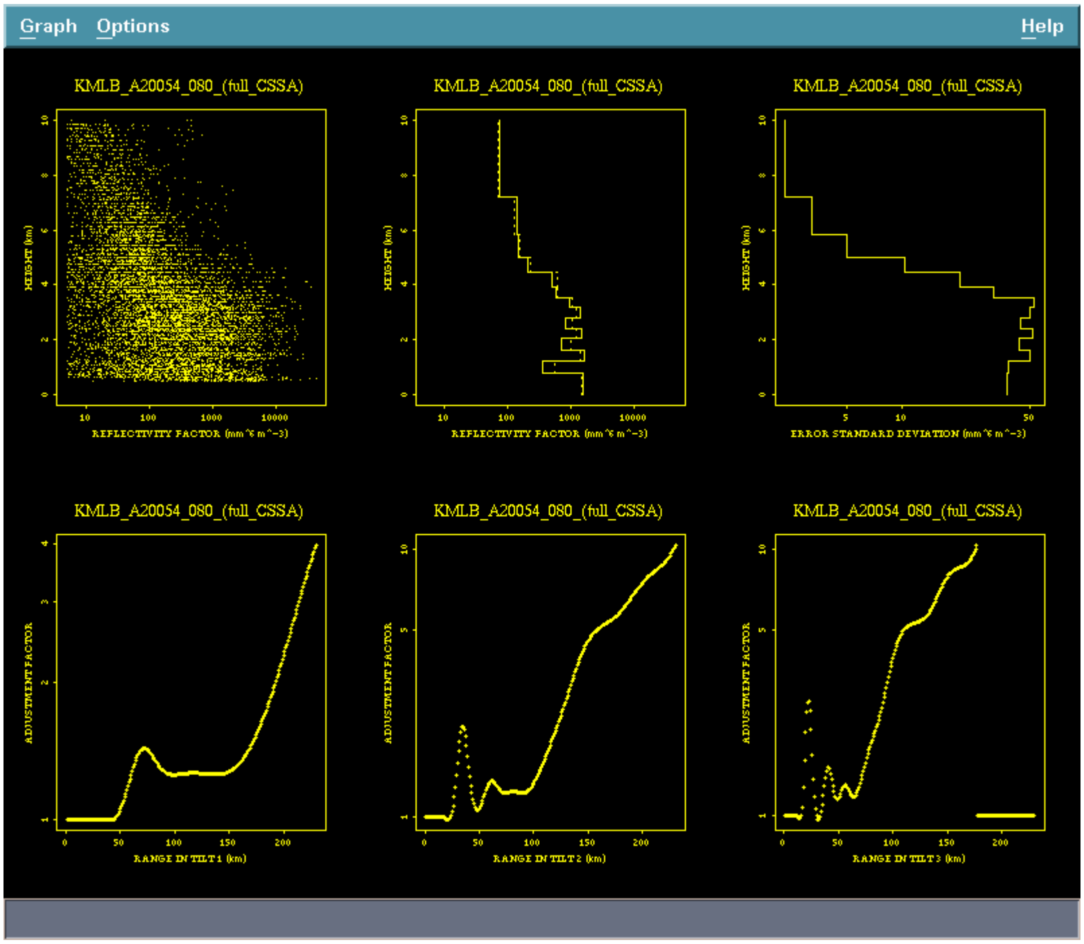

Figure 87. As in Fig. 86, except for RCA/full CSSA.

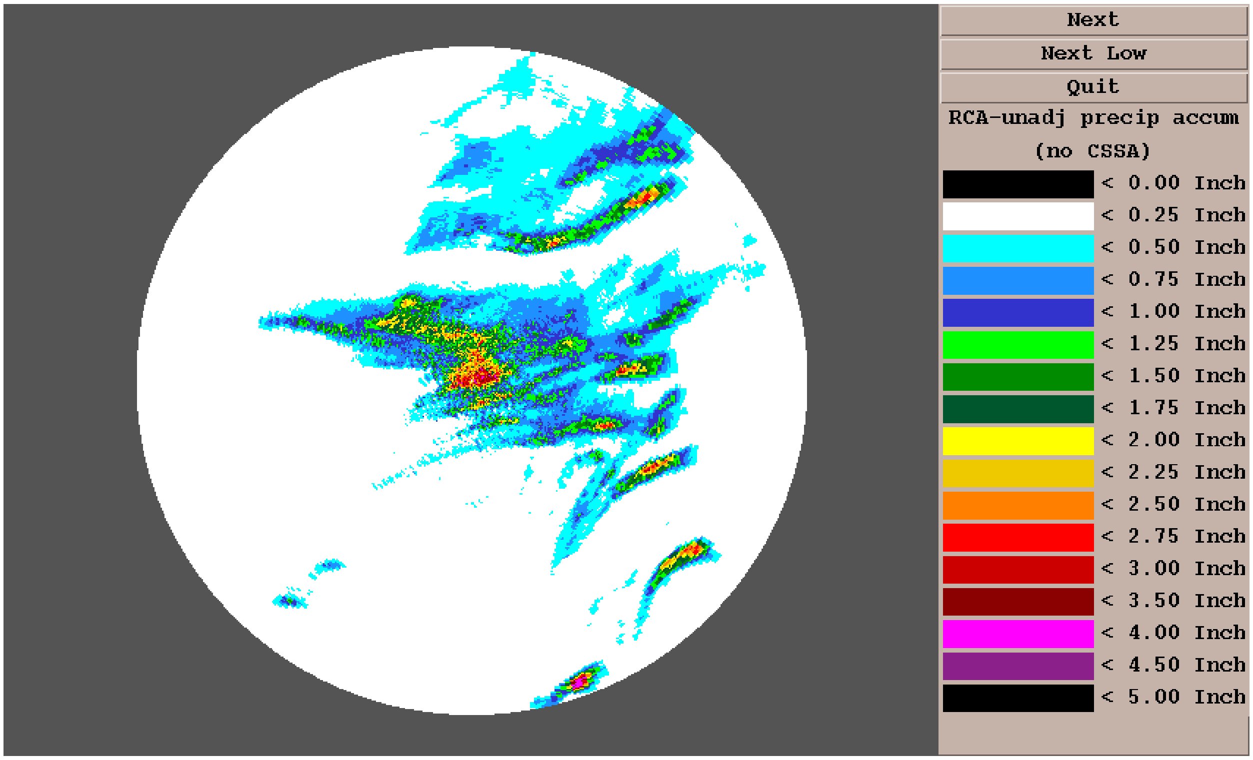

Figure 88. Rainfall over ~6 h in KMLB umbrella, without range correction.

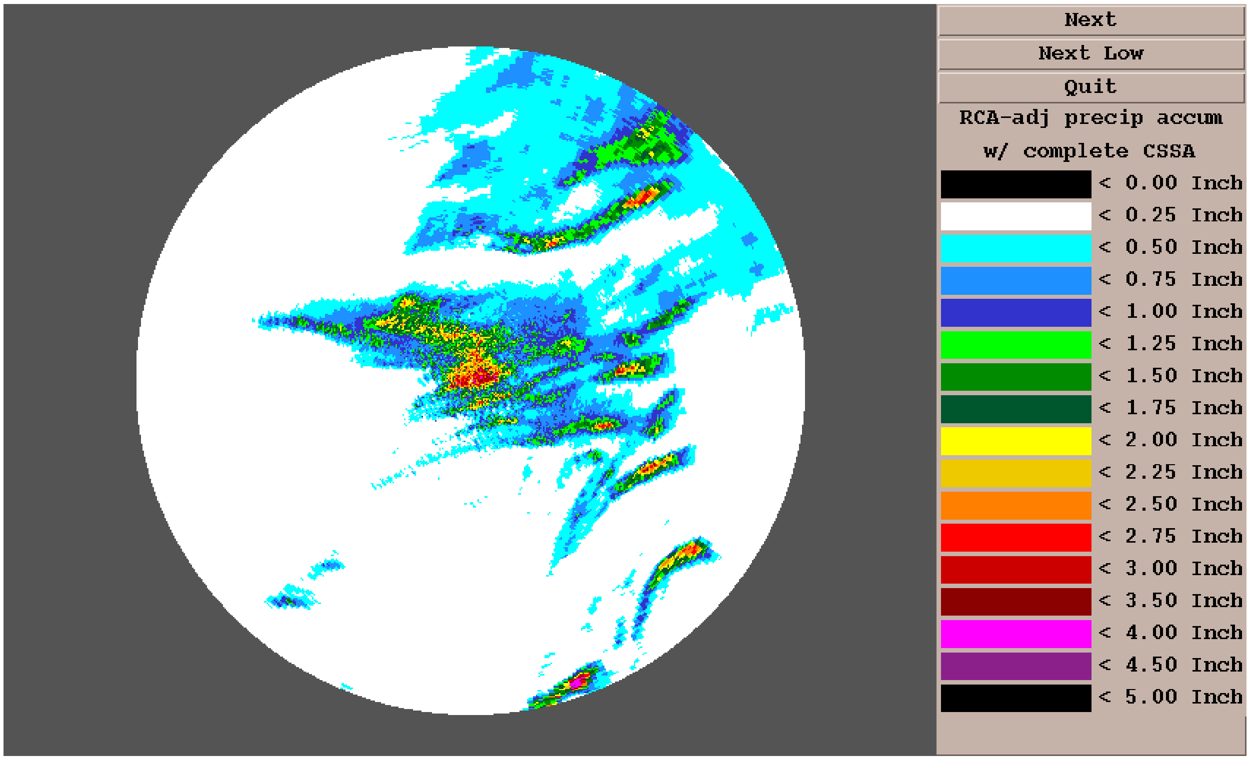

Figure 89. As in Fig. 88, except with range correction with full CSSA.

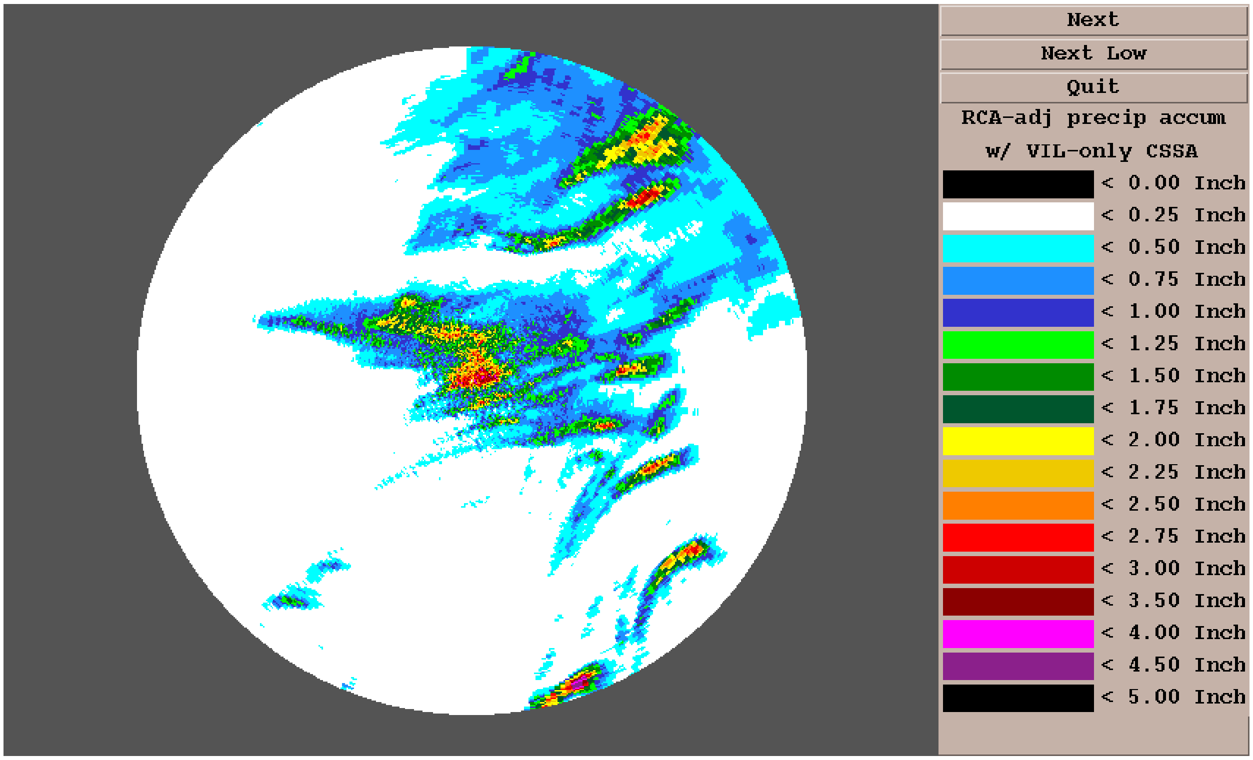

Figure 90. As in Fig. 88, except with range correction using VIL-only CSSA.

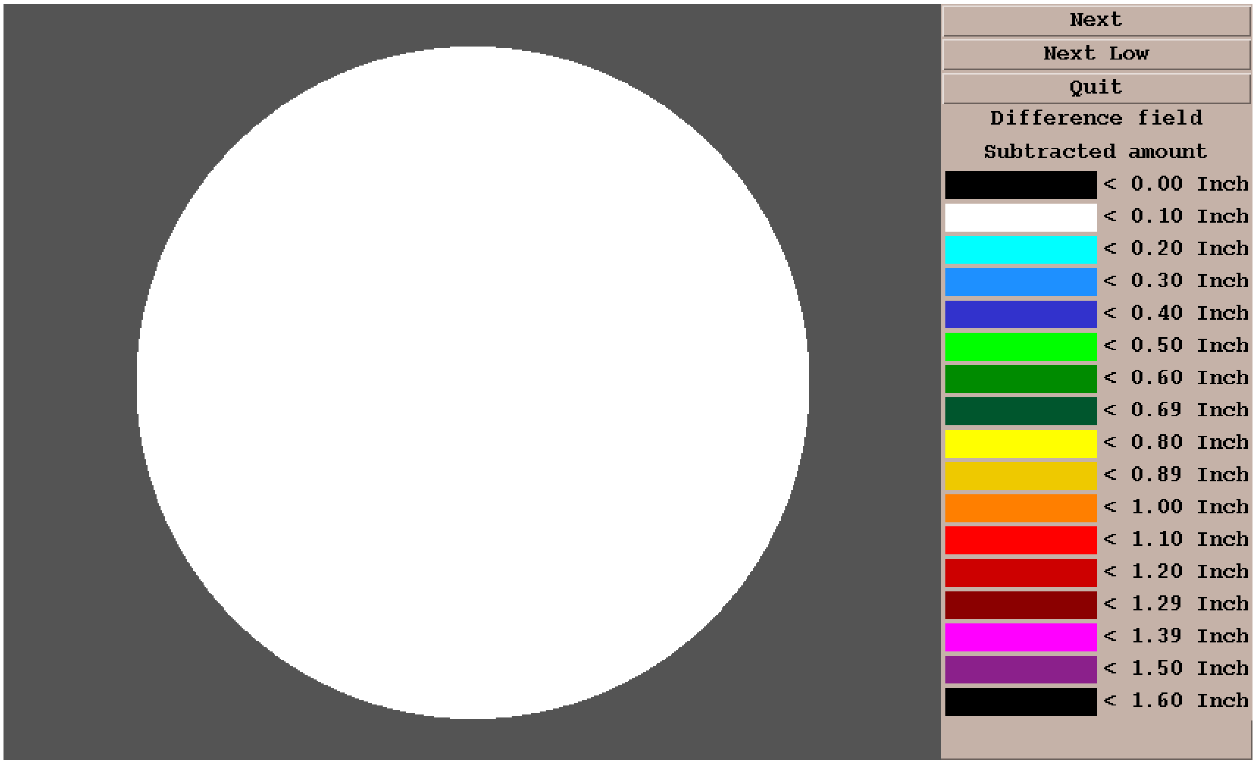

Figure 91. Rainfall apparently subtracted by RCA/full CSSA, corresponding to KMLB case as shown in Figs. 88 and 89.

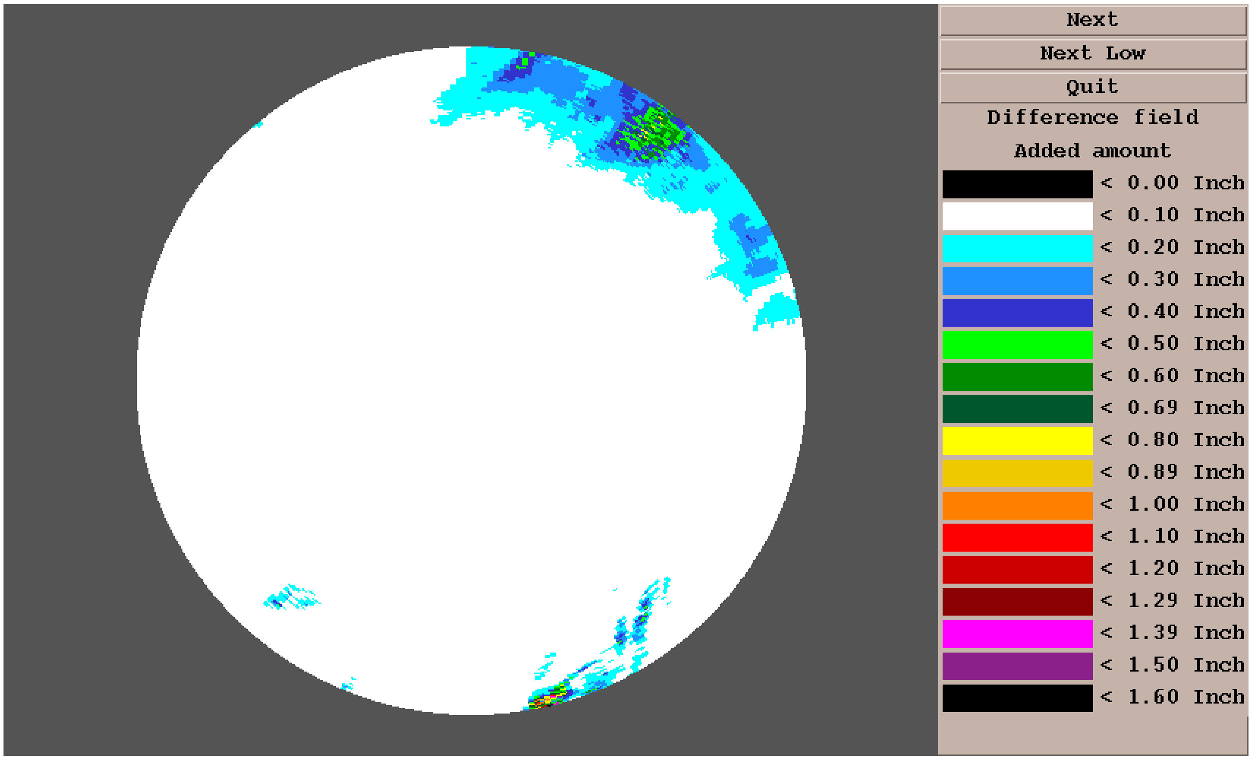

Figure 92. Rainfall apparently added by RCA/full CSSA, corresponding to KMLB case as shown in Figs. 88 and 89.

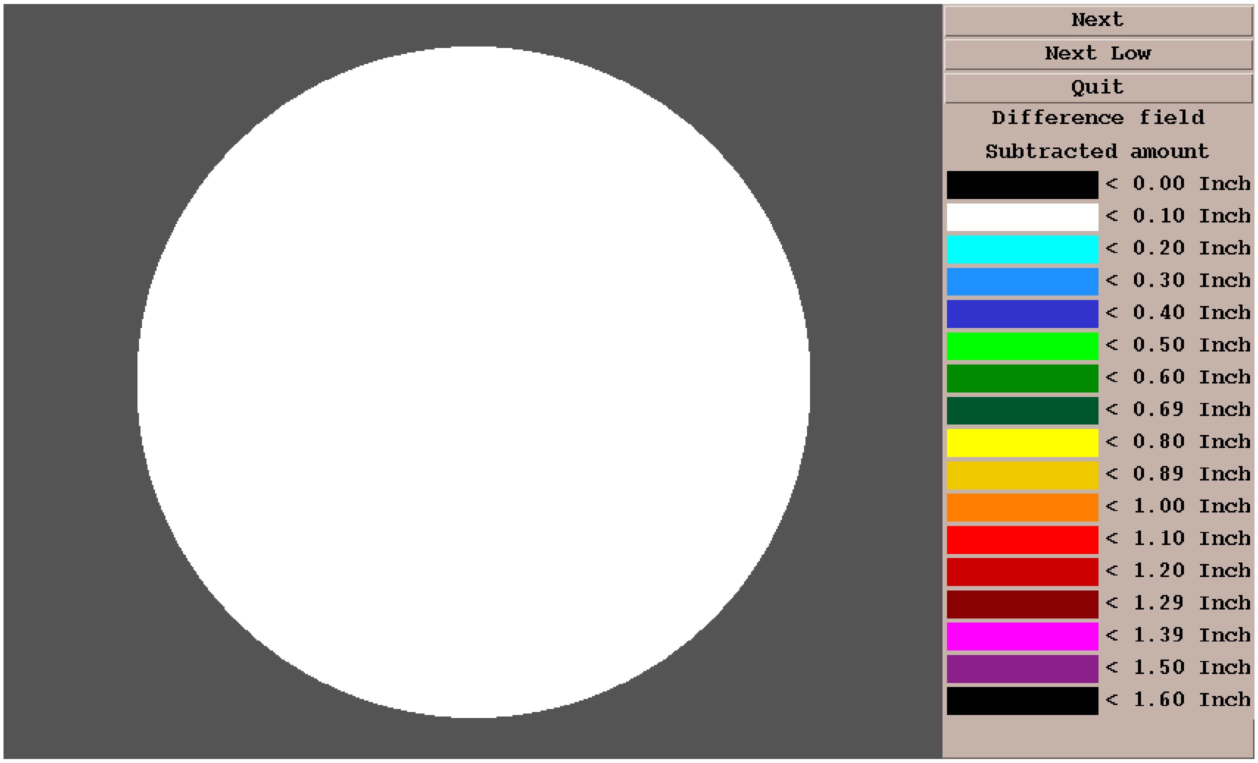

Figure 93. Rainfall apparently subtracted by RCA/VIL-only CSSA, corresponding to KMLB case as shown in Figs. 88 and 90.

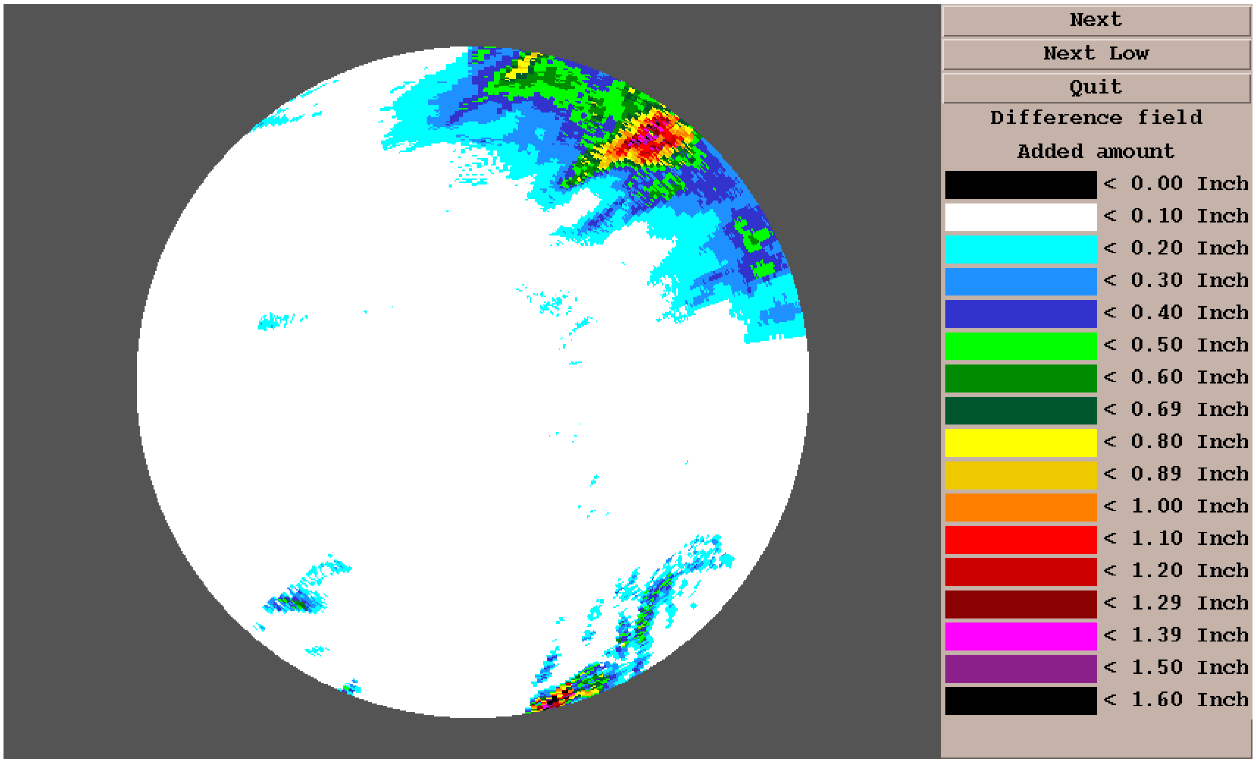

Figure 94. Rainfall apparently added by RCA/VIL-only CSSA, corresponding to KMLB case as shown in Figs. 88 and 90.

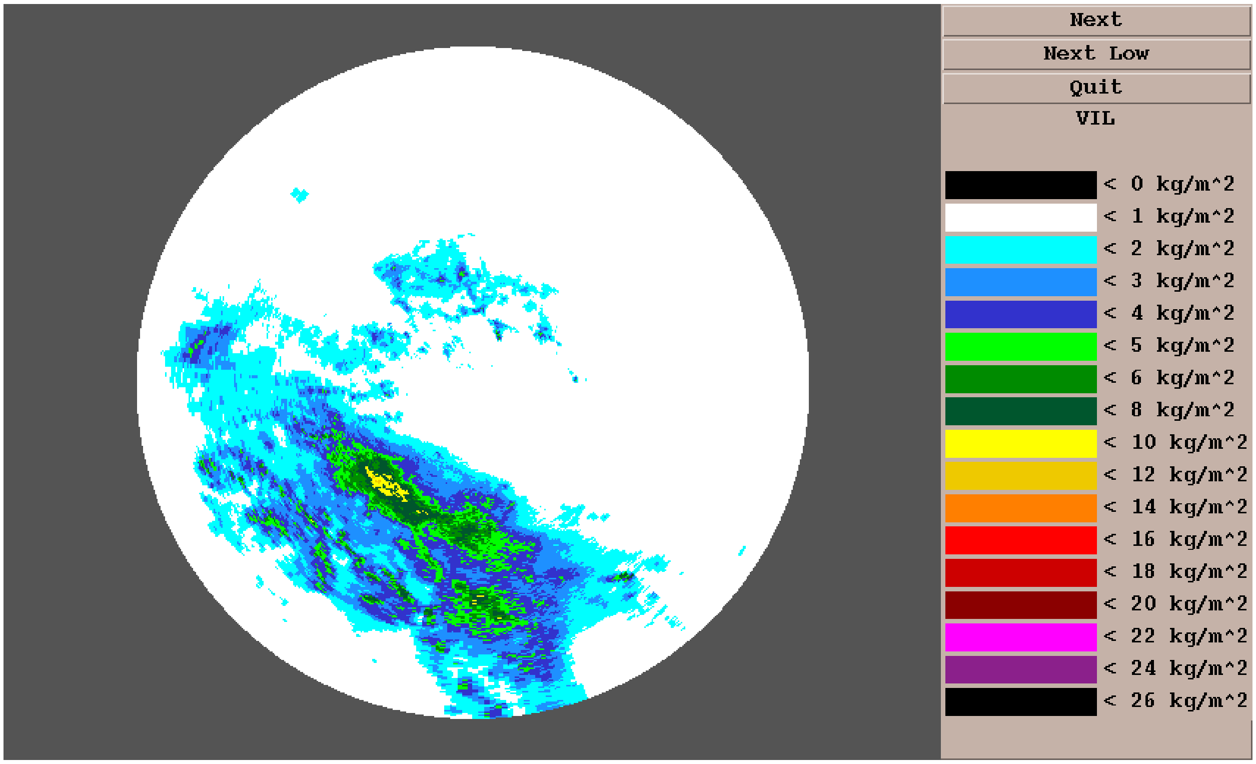

Figure 95. VIL field in KOKX umbrella, 19 October 1996.

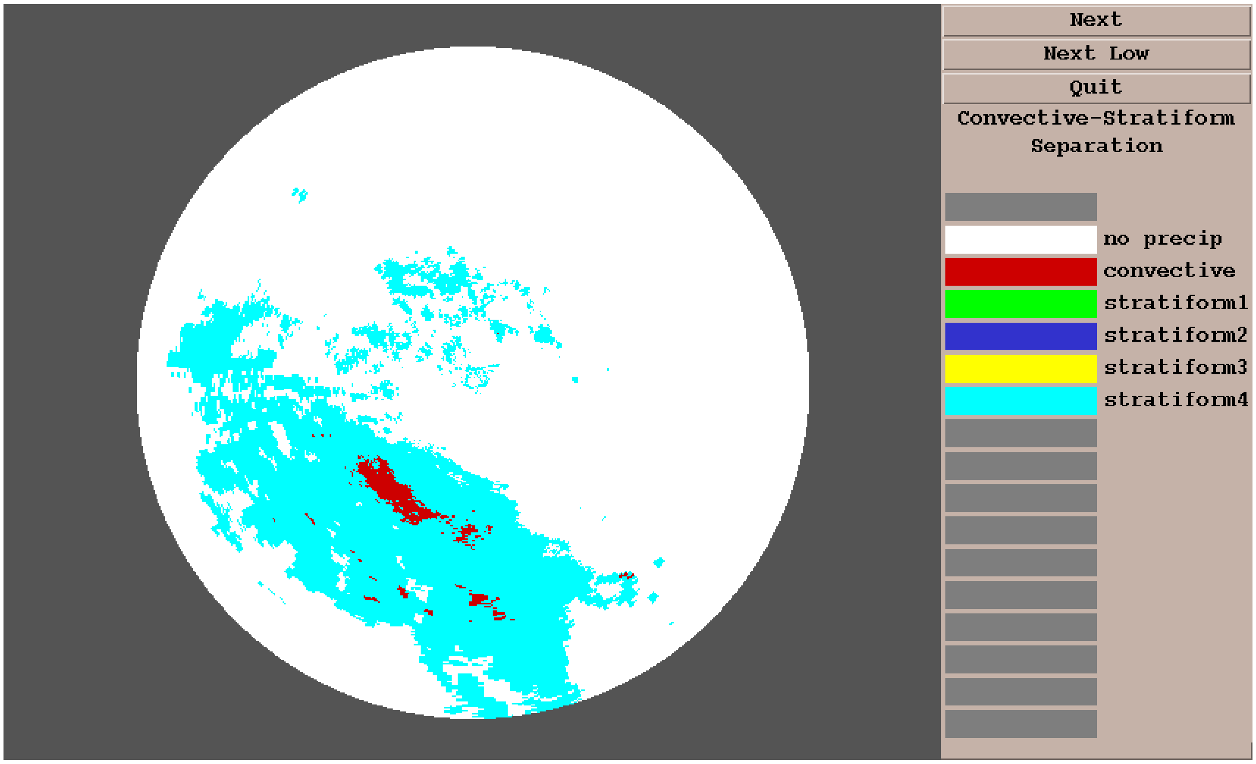

Figure 96. Output of VIL-only CSSA, KOKX umbrella.

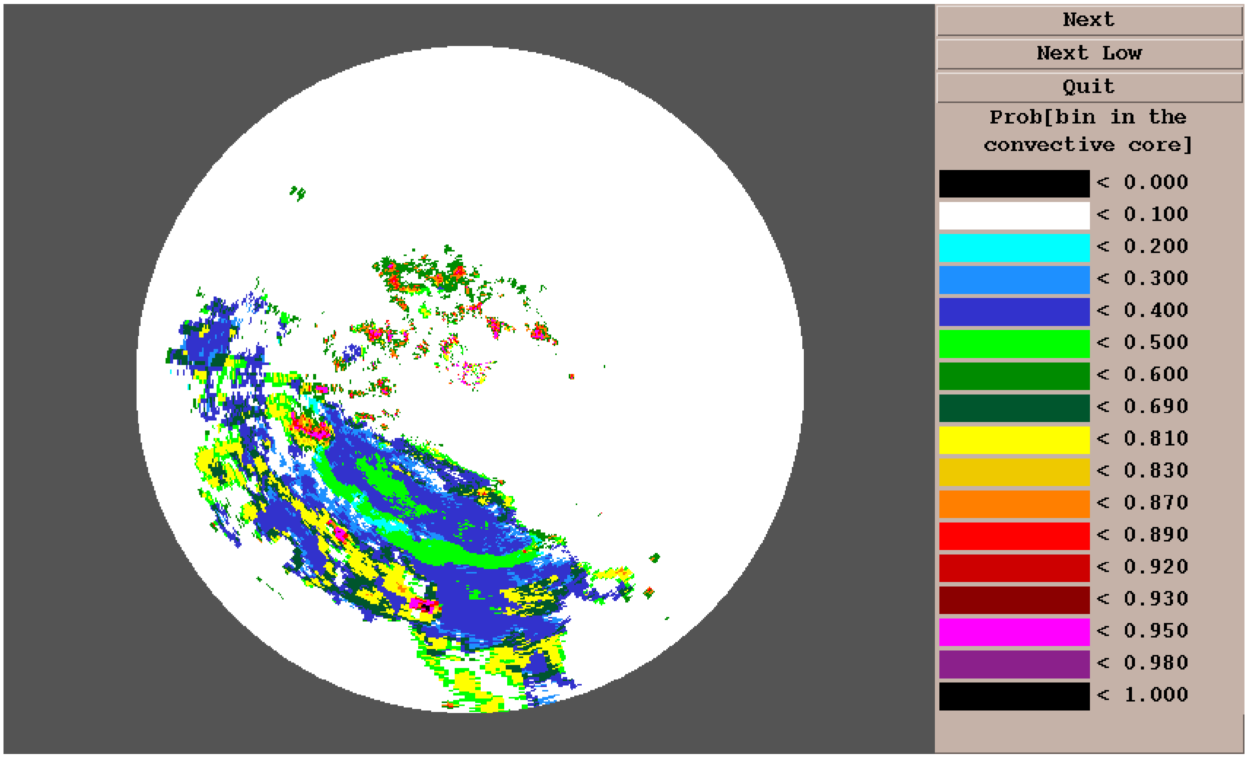

Figure 97. Output of full CSSA, KOKX umbrella.

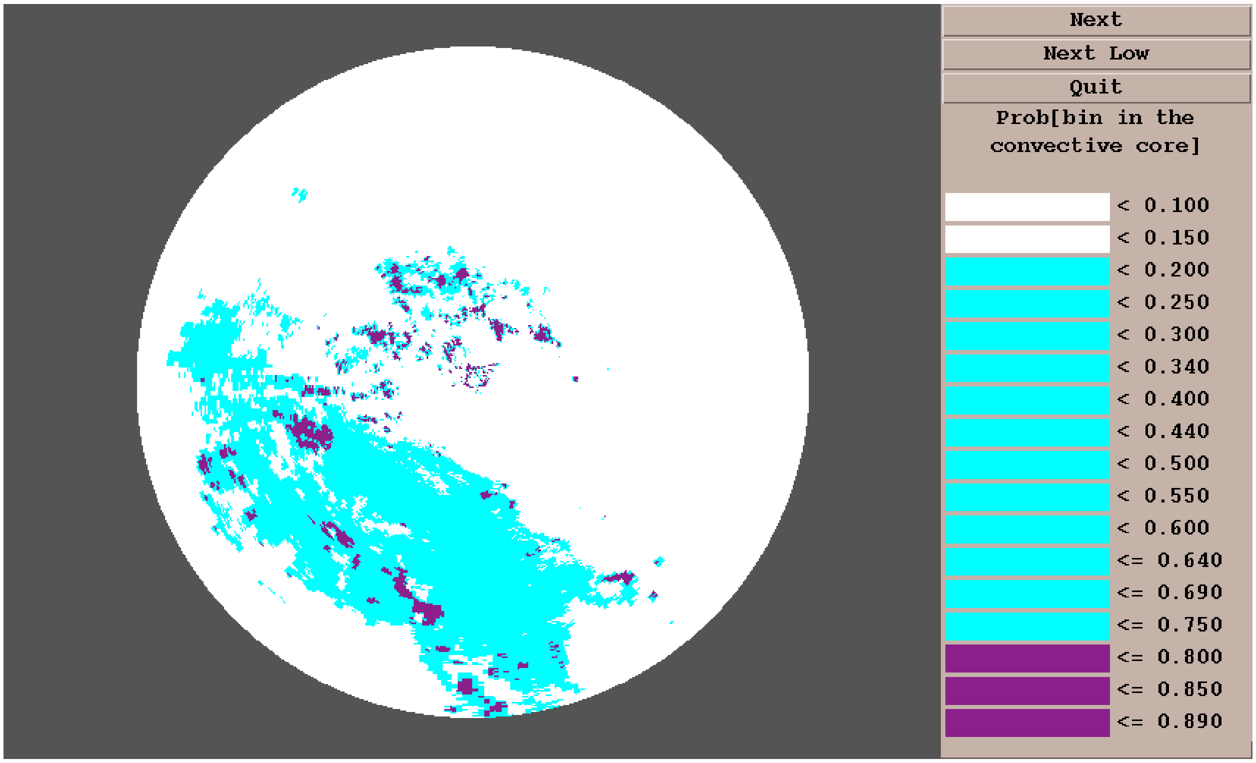

Figure 98. Categorical CSSA, KOKX umbrella, corresponding to Fig. 97.

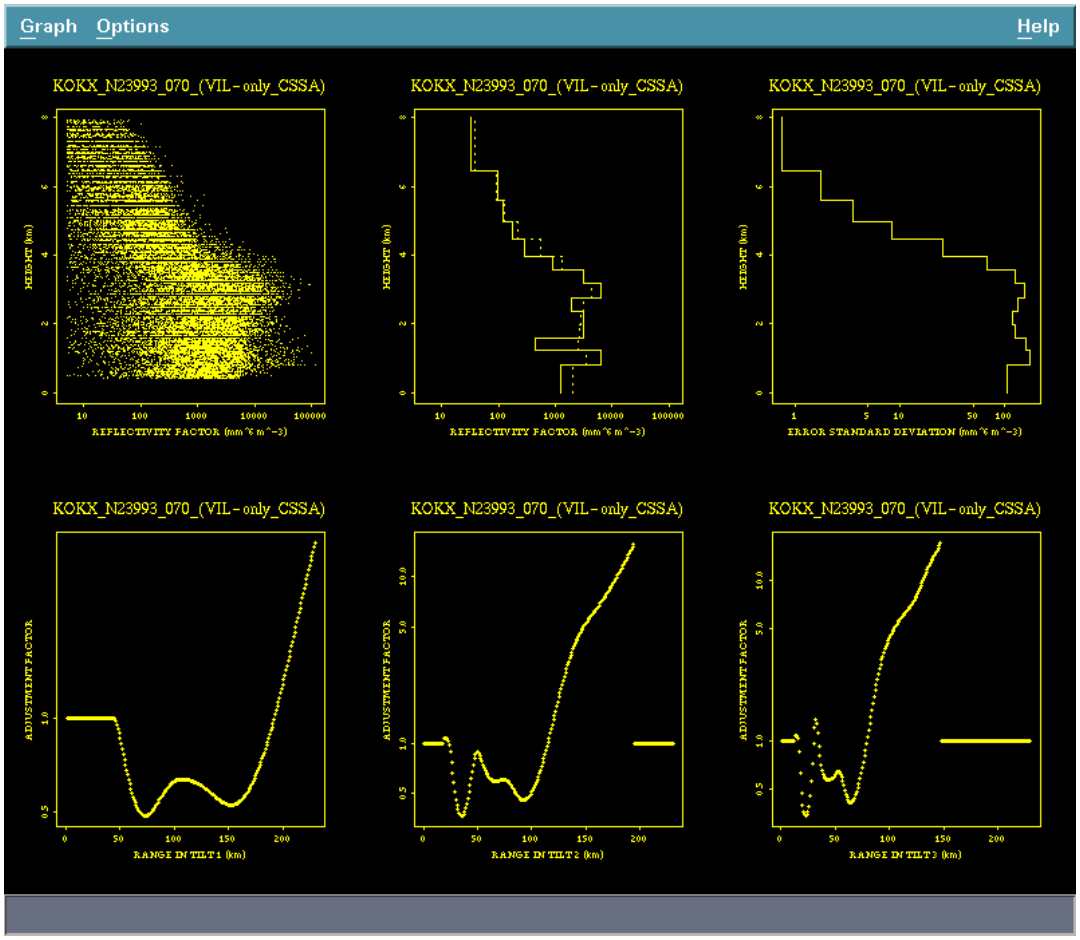

Figure 99. VPR and adjustment factor curves from RCA/VIL-only CSSA, KOKX umbrella.

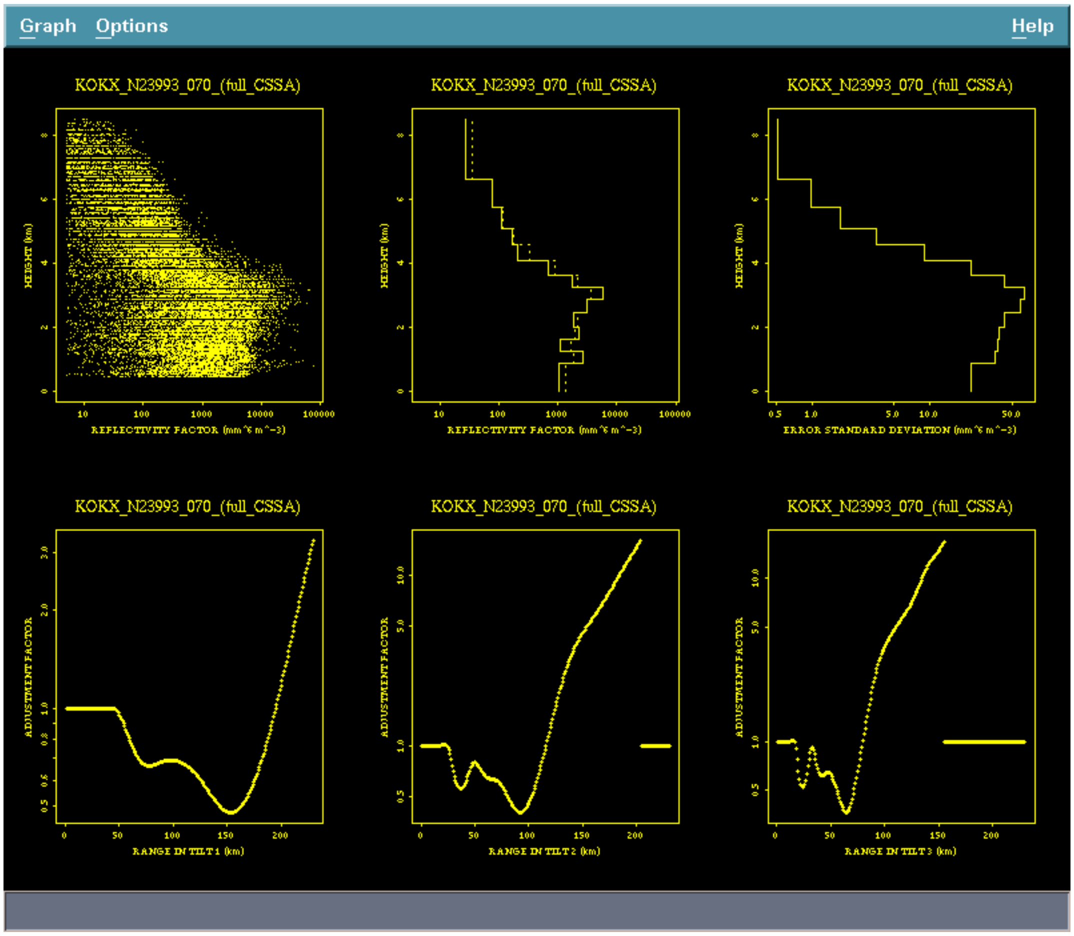

Figure 100. As in Fig. 99, except for RCA/full CSSA.

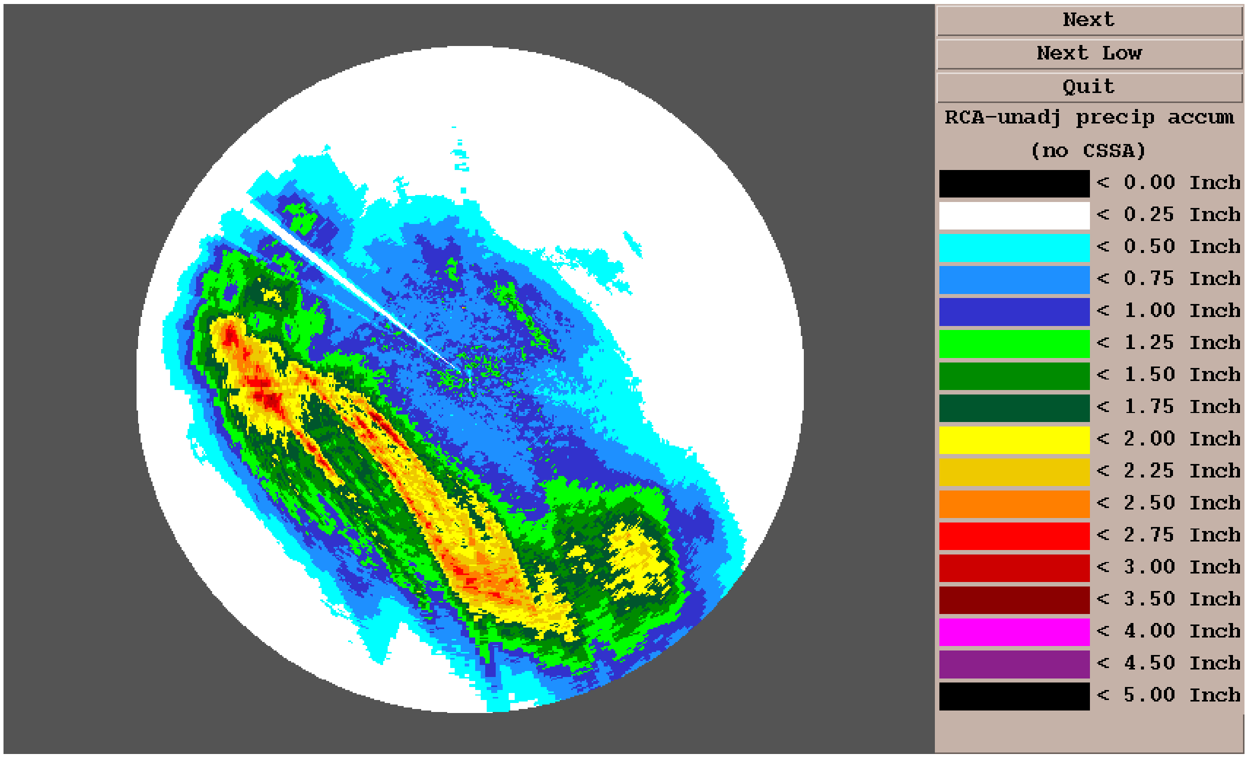

Figure 101. Rainfall over ~6 h in KOKX umbrella, without range correction.

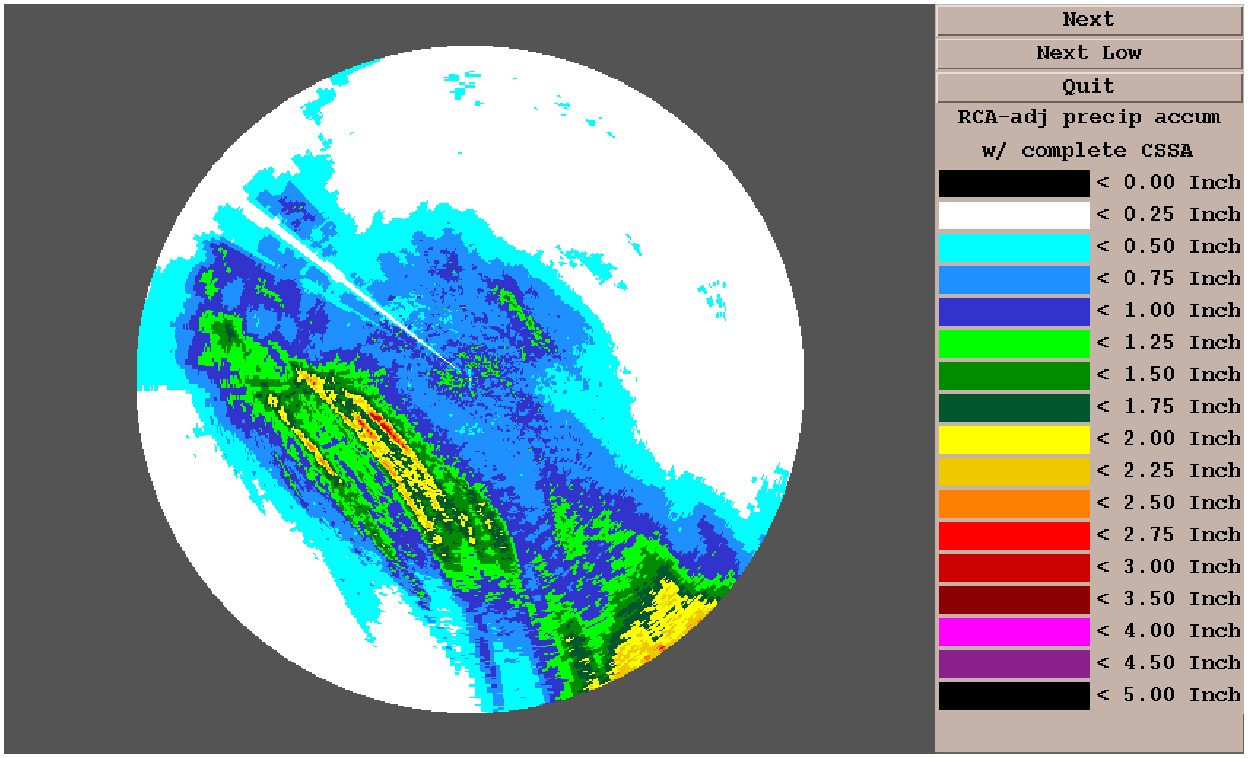

Figure 102. As in Fig. 101, except using range correction with full CSSA.

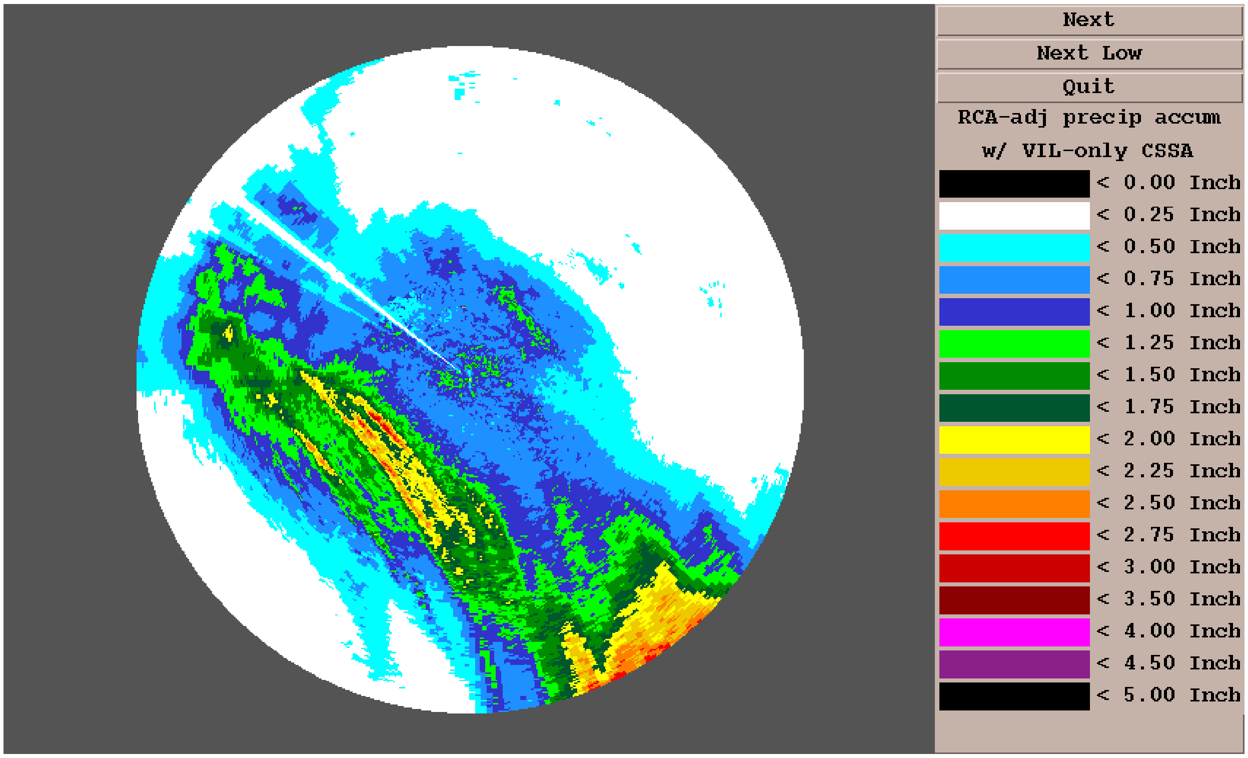

Figure 103. As in Fig. 101, except with range correction using VIL-only CSSA.

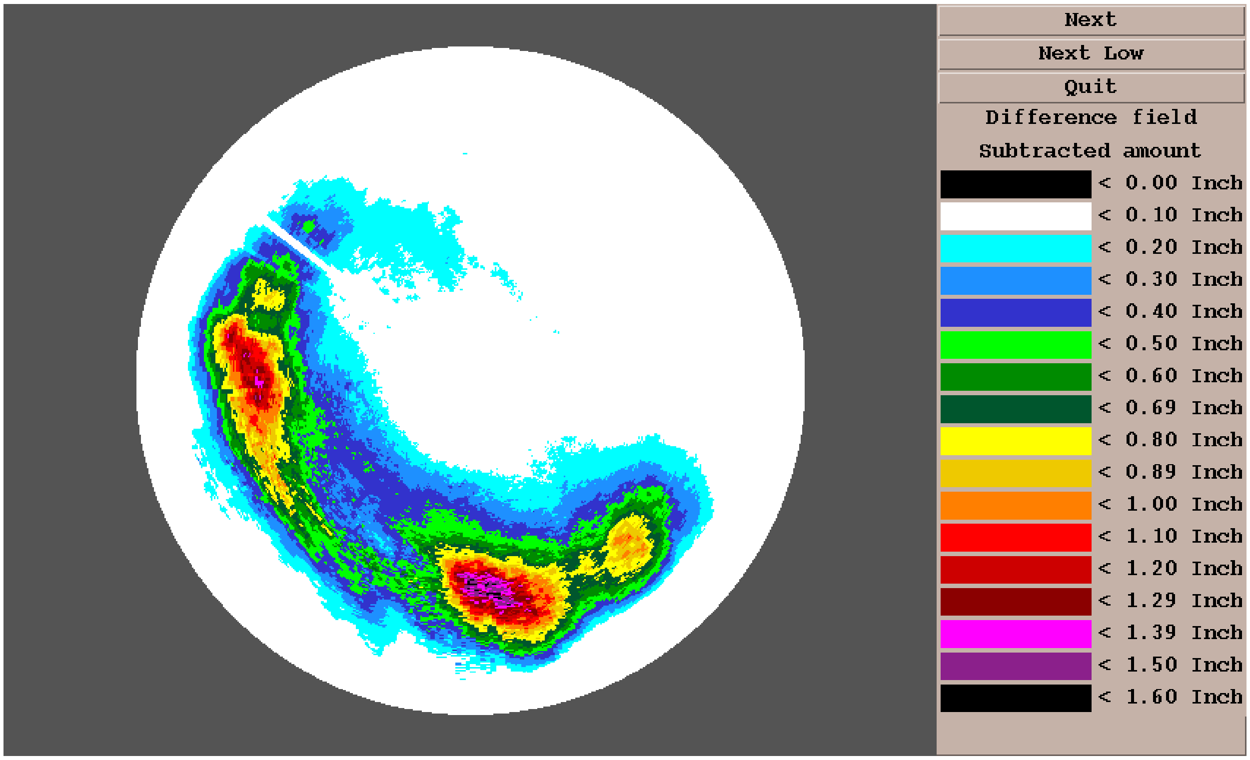

Figure 104. Rainfall apparently subtracted by RCA/full CSSA, KOKX umbrella, corresponding to rainfall in Figs. 101 and 102.

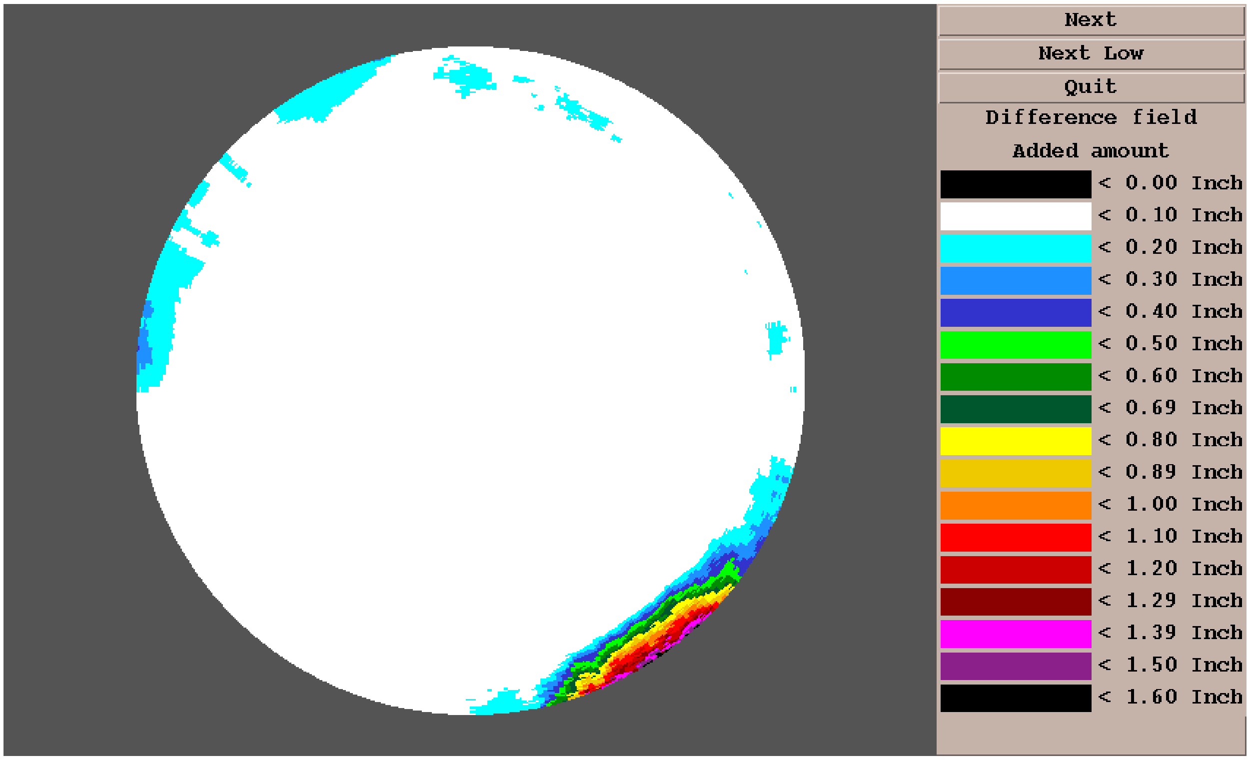

Figure 105. Rainfall apparently added by RCA/full CSSA, KOKX umbrella, corresponding to rainfall in Figs. 101 and 102.

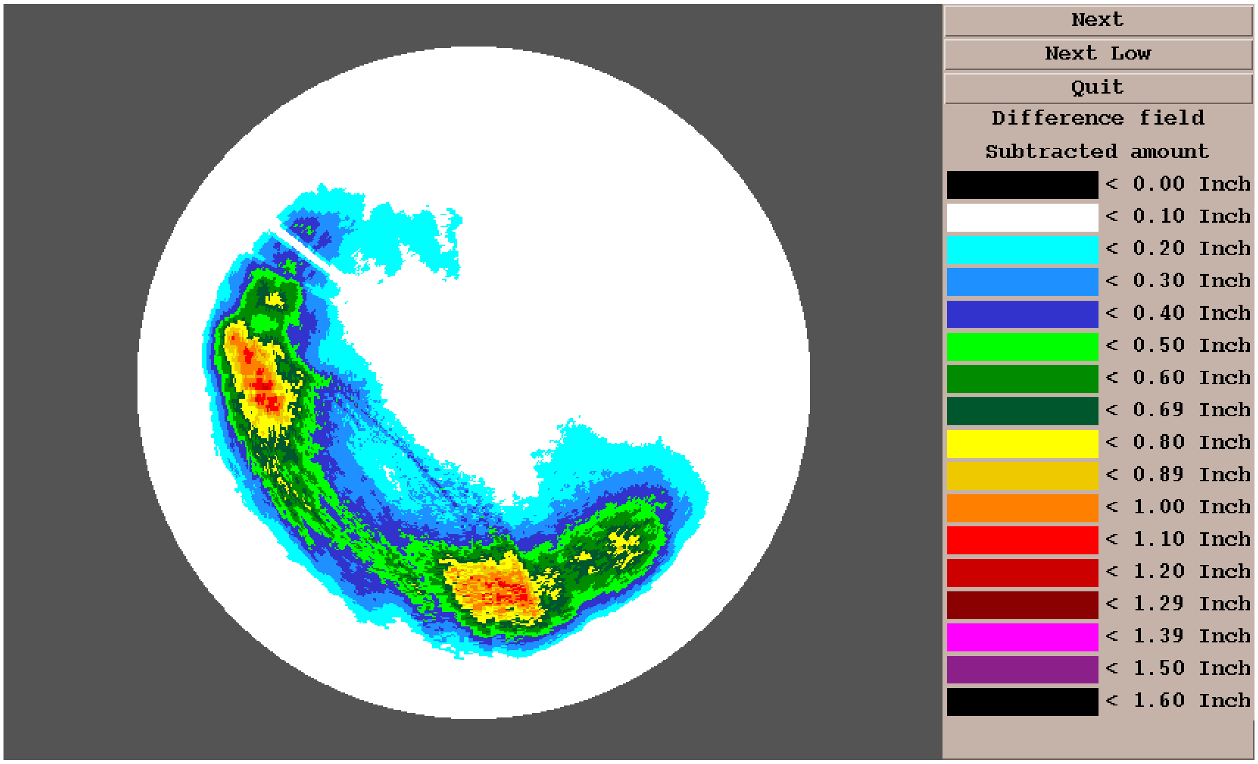

Figure 106. Rainfall apparently subtracted by RCA/VIL-only CSSA, KOKX umbrella, corresponding to rainfall in Figs. 101 and 103.

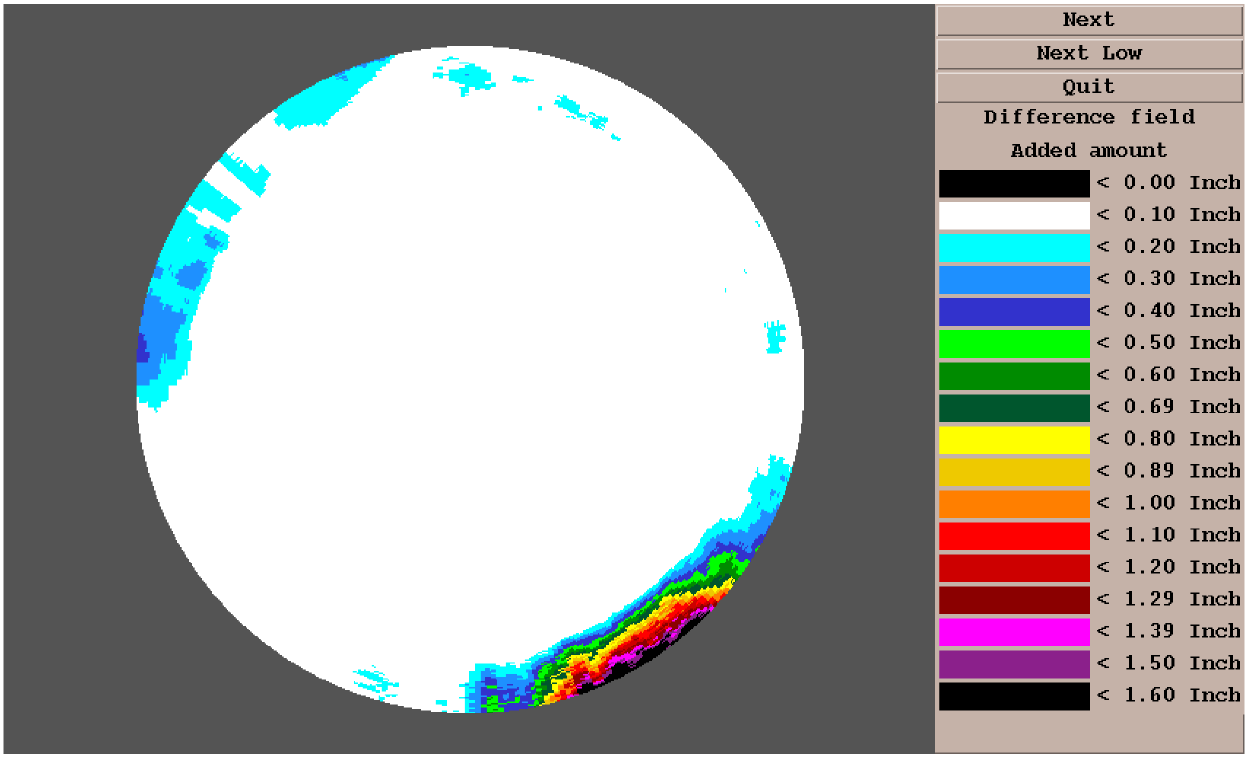

Figure 107. Rainfall apparently added by RCA/VIL-only CSSA, KOKX umbrella, corresponding to rainfall in Figs. 101 and 103.